BIOREMEDIATION OF VOLATILE ORGANIC COMPOUNDS IN A CONTINUOUS STIRRED TANK BIOREACTOR

A Thesis Submitted to the College of

Graduate Studies and Research

In Partial Fulfillment of the Requirements

For the Degree of

Doctor of Philosophy

In the Department of Chemical Engineering

University of Saskatchewan

Saskatoon

By

Yonghong Bi

PERMISSION TO USE

In presenting this thesis in partial fulfillment of the requirement for the postgraduate degree from the University of Saskatchewan, I agree that the Library, University of Saskatchewan, may make this thesis freely available for inspection. Moreover, I agree that permission for copying this thesis for scholarly purposes may be granted by the professors who supervised this thesis work recorded herein or, in their absence, by the Head of the Department or the Dean of the College in which my thesis work was done. It is understood that due recognition will be given to me and to the University of Saskatchewan in any scholarly use which may be made of any material in this thesis. Copy or publication or any other use of the material in this thesis for financial gain shall not be allowed without my written permission.

Request for permission to copy or to make any use of material in this thesis in whole or in part should be addressed to:

Head of the Department of Chemical Engineering
University of Saskatchewan
57 Campus Drive
Saskatoon, Saskatchewan
Canada S7N 5A9

ABSTRACT

The mass transfer of ethanol and toluene from air stream to liquid phase, and bioremediation of contaminated air streams containing either ethanol or toluene have been investigated using a stirred tank bioreactor. This investigation was conducted in six phases:

1) mass transfer experiments involving the transport of toluene and ethanol from contaminated air streams into the liquid phase,
2) study of air stripping effects of ethanol and toluene out of the liquid phase,
3) batch growth experiments to determine growth kinetic models and model parameters,
4) bioremediation of ethanol or toluene as the sole substrate to determine the capacity of *Pseudomonas putida* (*P. putida*) (ATCC 23973) growth on these substrates,
5) toluene removal from contaminated air streams using ethanol and benzyl alcohol as co-substrates, and
6) modelling the above studies using metabolic pathways to better understand the bioremediation process.

Preliminary oxygen mass transfer studies showed that the presence of ethanol in the liquid phase enhances the overall oxygen mass transfer coefficients. Increasing the ethanol concentration from 0 to 8 g/L caused the oxygen mass transfer coefficients to increase from 0.015 to 0.049 s^{-1}, and from 0.017 to 0.076 s^{-1}, for impeller speeds of 450

and 600 rpm, respectively. Mass transfer studies using ethanol vapor in the air stream demonstrated complete absorption into the aqueous phase of the bioreactor at all operating conditions investigated (air flowrates up to 2.0 L/min and inlet concentrations up to 95.0 mg/L) and therefore mass transfer coefficients for ethanol absorption could not be determined. On the other hand, toluene mass transfer coefficients could be measured and were found to be 8.3×10^{-4}, 8.8×10^{-4} and 1.0×10^{-3} s^{-1} at agitation speeds of 300, 450 and 600 rpm, respectively. The ethanol air stripping parameters (β values) were determined (at initial ethanol liquid concentration of 8.6 g/L) to be 0.002 and 0.007 h^{-1} for air flow rates of 0.4 L/min (0.3 vvm) and 1.4 L/min (1 vvm), respectively. The toluene air stripping rates, at initial liquid toluene concentration of 440 mg/L, were found to be 1.9, 5.3, 10.4, and 12.6 h^{-1} for air flow rates of 0.4, 0.9, 1.4, 2.1 L/min, respectively, which is much higher than those of ethanol at the same air flow rates and stirring speed of 450 rpm. It was also observed that benzyl alcohol was not stripped to any detectable level at any of the operating conditions used in this study.

The growth of *P. putida* using toluene as sole substrate was carried out at several operating conditions by varying the dilution rates (D) from 0.01 to 0.1 h^{-1}, the toluene air inlet concentration from 4.5 to 23.0 mg/L and air flow rates of 0.25 to 0.37 L/min (resulting in inlet toluene loadings from 70 to 386 mg/L-h). Steady state operation could not be achieved with toluene as the sole substrate. Ethanol and benzyl alcohol were therefore used as co-substrates for the toluene removal process. In order to understand the kinetics of *P. putida* growing on ethanol or benzyl alcohol, batch growth experiments were carried out at different initial substrate concentrations. The specific growth rates determined from the batch runs showed that ethanol had no inhibition

effect on the growth of *P. putida*. The growth on ethanol followed the Monod equation with the maximum growth rate of 0.56 h^{-1} and yield of 0.59. The results from the batch growth experiments on benzyl alcohol showed that benzyl alcohol inhibits the growth of *P. putida* when the initial concentration of benzyl alcohol in the growth media is increased. The maximum growth rate was 0.42 h^{-1} in the inhibition model and the yield value was 0.45.

By operating the bioreactor in continuous mode using a pure strain of *P. putida*, it was possible to continuously convert ethanol into biomass without any losses to the gas phase or accumulation in the bioreactor at inlet ethanol concentrations of 15.9 and 19.5 mg/L. With ethanol as a co-substrate, toluene was efficiently captured in the bioreactor and readily degraded by the same strain of *P. putida*. A toluene removal efficiency of 89% was achieved with an ethanol inlet concentration of 15.9 mg/L and a toluene inlet concentration of 4.5 mg/L. With the introduction of benzyl alcohol as co-substrate at a feed rate of 0.12 g/h, the toluene removal efficiency reached 97% at toluene inlet concentrations up to 5.7 mg/L. All the experimental results at steady state were obtained when the bioreactor operated in a continuous mode at a dilution rate of 0.1 h^{-1}, an air flowrate of 0.4 L/min, an agitation speed of 450 rpm and a reactor temperature of 25.0^{o}C. The results of this study indicate that the well-mixed bioreactor is a suitable technology for the removal of VOCs with both high and low water solubility from polluted air streams. The results were achieved at higher inlet pollutant concentrations compared to existing biofilter treatments.

A metabolic model has been developed to simulate the bioremediation of ethanol, benzyl alcohol and toluene. For continuous steady state operations, ethanol as

a sole substrate required less maintenance for biomass growth (0.010 C-mol/C-mol-h) than bioremediations in the presence of toluene, as seen with the ethanol/toluene mixture (0.027 C-mol/C-mol-h), and the benzyl alcohol/toluene mixture (0.069 C-mol/C-mol-h).

ACKNOWLEDGMENT

Of the countless people instrumental in the completion of my project, I feel that I am most sincerely indebted to Dr. G.A. Hill, and Dr. R.J. Sumner for their devotion, guidance, and encouragement throughout this whole project. Without their earnest and keen involvement, my objectives would not have been achieved.

I am also very grateful to other members of the advisory committee, such as Dr. T.G. Crowe, Dr. D-Y Peng, Dr. A. Phoenix, and Dr. T. Pugsley for their immensely helpful suggestions, the staff in the Department of Chemical Engineering, especially Ms. J. Horosko, Mr. D. Claude, and Mr. T. Wallentiny, as well as the Chemical Engineering graduate students: Is, Annie, Erin, Tracy, and Yupeng.

Finally, I render my sincerest gratitude to my husband R. Wu and my son WuDi for their continuous encouragement during my years of graduate studies. I also wish to express my deepest appreciation and thanks to all my family members and friends who gave me the emotional and spiritual encouragement I needed throughout all my academic pursuits.

The financial support provided by Dr. G.A. Hill and Dr. R.J. Sumner, NSERC, and University of Saskatchewan in the form of a Graduate Scholarship and a Teaching Assistantship is also gratefully acknowledged.

To the memory of my mother

TABLE OF CONTENTS

LIST OF FIGURES

LIST OF TABLES

NOMENCLATURE

a – Interfacial area, m^2/m^3
C – Substrate or biomass concentration, C-mol/L
C_{gin} – The gas inlet concentration, mg/L
C_L^* - The liquid equilibrium concentration calculated using the gas concentration data and the Henry's constant, mg/L
C_L - The liquid concentration of the organic compound at any point in time, t, mg/L
$C_{o_2}^*$ - The maximum oxygen concentration in the liquid, mg/L
D – dilution rate (flowrate/working volume), h^{-1}
d_b – Gas bubble size, mm
K – the amount of ATP needed for the formation of 1 C-mol biomass from precursors, C-mol
k_La- overall mass transfer coefficient, s^{-1}
K_s - The Monod half-saturation constant, mg/L
m – Maintenance requirement for biomass growth, C-mol/c-mol h
n – The power efficient in the inhibition model, dimensionless
Q – Gas flowrate, L/h
S – Substrate concentration, g/L
S_m – The maximum substrate concentration above which growth is completely inhibited, g/L
t – time, minutes or hours
V – Liquid working volume, L
X – Biomass concentration, g/L
y- gas phase concentration, C-mol/L
$Y_{x/s}$ – Yield of biomass in grams per gram substrate consumed
Y^{max} - The maximal yield.

Greek Symbol
β – air stripping coefficients, h^{-1}
δ – P/O ratio
ϕ - The flow of substrate or biomass into the system (C-mol/L h)
ε – gas holdup, %
θ – stoichiometric matrix for bioremediation reactions
μ – specific growth rate of cells, h^{-1}
μ_{max} - The maximum specific growth rate, h^{-1}
ν – reaction rates

Subscript

0 – initial concentration
1,2,3,4 – reaction number
b – benzyl alcohol
bt – benzyl alcohol and toluene mixture

bx – biomass yield from benzyl alcohol
c – continuous mode
e- ethanol; ex – Biomass yield from ethanol
et – ethanol and toluene mixture
in- Inlet concentration in gas phase
m – maximum value
out – Outlet concentration in gas phase
t – toluene
x-biomass

Superscript

* - Equilibrium value

CHAPTER ONE – INTRODUCTION

1.1 Air Pollution in North America

All unwanted chemicals or other materials found in the air which can harm health, property and the environment are called air pollutants. Public concern about air pollution is rapidly growing. Authorities in many countries have adopted stringent regulations that limit emissions to protect public health and the environment. The emissions of various air pollutants that affect our health and contribute to air pollution problems such as smog (smoke + fog) are tracked by Environment Canada. Most of our industrial and agricultural processes, transport operations and energy production systems generate gaseous emissions often of a polluting nature.

The thick, yellowish haze that can hang over our skylines is smog, and it is affecting our health. Smog can irritate the eyes, nose and throat. As levels increase, smog can cause more serious health problems such as asthma attacks, coughing, chest pain and decreased lung function. Crops, trees and other vegetation are also affected. The main ingredient in smog is ground-level ozone, formed when nitrogen oxides (NO_x) and volatile organic compounds (VOCs) react in stagnant sunlight (Environment Canada, 2005a).

VOCs are an aggregate grouping of almost 1000 organic substances that readily volatilize. VOC substances of interest to the Environment Canada's National Pollutant

Release Inventory (NPRI) are those that contribute to the formation of ground-level ozone and secondary particulate matter. Volatile chemicals produce vapors readily at room temperature and atmospheric pressure. VOCs include gasoline, industrial chemicals such as benzene, and solvents such as toluene and xylene. Many volatile organic chemicals such as benzene and toluene are recognized by the US Environmental Protection Agency (EPA) as hazardous air pollutants. In North America, both Canada and the United States have signed protocols /agreements and have established specific target reductions of VOC emissions and appropriate schedules for implementation. The regulatory incentives are therefore in place for the development and application of cost effective control measures.

Toluene ranks high on lists of toxic compounds emitted to the air. In 1993, toluene ranked highest on the Toxics Release Inventory (TRI) "top ten" list of chemicals with large emission rates to the air, with 8.1×10^7 kg/yr of toluene emitted (Reece et al., 1998). Toluene thus accounted for 10.6% of the total TRI released to the air. Sources of these emissions are numerous. Toluene occurs naturally in crude oil, and it is also produced in the process of making gasoline and other fuels from crude oil and making coke from coal. Toluene is used in making paints, paint thinners, fingernail polish, cleaning agents, and in chemical extractions. The major emissions of toluene are released from the plastic manufacturing, car assembly, and printing industries.

Ethanol is released to the atmosphere by many different industries such as bakeries, candy, confectionary, food, beverage manufacturing including breweries, and vinegar fermentation (Leson and Winer, 1991). Chemical inventories are generated to determine the quantity and nature of atmospheric emissions, sometime with unexpected

results (van Groenestijn and Hesselink, 1993). For instance, the inventory results indicated that ethanol and hexane account for 90% of the emissions of VOCs from the food and beverage industries (Passant et al., 1992). It was reported that nearly two-thirds of the total release of toxic chemicals was emitted to the air (Doerr, 1993).

Toluene was chosen in this investigation as the first model air pollutant of VOCs, since it is one of the compounds categorized by the US EPA as a hazardous air pollutant, due to its toxicity and volatility. Ethanol is the second model air pollutant selected for this study, since contrary to toluene it is highly water soluble and easy to bioremediate.

As for any pollution control technology, the major driving force for development of biological VOC treatment technologies is the continued extension and implementation of air pollution control regulations. In addition, biological VOC treatment technologies are viewed as pollution prevention or green technologies.

The stirred tank reactor has been selected in this study due to its being a popular biochemical experimental setup with the following positive characteristics: 1) efficient biomass retention; 2) a homogeneous distribution of substrates, products and biomass aggregates over the reactor; 3) reliable, continuous operation for more than 1 year; and 4) stable conditions under substrate-limiting conditions (Strous et al., 1998). Since ethanol is miscible with water, the stirred tank reactor (acting as a bioscrubber) may represent the best choice for treatment of ethanol contamination in the air. Once ethanol is available in the aqueous phase, the bacteria will be able to degrade it. Existing gas phase bioreactors such as biofilters can not treat high concentrations of toluene vapor in the air due to its high toxicity. In addition, a major disadvantage of biofilters, limiting

their use as bioreactors for biological waste-gas treatment, is clogging by the formation of excessive amounts of biomass within the filter pores.

1.2 **Research Objectives**

In order to drastically reduce the amounts of VOCs such as toluene and ethanol being released into the air yearly, and to gain more knowledge about ethanol and toluene removal using a stirred tank bioreactor, the following objectives for this project have been set:

1) To study ethanol and toluene mass transfer from air into a well-mixed stirred tank bioreactor (STR);
2) To investigate the effect of ethanol concentration in the aqueous phase on the rate of oxygen mass transfer;
3) To study the bioremediation of ethanol or toluene contaminated air using a well-mixed bioreactor.
4) To investigate the bioremediation of mixtures of toluene and ethanol or benzyl alcohol in a continuous stirred tank reactor (CSTR)
5) To model the combined mass transfer and bioremediation processes and predict their behavior.

1.3 Structure of the Thesis

This thesis contains six chapters. Chapter 1 introduces the background and the objectives in this study. Chapter 2 gives a survey of the literature relevant to this study, which includes the biological and non-biological treatment of VOCs, and describes the previous work and development in the modeling of VOC treatment. Chapter 3 illustrates the experimental procedures and materials applied in this project. The

experimental results are presented and discussed in Chapter 4, which includes the experimental results from mass transfer of ethanol and toluene from contaminated air streams into liquid phases, enhancement of oxygen mass transfer by ethanol addition, and the results from bioremediation of ethanol and toluene in a batch and continuous STR. Chapter 5 presents and discusses the modeling of combined mass transfer and bioremediation of ethanol and toluene from contaminated air in a batch and continuous STR, and the results predicted by the model. Chapter 6 draws the conclusions from this work and gives recommendations for future studies.

CHAPTER TWO – LITERATURE REVIEW

Volatile organic compounds (VOCs) are a class of carbon-containing chemicals which are derivatives of the basic chemicals found in living organisms and in products derived from living organisms, such as coal, petroleum and refined petroleum products. Most VOCs are derived from petroleum with a small amount coming from wood and coal. The emissions from the incomplete combustion of hydrocarbons in motor vehicles play an important role in the VOC total emission (See Tables 2.1 and 2.2). Of the industrial sources, upstream oil and gas industries, petroleum refineries, oil sands, and wood industries contribute the larger amount of VOC emissions. In the category of non-industrial fuel combustion, residential fuel wood combustion plays an important role for VOC emissions. In the open sources, agriculture (animals) plays a major role, as does forest fires.

Table 2.1 VOC Emissions in Canada in the Year 2000 (Environment Canada, 2005b)

Category	**VOC Emissions (thousand tonnes)**
Industrial Sources	992
Non-industrial Fuel Combustion	158
Transportation	727
Incineration	2
Miscellaneous	550
Open Sources	320
National Total	**2,749**

Table 2.2 VOC Emissions in the U.S. in the Year 2000 (EPA, 2005)

Category		**VOC Emissions (thousand tonnes)**
Fuel Combustion	Industrial	235
	Non-industrial	949
Industrial Processes	Chemical and Allied Product Manufactures	254
	Metals Processing	67
	Petroleum and Related Industries	428
	Other Industrial Processes	454
	Solvent Utilization	4,831
	Storage and Transport	1,176
	Waste Disposal and Recycling	415
Transportation		7,969
Miscellaneous		773
National Total		**17,511**

VOCs are of concern as primary pollutants causing immediate toxicity and odour, and as secondary pollutants promoting chemical reactions resulting in smog formation. Efforts to reduce the amounts of these compounds released to the atmosphere are motivated by problems related to health and the environment. The public, government, and industry have all increased efforts to reduce the levels of these compounds released to the environment. There is a building requirement for industries to reduce VOCs emissions and to adapt existing equipment to new regulations.

To meet the emission standards, various techniques for air treatment have been or are being applied and developed. These techniques for VOC treatment have been reviewed by several groups (Cross and Howell, 1992; Dueso, 1994; Hounsell, 1995). Amongst these are conventional methods and biological methods. The conventional methods are the most common methods used in industry today, but biological air

treatment methods are increasingly attractive alternatives and emphasis is placed on these biological methods in this literature survey.

2.1 Non-Biological Treatments of VOCs

Non-biological (i.e., conventional) treatments of VOCs include adsorption, absorption, condensation, membrane separation, and combustion, which will be briefly described below.

Adsorption

Adsorption can be used in pre-concentration for subsequent destruction or recovery. Adsorbents are placed in vertical or horizontal fixed beds. For polluted air flows greater than 15,000 m^3/h, parallel designs are needed (Dueso, 1994). The adsorbing materials currently available on the market are activated carbon and hydrophobic zeolites. The adsorption capacity favours activated carbon (Hussey and Gupta, 1998). Carbon is a relatively cheap support material, which is stable in both strongly acidic and alkaline environments and, due to its high porosity, large surface areas can be obtained. Activated carbon adsorption is a well-established method for controlling VOCs in gas streams (Fang and Khor, 1989; You et al., 1994; Reece et al., 1998; Heinen et al., 2000). Activated carbon adsorbs 90-95% of incoming VOCs if the carbon is regenerated or replaced regularly. The VOCs remain unchanged by sorption and in some cases can be recovered economically. Removal effectiveness decreases as the carbon becomes saturated, and any water vapour present interferes with VOC sorption. Also, under the dry conditions of gas sorption, activated carbon is flammable (Bohn, 1992). However, zeolites appear more suitable when facing high humidity levels

(paint shop effluents, for instance). Synthetic zeolite has a much greater adsorption capacity than carbon at low solvent concentrations, but carbon has a higher capacity at high concentrations (Hussey and Gupta, 1998). Treatment with adsorption merely transfers the contaminants from one phase to another, rather than transforming it into less harmful compounds. Therefore, a further oxidation process is required to destroy or recover the contaminants.

Absorption

Packed towers are used most of the time for absorption. The main application fields are refineries, petrochemical plants, and the pharmaceutical industry (Dueso, 1994). Absorption efficiency depends on:

- The transfer coefficient of organic compounds between the gaseous phase and the absorbing liquid phase (water or organic liquid depending on whether the organic compounds are soluble or insoluble in water);
- The efficiency of the gas/liquid contact in the counterflow washing column;
- The contact time.

Similar to treatment with adsorption, absorption also transfers the contaminants from one phase to another, therefore, a further oxidation process is required to destroy or recover the contaminants.

Condensation

Condensation is obtained by increasing pressure beyond the saturation pressure, or by decreasing temperature below the saturation temperature, or by combining the two. This type of process requires a low temperature as compounds to be trapped are volatile. Therefore, this process is relatively expensive and rarely used.

Membrane Separation Technology

The VOCs can be separated from air using membranes via a selective transfer through the separation layer. On the permeate side, the strongly loaded gas stream is condensed to recover the solvents. The majority of the selective layers used for VOC separation from air are silicone-based membranes (elastomer). By comparison to several other separating processes based on solvent recovery, membrane technology presents the important advantage that it can be made to withstand high temperatures (up to 200^{o}C). Most uses of this technique are applied in the field of gasoline recovery (Dueso, 1994).

Thermal Incineration

Thermal incinerations are used in diverse application fields including printing works, coil coating, coating installation, and drying ovens in paint shops. Catalytic incineration uses a catalytic bed composed of an inert support, with a metallic or ceramic base, in a tubular structure, on which a precious metal or metallic oxide catalyst has been deposited. These methods have been applied to offset printing, coating, drying ovens of paint shops, and odorous gas treatment (Dueso, 1994). Wilcox and Agardy (1990) carried out thermal destruction of air toxic VOCs using packed bed technology. The In-Process Technology thermal processor operation is based on a packed bed technology where vapor phase VOCs entering the unit, flow through a stationary bed of special inert material heated by electrical energy to a temperature up to 1093^{o}C. The destruction efficiencies for the VOCs tested (such as toluene and ethanol) in a bench scale unit were greater than 99.99% (Wilcox and Agardy, 1990). Depending on the pollutant, temperature, and type of the adsorbent or catalyst, adsorption or catalytic

combustion provides 70 to 90% air purification efficiency at space velocity ranging from 3200 to 30000 h^{-1} (Chuang et al., 1992; Carno et al., 1996).

2.2 Bioremediation of VOCs

Biological treatments of VOCs have been reviewed by different workers (Bohn, 1993; Van Groenestijn and Hesselink, 1993; Edwards and Nirmalakhandan, 1996). For the biological removal of contaminants from waste gases the contaminants have to be transferred from the gas phase to the liquid phase surrounding the microorganisms or directly to a biofilm. The driving force for this mass transfer depends on the concentration in the gas phase, the air/water partition coefficient and the concentration in the aqueous phase surrounding the microorganisms (Hartmans, 1997). Therefore, there are three important parameters determining if biological waste gas treatment is feasible: 1) the pollutant concentrations in the treated air, 2) the air/water partition coefficient of the contaminant, 3) the kinetics of the microorganism(s) degrading the contaminant of interest. Various bioreactor designs have been utilized to degrade VOCs in waste gases including biofilters, trickle beds, and bioscrubbers.

2.2.1 Biofiltration

Biofiltration is the oldest and most widely used of the biological air purification techniques. In biofiltration, the gas to be treated is forced through a bed packed with material on which microorganisms are attached as a biofilm. Biodegradable volatile compounds are adsorbed by the bed material and the biofilm, and subsequently biologically oxidized into biomass, CO_2 and H_2O. Usually, the packing material is a mixture of a natural fibrous substance with a large specific surface area and a coarse

fraction. The fibrous substance is the active fraction that contains most of the microorganisms and nutrients. Compost and peat are often used in this application. The coarse fraction serves as support material, prevents high-pressure drops in the filter and may consist of inert materials such as wood bark, wood chips, or modified activated carbon (Kiared et al., 1996; Marek et al., 2000). A well-designed air distribution system is required to assure even flow through the filter. Moisture can be added to the filter container as the conditions dictate. Biofilters can be run in parallel or in series.

A number of experimental studies in the last decade (Shareefdeen et al., 1993; Togna and Singh, 1994; Weber and Hartmans, 1995; Kiared et al., 1996; Song and Kinney, 1999; Ramirez-Lopez et al., 2000) have established biofiltration as an efficient treatment process and reliable technology for the control of volatile organic compounds. The compounds to be treated must be readily biodegradable and non-toxic; thus, biofilters have treated alcohols, ethers, ketones, and organic amines at reasonably high concentrations. Biofiltration of methanol vapour has been evaluated using a mixture of compost as filter materials in which an elimination capacity of 112.8 g m^{-3} h^{-1} was achieved (Shareefdeen et al., 1993).

2.2.1.1 Ethanol Removal by Biofiltration

Biofiltration has been the most widely used means to remove ethanol vapour from air streams (Hodge and Devinny, 1994; Shim et al., 1995; Kiared et al., 1996; Cioci et al., 1997; Arulneyam and Swaminathan, 2000; Ramirez-Lopez et al., 2000). Three different packing materials were studied for the biofiltration of ethanol vapor and elimination rates up to 219 g m^{-3} h^{-1} were achieved (Hodge and Devinny, 1994). A fixed film spiral bioreactor containing immobilized activated sludge microorganisms has been

used to degrade ethanol vapours and a maximum elimination capacity of 185 g ethanol h^{-1} m^{-3} of reactor volume was achieved (Shim et al., 1995). Critical ethanol loading, defined as the maximum loading to achieve greater than 99% elimination at various residence times have been determined, with typical maximum ethanol loadings of 180 and 109 g ethanol h^{-1} m^{-3} of reactor volume at residence times of 12.4 and 1.5 minutes, respectively.

The performance of a continuously operated biofilter for removal of ethanol vapour at relatively high inlet concentrations was examined and a maximum elimination capacity of 195 g m^{-3} h^{-1} was achieved (Arulneyam and Swaminathan, 2000). Concentrations as high as 10 g m^{-3} could be degraded at a gas velocity of 15 m h^{-1}; however, higher concentrations and higher gas flow rates reduced the removal efficiency due to mass transfer limitations and short residence times. They also observed that at all gas flow rates, the elimination capacity increased with increasing ethanol concentration until a threshold concentration after which it remained constant. Ethanol vapour was removed using a bioreactor (2.7 m^3) packed with a novel microbial support consisting of a highly porous inorganic matrix coated with a thin layer of activated carbon (Cioci et al., 1997). The plant was operated continuously for two months, and the inlet waste air was maintained at a temperature of 20^0C and a gas flow rate of 200 m^3 h^{-1} throughout the experimentation. The ethanol concentration was varied between 90 and 2200 mg m^{-3}, and removal efficiencies ranging from 80 to 99.9% were obtained. An aerobic biodegradation with a concentration of 1 g ethanol m^{-3} was studied in an experimental biofilter using wood bark as a packing material (Ramirez-Lopez et al., 2000). With the addition of nutrient, after 45 days of continuous biofilter operation

an elimination capacity of 107 g $m^{-3}h^{-1}$ equivalent to 100% removal efficiency was reached. An increase in the temperature of the bed from 17 to 25^{o}C and a variation in the pH from 7.3 to 4.0 were observed. The changes in pH were due to the acidic metabolic products, such as acetic acid and acetaldehyde (Ramirez-Lopez et al., 2000).

2.2.1.2 Toluene Removal by Biofiltration

Air containing toluene vapour has been biologically treated in different types of vapor phase bioreactors such as in biofilters (Chozick and Irvine, 1991; Morales et al., 1994; Shareefdeen and Baltzis, 1994; Parvatiyar et al., 1996; Song and Kinney, 1999; Darlington et al., 2001), in a filter-bed reactor (Bibeau et al. 1997), and in a biological trickle-bed reactor (Weber and Hartmans, 1996; Pedersen and Arvin, 1999). The maximum removal rates of 4.5 and 25 g $m^{-3}h^{-1}$ for benzene and toluene, respectively, were achieved in the laboratory scale biofilter (Shareefdeen and Batzis, 1994). A maximum removal rate of 25 g toluene $m^{-3}h^{-1}$ was also obtained by Morales et al. (1994) in a bench-scale biofilter.

Kiared et al. (1996) reported that removal efficiency reached around 80% and 70% for ethanol and toluene, respectively, using a laboratory scale biofilter with the inlet concentration of ethanol at 1.89 g m^{-3} and that of toluene at 0.75 – 3.76 g m^{-3}. A higher removal efficiency of ethanol (up to 100%), for an ethanol inlet concentration below 3.0 g m^{-3}, was also reported by other authors (Arulneyam and Swaminathan, 2000). However, with an increase of ethanol inlet concentration up to 10.0 g m^{-3}, the removal efficiency dropped to 68% only. Toluene removal efficiency was reported to be 70% at inlet concentrations below 2.2 g m^{-3} (Bibeau et al., 1997) while the removal efficiency was approximately 30% with an inlet concentration range between 2.2 to 6.0

g m^{-3}. This would suggest that the removal efficiency decreased with increasing inlet concentration using a biofilter. The higher removal efficiency of toluene, up to 93%, was achieved using a pilot-scale biofilter at an inlet concentration of 2.63 g m^{-3} and a gas flowrate of 5.5 m^3/h (Jorio et al., 1998).

When compared with conventional treatments, such as adsorption, water and chemical scrubbing, catalytic oxidation, and incineration, biofiltration offers a number of advantages (Bohn, 1992). They include low installation and maintenance costs, and the fact that the components to be removed are generally converted into non-toxic compounds. However, the application of this technology is hindered by a number of drawbacks. One of the major limitations is represented by the organic nature of the support material, which leads to the formation of agglomerates and sludge, requiring the packing material to be replaced from time to time. To attain optimal microbial growth conditions, accurate control of pH and moisture levels are required. Moreover, a poor adaptability to changes in gas composition is generally observed.

2.2.2 Biotrickling Filter

A geometry of the biotrickling filter is similar to a biofilter with the exception that moisture is sprinkled on the top of the filter media and allowed to trickle down through the filter media, therefore requiring somewhat greater porosity. Trickle-bed bioreactors represent the second generation of biological air purification devices. They are based on the use of adapted bacterial monocultures or mixed cultures immobilized on granular materials, such as synthetic polymers or activated carbon (Hekmat and Vortmeyer, 1994; Togna and Singh, 1994; Weber and Hartmans, 1996). Biotrickling filters can also be run in series or in parallel.

Experimental research on laboratory-scale trickle-bed reactors was performed in order to quantify degradation rates of various organic pollutants utilizing different types of inert carrier materials (Kirchner et al., 1987, 1989, 1991; Hekmat and Vortmeyer, 1994). Despite the obvious improvement over biofilters, trickle-bed bioreactors have two limitations that have precluded their use in industrial air purification. First, diffusion of pollutants through the aqueous phase toward the biofilm appears to be rate limiting (Kirchner et al., 1989, 1991). Thus, the removal of pollutants sparingly soluble in water (e.g., toluene) is much less efficient (Kirchner et al., 1991; Kozliak et al., 2000). Secondly, increasing the pollutant inlet concentrations above 50 g m^{-3} causes an oxygen diffusion limitation. Therefore, the reactors are efficient only for the removal of low pollutant concentrations (Kirchner et al., 1992, 1996).

Fibers are suggested for bacterial immobilization in trickle-bed bioreactors used for the removal of VOCs from air. An overview of air purification from VOC using fiber-based trickle-bed bioreactor was given by Kozliak and Ostlie-Dunn (1997). Efficient removal is achieved for ethanol. Specific pollutant elimination capacity per unit fiber-based biocatalyst volume (up to 4000 g $m^{-3}h^{-1}$) exceeds those of biological air purification methods and is comparable to chemical methods (Kozliak et al., 2000). They concluded that the higher air purification efficiency is due to the greater surface-to-volume ratio of fibers when compared with granules, which results in a more efficient substrate mass transfer.

Clogging of the fibers due to the formation of excessive amounts of biomass can be a major disadvantage, limiting the use of trickle-bed reactors for biological waste-gas

treatment, This excessive biomass formation should be prevented by limiting the amount of inorganic nutrients available for growth.

2.2.3 Bioscrubbers

In bioscrubbers, contaminated gas is contacted generally with water in a spraying tower with inert packing resulting in absorption of toxic compounds from the air into the water phase, followed by the biological treatment of the contaminated water. Thus, a bioscrubber consists of a scrubber and a bioreactor with activated sludge. The aqueous phase (often with suspended microorganisms) is continuously recirculated over the two separate units. In contrast to biofilters, the liquid phase in the bioscrubbers is mobile, which allows better control of the reaction conditions. In addition, temperature, pH and ionic strength can be monitored and controlled more easily (van Groenestijn and Hesselink, 1993). A drawback compared to biofilters is the lower specific gas/liquid surface area. Bioscrubbers are restricted mainly to the removal of the water-soluble compounds from the air. In the bioscrubbing system, the two units can also be integrated where the contaminant is transferred from the gas phase to the liquid phase and biodegraded.

2.2.4 Liquid Phase Bioreactor

Volatile organic chemicals from waste gas can act as energy sources for microbial growth. The purification of waste gases by microorganisms (primarily bacteria) is carried out as the microorganisms search for food sources for growth. The microbes consume the pollutants from the surrounding aqueous phase, which in turn absorbs the pollutants from the gas phase. Thus, the mass transfer of the pollutants into

the liquid phase surrounding the microbes is important. Once the pollutant is available to the microbe in the aqueous phase, the microbes can oxidize these compounds into final products such as CO_2, H_2O and biomass (Vega et al., 1989).

Ethanol can be degraded in both aerobic and anaerobic environments, faster than other gasoline constituents and oxygenates (Chapelle, 1993). Only large concentrations (more than 100,000 g m^{-3}) of alcohols are not biodegradable due to their toxicity to most microorganisms (Brusseau, 1993; Hunt et al., 1997). Such high concentrations could be encountered near the sources of ethanol releases. The aerobic biodegradation of ethanol at temperatures between 50 and 60^{o}C was evaluated, and the results demonstrated that mixtures of carbonaceous compounds of the types found as pollutants in petrochemical industry wastewaters can be effectively biooxidized at elevated temperatures (50-57^{o}C) during continuous operation at dilution rates < 0.2 h^{-1} (Hamer et al., 1989). *Acetobacter aceti* was used to metabolize ethanol (Hill and Daugulis, 1999; Wei et al., 1999). A defined medium with no vitamin or amino acid supplements has been used such that ethanol was the sole carbon substrate. Hill and Daugulis (1999) reported that growth on ethanol at a few thousand milligrams per litre (below the known inhibitory level) resulted in a maximum specific growth rate of 0.16 h^{-1} with a 95% yield of acetic acid, followed immediately by acetic acid consumption at a growth rate of 0.037 h^{-1}. Wei et al. (1999) also reported the growth rate of 0.05 h^{-1}on ethanol, and a removal efficiency of 99.7% in a bioscrubber at the ethanol loading rate of 220 g $m^{-3}h^{-1}$. Due to its high acetic acid production and low growth rate, *Acetobacter aceti* was not chosen as the microorganism in this study.

The simultaneous degradation of toluene and ethanol by *Pseudomonas* GJ 40 and *P.* GJ31 was conducted by Corseuil *et al*. (1998) in a continuous-flow bioreactor that operated as a chemostat (working volume 0.75 L; minimal salts medium pH 7.0; 30^{o}C; dilution rate 0.1 to 0.5 h^{-1}; air flow rate 1.5 L/h). Both *Pseudomonas* strains were capable of fast growth on ethanol. A pure culture of *Pseudomonas putida F1* (*PpF1*) was reported to simultaneously degrade ethanol and toluene with no apparent inhibitory effect up to 500 g ethanol m^{-3} (Hunt et al., 1997). The results demonstrated that the growth of *PpF1* on ethanol was faster than other substrates, including toluene.

Microorganisms that grow on toluene have been isolated (Alvarez and Vogel , 1991; Lodaya et al., 1991; Vipulanandan et al., 2000). The degradation of toluene has also been investigated using activated sludge (Goldsmith and Balderson, 1988; Alvarez and Vogel, 1991; Lodaya et al., 1991; Falatko and Novak, 1992; Goudar et al. 1999; Vipulanandan et al., 2000; Nakao et al., 2000). Vipulanandan et al.(2000) conducted the biodegradation of liquid toluene in continuously stirred batch reactors using activated sludge (mixed culture) from a wastewater treatment plant. Toluene concentrations up to 100 g m^{-3} were degraded with a lag time of 19 days and a total time of 28 days for complete biodegradation of toluene. They also found that the lag time for toluene degradation increased with initial toluene concentration.

Vecht et al. (1988) investigated the growth of *Pseudomonas putida* (ATCC 33015) in batch and continuous cultures on toluene as sole carbon and energy sources. Toluene vapour was introduced into the culture through the air stream. A mass balance was performed on the chemostat culture. About 60% of the toluene was recovered in the outlet air stream. Up to 70% of the toluene which entered into the solution was

converted into biomass, and the balance was converted into carbon dioxide and unidentified byproducts. The highest specific growth rate associated with toluene, 0.13 h^{-1},was achieved in a chemostat culture.

Typically, air streams that are well suited for bioremediation have a low VOC concentration (<1000 ppmv), a low particulate concentration to prevent plugging of the reactor, and a temperature suitable for bioremediation (10-45^{o}C). Pre-treatment to meet these conditions may be necessary for some airstreams.

2.2.5 Comparison of VOC Treatment Techniques

Oxidation rates of VOCs from industrial waste air vary from a fraction of a second in incinerators to seconds in chemical scrubbers to minutes or days in biofilters. The faster reactions require fuel, chemicals and maintenance. The slower, inexpensive microbial reactions in biofilters require large reactor volumes and bed areas.

Incineration at high temperatures occurs very quickly and is more than 99% effective (Bohn, 1992). The costs associated with this method are very high due to the large quantities of fuel required. Production of NO_x and SO_x can occur with incineration, creating further environmental problems. The incineration temperature can be lowered with catalysts resulting in lower fuel consumption, but results in higher maintenance costs.

For pollutants with high solubility in water, liquid treatment methods are often used where waste gas is contacted with water. A combination of water washing systems with liquid phase treatment is an important current research topic. Water washing and activated carbon adsorption transfer the VOCs to water or carbon, and the VOCs must be consumed later. Water washing is rarely effective for VOC treatment because it

removes only water-soluble gases. Water usage is high and average costs are considerable.

Biofiltration requires a longer retention time, so the volume of soil or compost bed must be relatively large compared to the space required for other methods, thus the installation and maintenance costs will be higher. Thermal oxidizers are commonly used to destroy the concentrated VOCs. The operating cost benefits of using a concentrator in conjunction with a small oxidizer make this a very attractive option (Hussey and Gupta, 1998).

Biological treatments of waste gases have the specific advantage of microbial metabolism. Whereas other conventional methods may not eliminate the pollutants, microbes convert the pollutant into their metabolic products. These processes generally do not lead to further environmental problems and the cost is low because they are carried out at normal temperatures and pressure (Ottengraf, 1986). These processes are cheap, reliable and do not usually require complex facilities. Bohn (1992) reported the cost of a typical biological air treatment system as $8 per million cubic feet of air treated compared to other costs shown in Table 2.3.

Among all the technologies of waste gas treatment, the main advantages of biological treatment are high removal efficiencies, low installation, operation and maintenance costs, and high reliability. Most importantly, biological treatments can convert many organic compounds into oxidation products such as biomass, water and carbon dioxide.

Table 2.3. Overall costs of air-pollution control by several methods

Treatment Method	Total cost (in 1991 U.S.dollars) per 10^6 ft^3 of air
Incineration	$130
Chlorine Scrubbing	$60
Activated carbon adsorption (with regeneration)	$20
Typical biological air treatment (biofiltration)	$8

Source: Adapted from Bohn (1992).

Like all treatment technologies, certain limitations exist for biofilters. Biofilters cannot treat high concentrations of toluene vapor in the air stream due to its high toxicity. In addition, biofilters may clog due to the formation of excessive amounts of biomass normally found at the entrance zone of the biofilter. On the other hand, in a well-mixed bioreactor, microbial cells are freely suspended in an aqueous media and the risk of clogging is negligible. Furthermore, well-mixed vessels are used abundantly in industry due to the homogeneous nature of the mixture and excellent mass transfer characteristics. In order for microbial cells to capture waste chemicals from a polluted air stream, those chemicals must first be transferred to the aqueous phase where the cells can grow and multiply. Thus, the mass transfer of the pollutants into the liquid phase surrounding the microbes is a critical feature of any biological waste gas treatment process.

2.2.6 Pseudomonas

It is well known that bacteria belonging to the genus *Pseudomonas* utilize a large number and variety of compounds as carbon and energy sources (Stanier et al., 1966). While toluene is not readily degraded by all microorganisms, several strains of *Pseudomonas putida* have demonstrated a toluene-degrading ability (Gibson et al., 1970; Vecht et al., 1988; Keuning and Jager, 1994; Romine and Brockman, 1996; Reardon et al., 1994, 2000; Kim and Jaffe, 2000; Brown *et al*., 2000). Reardon et al.(1994) measured the kinetics of toluene biodegradation by *Pseudomonas putida* F1 (*PpF1*) and the maximum growth rate of *PpF1* on toluene was found to be 0.86 h^{-1}. Reardon et al. (2000) also reported the kinetics of *PpF1* growing on mixtures of benzene, toluene, and phenol. Toluene significantly inhibited the biodegradation rate of benzene and phenol. Brown et al. (2000) have reported toluene removal from aqueous streams in a cyclical bioreactor using *Pseudomonas putida* (ATCC 23973), which is the same strain used in this study. Liquid toluene was added to the self-cycling fermentor by diffusion across a silicone membrane.

2.3 Modeling of Microbial Growth

2.3.1 Monod Model

Microbial growth is the result of both replication and change in cell size. In a suitable nutrient medium, organisms extract nutrients from the medium and convert them into biological compounds. A typical bacterial growth curve in a batch culture appears in the following order: lag phase, exponential phase, stationary phase, and death phase (Shuler and Kargi, 2002). The lag phase starts with inoculation of the

microorganism and involves adaptation to the new environment. In this phase, the cell number does not increase significantly, but the cells may grow in size. The length of this phase depends on the history and amount of the inoculum utilized. In the exponential growth phase (i.e., logarithmic phase), the cells have adjusted to the new environment and the rate of biomass formation is:

$$\frac{dX}{dt} = \mu \cdot X \qquad (2\text{-}1)$$

where μ is the specific growth rate, and X is the biomass concentration.

The growth of the cell eventually reaches a phase during which there is no further change in bacterial cell numbers, which is called the stationary growth phase. A bacterial population may reach stationary growth conditions when a required nutrient is exhausted, when inhibitory end products accumulate, or when environmental conditions change. Eventually, with nutrient depletion or toxic product accumulation, the cells start to be destroyed by enzymes, i.e. the death phase begins. The number of viable bacteria cells begins to decline.

When sufficient nutrients are present, the availability of organic substrate (carbon source) is normally the rate-limiting factor. Under these conditions, the well-known, unstructured, Monod equation is most often used to describe the relationship between the substrate concentration and the specific growth rate:

$$\mu = \mu_{\max} \frac{S}{K_s + S} \qquad (2\text{-}2)$$

where μ_{max} is the maximum growth rate when $S >> K_s$; K_s, the saturation constant, is the substrate concentration at which μ is a half of its maximum value.

2.3.2 Growth Models with Inhibition

At high concentrations of all substrates, growth becomes inhibited and growth rate depends on inhibitor concentrations. The inhibition pattern of microbial growth is analogous to enzyme inhibition. If a single enzyme-catalyzed reaction is the rate-limiting step in microbial growth, then kinetic constants are biologically meaningful. Often, the underlying mechanism is complicated and kinetic constants of unstructured growth models do not then have biological meanings. The effects of increasing the inhibitor concentrations are similar to the effects of enzyme reaction inhibitors. Thus, the expressions for enzyme inhibition can be applied to model cell growth inhibition. Some enzyme inhibition models are shown below (Shuler and Kargi, 2002):

Non-competitive substrate inhibition (Haldane inhibition model):

$$\mu = \frac{\mu_{\max}}{(1+\frac{K_s}{S})(1+\frac{S}{K_i})} \tag{2-3}$$

if $K_i >> K_s$, then

$$\mu = \frac{\mu_{\max} S}{(1+S+\frac{S^2}{K_i})} \tag{2-4}$$

Competitive substrate inhibition:

$$\mu = \frac{\mu_{\max} S}{K_s(1+\frac{S}{K_i})+S} \tag{2-5}$$

where K_i is the inhibition constant.

Luong (1987) proposed an empirical relationship to correlate substrate inhibition:

$$\mu = \frac{\mu_m S}{K_s + S}(1-\frac{S}{S_m})^n \tag{2-6}$$

where S_m is the maximum substrate concentration above which growth is completely inhibited.

The products of the cellular metabolism may also inhibit growth resulting in a reduction of growth rate. The mechanism for inhibition of growth by products of metabolism is not well understood and may result from several effects (Blanch and Clark, 1997). Different models have been developed to represent experimental data (Bailey and Ollis, 1986, Shuler and Kargi, 1992, Blanch and Clark, 1997):

$$\mu = \mu_{\max}(\frac{S}{K_s + S})(1 - \frac{P}{P_m})^n \quad (2\text{-}7)$$

$$\mu = \mu_{\max}(\frac{S}{K_s + S})[1 - (\frac{P}{P_m})^n] \quad (2\text{-}8)$$

where P is the product concentration; P_m is the maximum product concentration at which the growth of the cell is completely inhibited; n is a constant that needs to be empirically determined (Levenspiel, 1980; Luong, 1987).

2.3.3 Growth on Multiple Substrates

All the unstructured models assume that there is only one limiting substrate, but often more than one substrate influences the specific growth rate. In these situations complex interactions can occur, which are difficult to model with unstructured models unless additional adjustable parameters are admitted (Nielsen et al., 2003).

For a multisubstrate biodegradation model, Guha et al. (1999) reported that biomass growth is due to the utilization of all the compounds according to:

$$\mu = \sum_{i=1}^{n} \mu_i \quad (2\text{-}9)$$

where μ is the total specific growth rate (h^{-1}), and the summation is taken over the n substrates. The specific growth rate on each substrate, μ_i, is related to the concentration of all the substrates through a multi-substrate Monod growth relationship by assuming that all components in the mixture share a common rate-limiting enzyme reaction pathway. The resulting equation is:

$$\mu_i = \frac{\mu_{\max,i} S_i}{K_{si} + \sum_j^n \frac{K_{si}}{K_{sj}} S_i} \tag{2-10}$$

Bailey and Ollis (1986) proposed the following two compound inhibition equation:

$$\mu = \frac{\mu_{\max} S}{S + K_s (1 + I / K_i)} \tag{2-11}$$

where I = liquid concentration of a competing compound (mg/L) and K_i is an inhibition constant (mg/L). This equation was applied to model biodegradation of mixtures with presence of toluene by a group of researchers (Machado and Grady Jr., 1989; Chang et al., 1993; Criddle, 1993; Bielefeld and Stensel, 1999).

2.3.4 Metabolic Modeling

The metabolic reactions for the aerobic metabolism of substrate can be separated into two groups: the energy consuming reactions and the energy generating reactions. The energy consuming reactions are due to the production of biomass while the energy producing reactions include substrate catabolism and oxidative phosphorylation. The system being considered is assumed to be of constant volume and it contains a certain number of moles of biomass. The stoichiometry of the energy-generating and energy-

demanding processes has to be first established according to the metabolic pathways of the substrate (see Appendix A for metabolic pathways of ethanol and toluene). Thus, the balance equations for each of the compounds present in the system has to be formulated by using the following equation:

$$\vec{r} = \alpha \cdot \vec{\nu} + \vec{\phi} \qquad (2\text{-}12)$$

Where $\vec{\nu}$ is the vector of the reaction rates (ν_1, ν_2, ν_3); α is a stoichiometry matrix of the three reactions; $\vec{\phi}$ is the vector of flow into the system (In-Out), and $\vec{r}$ is the vector of the overall conversion rates.

Metabolic modeling is based on fundamental biochemical principles, thus it is expected that process stoichiometry calculations using such fundamental principles can be applied to a wider set of operating conditions compared to "empirically" derived models. This approach of metabolic modeling has been successfully used in the modeling of different processes by researchers (Roels, 1980, 1983; Smolders et al., 1994; Wang et al., 2002).

2.4 Ideal Reactors

Ideal reactors are developed mainly on the assumption of an idealised flow pattern in the reactors. The flow pattern in the reactors are assumed to be either completely mixed and homogeneous (mixed reactors) or uniformly segregated and plug flow. Four of the most important models along with their mathematical performance equations are summarized below. The performance equations are derived for constant temperature and constant liquid density reactions that are common in many biochemical processes.

2.4.1 Batch Reactor

In a batch reactor, the reactants are initially added into the reactor and left to react for a certain period of time. The reactant can be either a pure chemical reaction or a biochemical one. The content of the reactor is kept mixed in order to have a uniform composition throughout the reactor. The process is unsteady state (changes with time) and the reactor content is discharged at the end of the process. The performance equation of a batch reactor can be derived from the material balance of substrate as (Levenspiel, 1972):

$$\frac{dX}{dt} = r_x \tag{2-13}$$

$$\frac{dS}{dt} = -r_s \tag{2-14}$$

in which t is the time, X is the biomass mass concentrations and r_x is the rate of biomass formation, S is the substrate mass concentrations and r_s is the rate of substrate consumption. Solving Equations (2-13) and (2-14) will give the concentrations of biomass (X) and substrate (S) at any desired time. If the temperature of the reactor changes, an energy balance will also be necessary for solving the performance equation of the batch reactor.

2.4.2 Fedbatch Reactors

In a fedbatch (semi-batch) reactor, an initial amount of reactant and/or medium is charged into the reactor (initial charge) which is also kept well mixed. More reactants or medium are added to the reactor as the reaction proceeds. The process is unsteady state and the contents of the reactor need to be discharged after a certain period of time. Fedbatch processes are often used in fermentation to minimize substrate inhibition, or to

avoid oxygen insufficiency. The performance equation of a fedbatch bioreactor can be easily derived from the material balance equations for the biomass and substrate as follows:

$$\frac{dX}{dt} = r_x - \frac{FX}{V} \tag{2-15}$$

$$\frac{dS}{dt} = \frac{F}{V}(S_f - S) - r_s \tag{2-16}$$

where F is the flow rate of the fresh media, S_f is the concentration of substrate in the feed, and V is the volume of fluid in the reactor. The volume of fluid in the reactor changes with the addition of liquid feed, F.

2.4.3 Continuous Stirred Tank Reactor (CSTR)

The continuous stirred tank reactor (CSTR) is an ideal steady state reactor. The reactants are charged continuously into the stirred tank and the product is continuously discharged from the reactor. Thorough mixing keeps a uniform concentration throughout the reactor. The performance equation of a CSTR for the substrate can be derived from the steady state version of the material balance equation as:

$$r_s = \frac{F}{V}(S_f - S) \tag{2-17}$$

in which S is the substrate concentration in the output stream and S_f is the substrate concentration in the feed; F is the flow rate of the fresh media which is the same as the output liquid flow rate to keep the liquid volume in the reactor, V, constant.

2.4.4 Plug Flow Reactor

The other ideal steady state reactor is called a plug flow reactor. The reactants are charged continuously into one end of a pipe and the product is continuously

discharged from the other end. The flow pattern in the ideal reactor is plug or piston flow with no back mixing. The performance equation of a single plug flow reactor for the substrate can be obtained from the material balance as:

$$\frac{V}{F} = -\int_{S_f}^{S} \frac{dS}{r_s} \qquad (2\text{-}18)$$

2.4.5 Reactors for Biochemical Processes (Bioreactors)

Many factors such as cost of equipment, scale of production, stability and safety, that can affect the choice of an optimum reactor. The most important single factor is the reaction kinetics. A poor choice of reactor type can increase the cost of reactor construction and operation as much as two orders of magnitude. For example, the volume of a CSTR reactor needed for 99% conversion for a first order reaction (or even zero and second order) is as much as 100 times more than a plug flow reactor (Levenspiel, 1972). However, the nature of many biochemical reactions resembles autocatalytic reactions which strongly favours the use of CSTRs instead of plug flow reactors (Levenspiel, 1972).

CHAPTER THREE – EXPERIMENTAL STUDIES

This chapter describes the materials and methods used in the experimental studies of this research. It covers the microorganisms, the growth nutrients and culture, and the organic chemicals used in this project. The analytical methods and the experimental procedures applied in this study will also be discussed in this section.

3.1 Microorganisms and Chemicals

3.1.1 Microorganism and Medium

Strains of *Pseudomonas* are well known for their ability to degrade aromatic hydrocarbons (Stanier et al., 1966; Reardon et al., 1994, 2000; Brown et al., 2000). *Pseudomonas putida* (ATCC 23973), which was used in this study, was kindly provided by Dr. W. A. Brown at McGill University (Montreal, Canada). Pictures of these bacteria were taken using a 505 Philips (Holland) scanning electron microscope (SEM) in the Department of Biology, University of Saskatchewan. The preparation of slides for SEM were based on the procedure reported by Klainer and Betsch (1970) and Hill (1974). The unicellular rod shape of *P. putida* is easily observed with the SEM pictures (See Figures B-1 and B-2).

The nutrient medium contained (grams in 1 litre of deionized, reverse osmosis water): KH_2PO_4, 1.5; K_2HPO_4, 5.0; $(NH_4)_2SO_4$, 2.0; NaCl, 5.0; $CaCl_2$, 0.06; $MgSO_4 \cdot 7H_2O$, 0.2; 0.1mL trace element solution (Dr. Brown, McGill University). The trace

element solution consisted of (grams in 100 mL water): $Na_2MoO_4 \cdot 2H_2O$, 0.5; $MnSO_4$, 0.5; $CuSO_4$, 0.5; $FeCl_3$, 0.5. The medium was prepared by mixing the appropriate inorganic chemicals with one liter of distilled water that resulted in a buffered medium with a starting pH of 6.7-6.9. The media, culture flasks and bioreactor were sterilized at 121^{o} C for at least 30 minutes and then the organic compounds were added in a biofilter cabinet to reach the desired initial concentrations.

3.1.2 Organic Chemicals

For all bioremediation experiments, only benzyl alcohol, ethanol and/or toluene were used as carbon sources. Ethanol (100%, Commercial Alcohols Inc., Brampton, Canada), toluene (99.5%, BDH, Toronto, Canada) and benzyl alcohol (99%, Aldrich Chemical Co., Milwaukee, USA) were used as the growth carbon sources. 1-butanol (99.4%, BDH, Inc., Toronto, Canada) was used as internal standard to prepare liquid samples for gas chromatography (GC) analyses. Antifoam "B" (BDH, Toronto, Canada) was added to the bioreactor at a concentration of approximately 1.5 g/L to prevent foam formation. Experimental observations in this study confirmed that the cells do not grow on Antifoam "B". The effect of Antifoam "B" on mass transfer was not studied.

3.2 Growth of Microorganisms

3.2.1 Shake Flask

The microorganisms used in the experiments were *Pseudomonas putida* (ATCC 23973). To propagate bacteria from the agar plates, a 250-mL Erlenmeyer flask with 100-150 mL sterile medium containing a certain amount of substrate (ethanol or benzyl

alcohol) was inoculated with two loops[1] of bacteria from a previously cultivated agar plate. The shake flask was placed on a rotary shaker at 200 rpm and maintained at room temperature (normally 25-30^{o}C) until the bacteria achieved their exponential phase of growth (12 to 24 hours depending on the age of the stored bacteria). This broth served as the inoculum source for all bioremediation experimental runs containing substrate, and was also used to propagate the bacteria on fresh agar plates.

3.2.2 Agar Plates

The agar plates were made by adding 3 grams of Bacto-agar to 100 mL of distilled water. These ingredients were stirred and heated to a temperature just below the mixtures' boiling point or until the solution became clear, then sterilized for 30 minutes at 121^{o}C. Under the biofilter cabinet hood, benzyl alcohol was added into the warm agar solution, and this agar solution with 0.1%(w/v) benzyl alcohol was poured into Petri dishes to make six agar plates. To propagate bacteria on fresh agar, several loops of broth solution from the shake flask (see the above section) were aseptically removed and streaked on agar plates. The sealed agar plates were then placed in the CO_2 incubator at 30^{o}C for 24 hours. These agar plates were renewed every two months to ensure that a fresh source of microbes was always available.

3.2.3 Inoculum

Initially 250 mL of medium is sterilized in a shake flask and then a certain amount of benzyl alcohol or ethanol was added into the flask under the biofilter cabinet. Two loops of bacteria taken from the agar plate were then added into the flask. Finally the flask was put on the shaker and agitated at 180 rpm at room temperature (25^{o}C) for a period of time that is within the log phase (predetermined to be 10-16 hours for

[1] A circular metal ring shaped instrument used for scooping bacteria from an agar plate.

growth on ethanol, 20-48 hours for growth on benzyl alcohol) to harvest the cells for bioreaction studies. Inoculation and transfer cultures are occasionally checked for contamination by Gram staining. Contamination was never observed.

3.3 Analytical Methods

3.3.1 Measurement of Biomass Concentration

The biomass concentrations were measured as optical density at a wavelength of 620 nm (OD_{620}) using a spectrophotometer (Milton Roy, 1001 Plus). The spectrophotometer had been calibrated using known dry weights of *Pseudomonas putida* (ATCC 23973) suspended in culture media. The absorbance was related to dry weight using a pre-determined calibration curve (See Figure B-3 in Appendix B). The calibration curve was developed by using the dry weight method described below.

A high biomass concentration was achieved in a shake flask with 250-mL of media following the method in Section 3.2.3. 100 mL of this broth (broth a) was then transferred to centrifuge tubes and centrifuged at 9900 rpm for 15 minutes to allow the microorganisms to settle to the bottom of the tube. The supernatant was then decanted. A few drops of distilled water were used to rinse the tube wall, followed by mixing using a vortex mixer. The procedures of centrifuging, decanting and rinsing were repeated two times. Finally, this solution was transferred to pre-weighed aluminum dishes and placed into a vacuum oven that was operated at a temperature of 65^{o}C and a pressure of –22 in Hg (gauge pressure) for 24 hours. Before the dishes were weighed, these samples were put in a dessicator for 1 hour to bring the dishes to equilibrium with room temperature. The difference in weight between the dried dish with biomass and

the original dish was used to calculate the original broth biomass concentration (milligrams per liter of broth). Another 100 mL of the same broth (broth a) was subjected to a number of dilutions and analyzed for optical density. These dilutions provided a range of known concentrations with measured optical densities and were used to plot the dry-weight calibration curve for *Pseudomonas putida*. Samples with optical densities exceeding the range of the calibration curve were diluted until their optical densities fell within the calibrated range.

3.3.2 Analyses of Organic Chemicals

Prior to measuring the substrate concentrations, samples from bioremediation experiments were centrifuged at 2500 rpm for 5 min to let the bacteria settle to the bottom of the tube, then the supernatant was mixed with an equal volume of an aqueous solution of 1-butanol, the internal standard, to measure substrate concentrations in the liquid samples.

Ethanol, toluene and benzyl alcohol concentrations in the liquid were analyzed using a GC (HP 5890) equipped with a Flame Ionizing Detector (FID) and capillary column (PTE^{TM}5 Fused Silica Capillary Column, 30 m, 0.25 mm ID, Supelco, Inc., PA, USA). The temperatures of the injector and detector were 210 ºC and 250 ºC, respectively. The oven temperature was ramped from 45 ºC to 150 ºC at the rate of 25^{o}C/min. 1-Butanol was used as the internal standard for all liquid sample analyses. Ethanol, toluene and benzyl alcohol standards were prepared as aqueous solutions for the calibration of the GC analyses. The calibration curves are shown in the Appendix B (See Figures B-4 to B-6).

Gas phase samples of toluene were collected from glass samplers placed in the flow lines (see Figure 3-1). 0.1 mL samples were taken from these samplers using a one mL gas-tight syringe and then injected into the GC. Air phase calibration standards for toluene concentrations were prepared by adding an amount of liquid toluene in the range of 10 to 60 μL into 160 mL, sealed serum bottles containing 55 mL of water at 25 ºC. Using the known Henry's constant and volumes of the gas and water phases in the bottles, the toluene concentrations in the gas phase could be calculated (Gossett, 1987; Cesario *et al*., 1997). The calibration curve is given in Appendix B (See Figure B-7). Reproducibility studies using calibration standards demonstrated that GC measurements for both liquid and gas toluene concentrations were repeatable to ± 8 %. Gas phase concentrations of ethanol were determined by passing the gas stream through a known amount of water (500 mL) in a flask for a measured interval of time (1hr), and then the liquid samples were analyzed using the GC. Similar reproducibility of measurement was achieved as that for toluene samples.

3.3.3 GC-MS Analysis

To identify and determine the molecular weight of metabolite byproducts recovered in the bioremediation experiments, the liquid samples were filtered through a nylon membrane with 0.2 μm openings. The filtered samples were analyzed using a GC-MS (Model VG70VSE, VG Analytical) at the Department of Chemistry, University of Saskatchewan.

3.4 Experimental Procedures

Figure 3-1 is a schematic of the experimental apparatus used throughout this investigation. Air stripping and bioremediation experiments were all performed at 25 ºC in a 3 L, baffled New Brunswick Scientific Bioflow III well-mixed bioreactor at a working volume of 1.5 L. One six-blade Rushton impeller was positioned 3.5 cm from the bottom of the vessel. For biodegradation investigations, air was normally supplied through two, metered inlet streams. All air flowmeters were calibrated using a Wet Test flowmeter and the calibration curves are given in Appendix B (See Figure B-8). In order to obtain the desired gas inlet concentration of ethanol or toluene, one air stream passed through a bubbler filled with either ethanol or toluene which was maintained in a water bath at 21.0 ± 0.5 ºC; the other stream by-passed the bubbler. These two air streams were then mixed downstream of the bubbler and directly entered the bioreactor. In this way, the concentration of ethanol or toluene entering the bioreactor could be precisely controlled. In some runs, a third stream was employed which passed through a second bubbler. Thus, ethanol and toluene could be simultaneously added to the bioreactor. For continuous runs, fresh sterile nutrient media was pumped into the bioreactor and spent fermentation broth was removed at identical flowrates.

3.4.1 Mass Transfer

Mass transfer studies of toluene and ethanol from contaminated air streams to the liquid phase, along with oxygen mass transfer studies, were carried out using a standard stirred tank bioreactor (model GF0014, Chemap AG, Switzerland). The liquid volume used was 12 liters and the operating temperature was maintained at 25 ± 0.5^{o}C for all runs. The general specifications of the reactor are presented in Table C-1. The

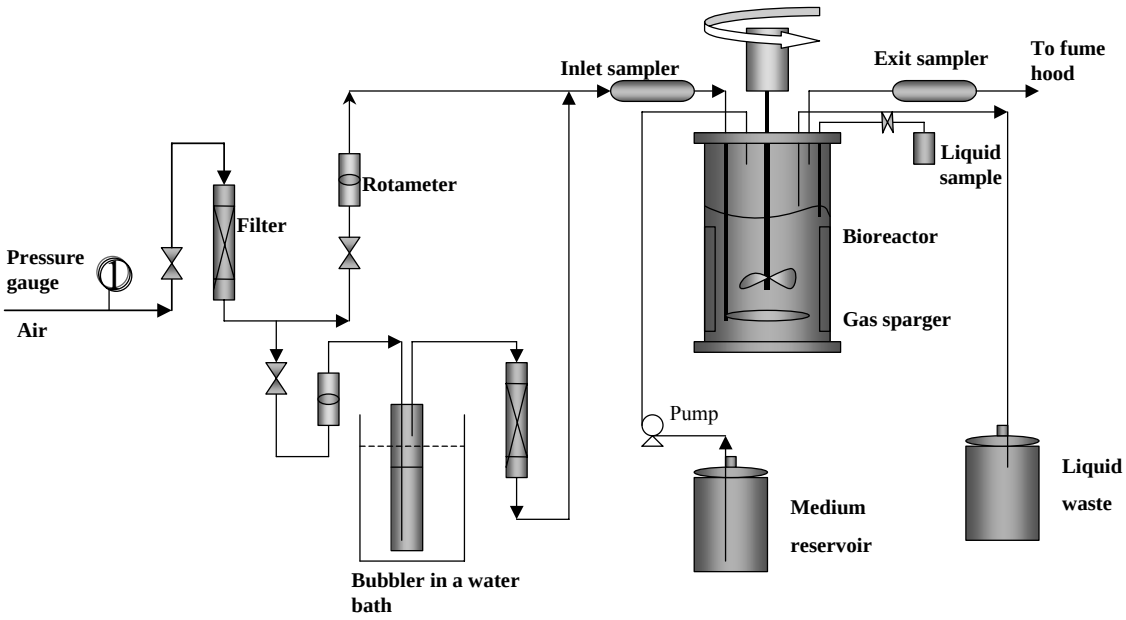

Figure 3-1 Schematic of the experimental apparatus

reactor consists of two turbine impellers, which were adjustable in height, and four evenly spaced baffles (size of 32.5 x 4.5 cm) which ensured that the fluid was thoroughly mixed. The impeller shaft was driven by a variable speed electric motor. Gas entered the reactor through a sparger (with 12, 2 mm diameter holes) located at the bottom of the tank, and its flowrate was measured using a mass flowmeter (Model 8891, Sierra Instruments, Inc.).

3.4.1.1 Mass Transfer of Ethanol and Toluene

For bioremediation to occur, VOCs need to first be absorbed from the contaminated air into the fermentation media. The polluted air stream was obtained by passing air at certain flow rate through a bubbler filled with either ethanol or toluene which was maintained in a water bath at 21.0 ± 0.5 ºC. In initial studies, this air steam, containing known concentrations of ethanol or toluene, was then bubbled through sterile media in the bioreactor at known gas (air-ethanol or air-toluene) flow rates and impeller speeds. The build-up of ethanol or toluene in the aqueous media was measured by GC analyses and samples were taken of the effluent air stream to confirm species mass balances. The collected data were used to determine mass transfer coefficients for absorption.

3.4.1.2 Effect of Ethanol Addition on Oxygen Mass Transfer

Oxygen transfer from air to an aqueous phase is frequently the rate-limiting step in aerobic fermentations due to the low solubility of oxygen in water. The effect of ethanol addition on oxygen mass transfer was conducted using the same reactor as mentioned above. The first step in conducting the measurements of oxygen transfer to the aqueous phase in the bioreactor involved deaerating the liquid using nitrogen gas.

Once the oxygen meter indicated a stable concentration near zero, the flow of nitrogen gas was stopped and air was introduced at a constant flow rate of 3.5 L/min (0.3 vvm). The concentration of oxygen in the aqueous phase was recorded every 10 seconds until the oxygen concentration was constant. Oxygen concentrations in the liquid were measured using an oxygen probe (type 50180, manufactured by Hach Company). The probe was connected to a Hach oxygen meter (model # 50175). The experiments were carried out at different impeller speeds (135, 300, 450 and 600 rpm) and at different ethanol concentrations (0, 1, 3, and 8 g/L ethanol in distilled water).

3.4.2 Air Stripping

Prior to conducting any bioremediation runs in a bioreactor, it was necessary to determine the quantity of each substrate that would be stripped by air. All organic compounds possess a certain affinity to vaporize from either the solid or liquid state. If the substrate is highly volatile, the amount of substrate available in the liquid phase for growth is significantly reduced through air stripping.

Air stripping studies for ethanol and toluene were carried out at a temperature of 25.0 °C and an impeller rotational velocity of 450 rpm using the Bioflow III bioreactor filled with 1.5L of solution at a preset initial concentration. In this case, known quantities of ethanol or toluene were initially placed in the aqueous media and the rate at which the chemical was removed by uncontaminated air bubbled through the bioreactor was determined. Samples of the liquid solution were taken at a certain time interval, and samples of the effluent air were taken to complete the species mass balance. The disappearance rate was used to evaluate the air stripping parameters according to Singh and Hill (1987).

3.4.3 Batch Growth

The batch growth experiments were carried out to study the growth rates of *P. putida* (ATCC 23973) on different substrates, however toluene was stripped too quickly from the bioreactor to carry out batch growth experiments (Brown et al., 2000). Therefore, bioremediation kinetics on ethanol or benzyl alcohol was determined from batch growth experiments.

A volume of 1.5 L of media was added to the bioreactor. The reactor, complete with the nutrient media, was sterilized at a temperature of 121^{o}C for 45 minutes. The inoculum was prepared in shaking flasks using the same chemical as the growth substrate (see Section 3.2.3 for preparation procedure). A certain amount of the selected substrate was added into the bioreactor to reach the desired initial concentration then 75-150 mL of inoculum was aseptically transferred from the shake flask into the bioreactor.

The media in the bioreactor thus contained either ethanol or benzyl alcohol at known initial concentrations. The temperature was controlled at 25.0 °C. In order to maintain efficient mixing in the reactor, and to gain sufficient oxygen supply from the air stream, an agitation rate of 450 rpm and an air flowrate of 0.4 L/min was set for all experiments. These operating conditions were based on the results from air stripping and mass transfer experiments. Samples of approximately 10 mL were taken at specific time intervals through the liquid sample port. Three to four mililitres of these samples were immediately analyzed for biomass concentration, and a 5 mL sample was

centrifuged and the supernatant was then analyzed for substrate concentration by GC analyses. Samples were always collected and analyzed in duplicate.

3.4.4 Continuous Bioremediation in a CSTR

In these experiments, sterilized nutrient media was continuously fed to the bioreactor and spent fermentation broth was continuously removed at dilution rates of 0.01 to 0.1 h^{-1}. The organic food source was provided from the contaminated air stream. Contaminated air, containing ethanol, toluene or mixtures of ethanol and toluene at various concentrations, was bubbled into the bioreactor using varying flow rates while the agitation speed and temperature were held at 450 rpm and 25.0 °C.

CHAPTER FOUR- EXPERIMENTAL RESULTS AND DISCUSSION

Introduction

This chapter will present and discuss the experimental results in the order of mass transfer and air stripping results, followed by the bioremediation results. Since we are dealing with air pollutants using a well-mixed bioreactor with the microorganisms in the liquid phase, the substrates (ethanol and toluene in this study) have to transfer from the gas phase into the liquid phase to be bioremediated. Moreover, due to high volatility of the VOCs, we also need to know air-stripping effects in the process. Therefore, before bioremediation experiments take place, experiments of mass transfer and air stripping were carried out.

4.1 Mass Transfer

4.1.1 Mass Transfer of Ethanol and Toluene

For toluene, mass transfer kinetics can be described by Equation (4-1) (Lyman *et al*., 1982):

$$\frac{dS_t}{dt} = k_L a \times (S_t^* - S_t) \qquad (4\text{-}1)$$

where $k_L a$ *is* the volumetric mass transfer coefficient for toluene, S_t^* is the liquid equilibrium concentration ($S_t^* = \frac{C_g}{H}$, i.e., the maximum solubility in water at experimental conditions, 530 mg/L, from Lyman *et al*., 1982), S_t is the liquid concentration of toluene at any particular time, t. The integration of Equation (4-1) gives:

$$\ln[\frac{(S_t^* - S_0)}{(S_t^* - S_t)}] = k_l a \cdot t \qquad (4\text{-}2)$$

Once the liquid toluene concentrations with respect to time have been measured, the volumetric mass transfer coefficient, $k_L a$, can then be determined by plotting $\ln[\frac{(S_t^* - S_0)}{(S_t^* - S_t)}]$ versus time (*t*). The slope of the straight line is the volumetric mass transfer coefficient, $k_L a$. At an air flow rate of 2.0 L/min and toluene inlet concentration of 105 mg/L, the $k_L a$ values for toluene (See Figure 4-1) were found to be 8.3×10^{-4}, 8.8×10^{-4}, and 1.0×10^{-3} s^{-1} at agitation speeds of 300, 450 and 600 RPM, respectively.

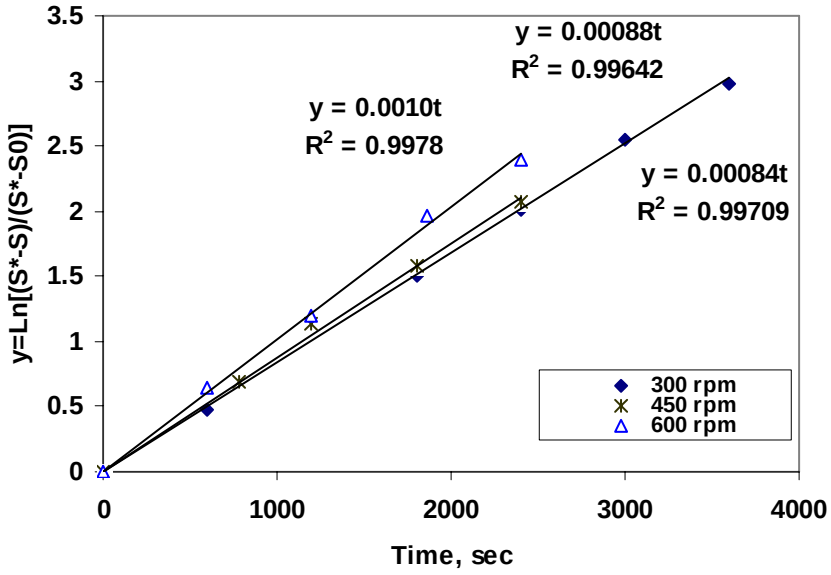

Figure 4-1 Determination of toluene mass transfer coefficients

Ethanol mass transfer results demonstrated that at inlet ethanol concentrations of 80.0 to 92.0 mg/L, air flow rates up to 3.8 L/min and mixing speeds of 135 to 600 RPM, ethanol was completely removed from the air streams by the aqueous phase in the reactor. Ethanol liquid concentrations can then be calculated from the material balance:

$$\frac{dS_e}{dt} = \frac{Q(C_{g,in} - C_{g,out})}{V} \qquad (4\text{-}3)$$

where S_e is ethanol concentration in the liquid phase (g/L), t is time in minutes, V is the working volume of the reactor (L), Q is the air flow rate (L/min), and $C_{g,in}$ (g/Lair) and $C_{g,out}$ (g/Lair) are the ethanol concentrations in the inlet and outlet air streams, respectively.

Figure 4-2a shows ethanol liquid concentrations with respect to time at an air flow rate of 2.0 L/min and 450 rpm. Figure 4-2 b shows ethanol mass transfer results at an air flow rate of 3.8 L/min and 300 rpm. The inlet gas concentration can be obtained from the slope of the straight line, i.e, $C_{g,in} = slope * \frac{V}{Q}$, since the outlet gas concentration (C_{gout}) is negligible (less than the detectable limit of 0.5 mg/Lair) compared to the gas inlet concentrations of 80.0 - 92.0 mg/L for the cases tested in this study. The total amount of ethanol added into the gas stream was measured to verify the calculated results of ethanol concentrations in gas and liquid phases, and an error of less than ±5.0% (error = (ethanol mass measured-calculated)/measured mass*100%) was obtained for ethanol mass transfer experiments.

Results from the ethanol mass transfer study indicated that ethanol liquid concentrations are limited only by the amount of ethanol introduced from the inlet air stream. Therefore, ethanol mass transfer will not be the rate-limiting step in bioremediation of ethanol from the contaminated air stream.

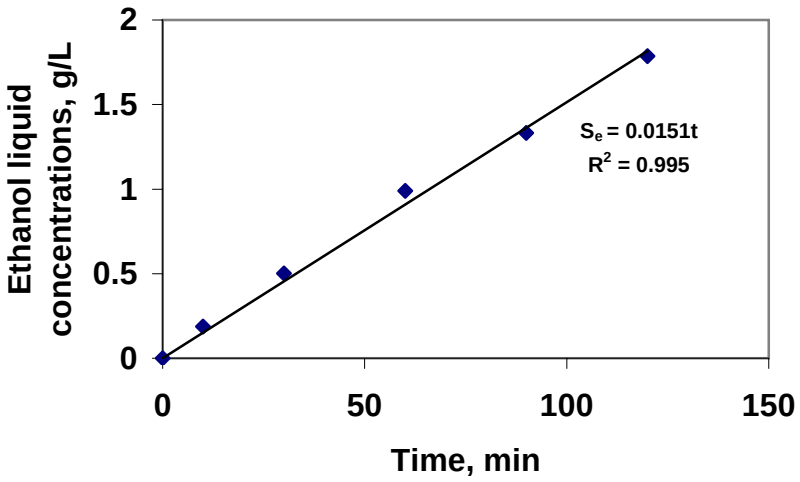

Figure 4-2a Ethanol mass transfer results at air flow rate of 2.0 L/min and 450 rpm

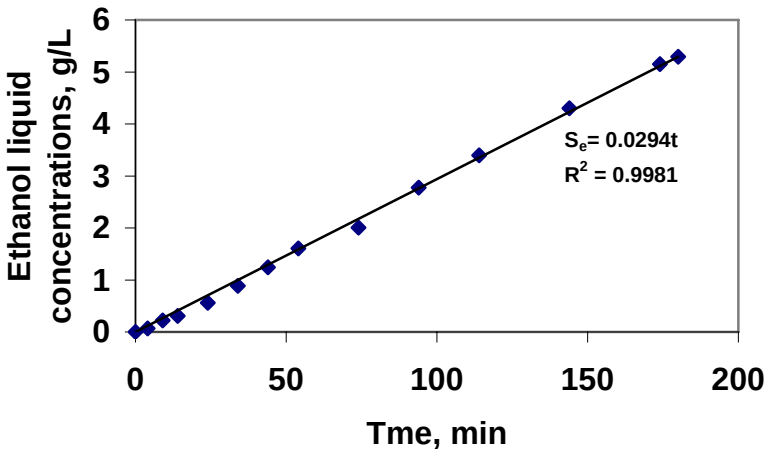

Figure 4-2b. Ethanol mass transfer results at air flow rate of 3.8 L/min and 300 rpm

4.1.2 Oxygen Mass Transfer

Mixing and ethanol addition effects on oxygen mass transfer from air to the aqueous phase were studied using a standard stirred tank bioreactor (as described in Section 3.4.1; See Table C-1 for specifications). The overall volumetric oxygen transfer

coefficient (k_La) in the well-mixed bioreactor was determined for different conditions by obtaining the coefficients associated with the best-fit (using Solver in Excel for non-linear, least square regression) of the dynamic oxygen concentration data using the following equation (Merchuk *et al.*, 1990):

$$C_t = C_{o_2}^* - \frac{(C_{o_2}^* - C_0)(e^{-tk_La} - t_e * k_L a * e^{-t/t_e})}{(1 - t_e * k_L a)} \quad (4\text{-}4)$$

where $C_{o_2}^*$ is the equilibrium (maximum) oxygen concentration in the solution (mg/L), C_t is oxygen concentration in the solution at time t (mg/L), C_0 is initial oxygen concentration in the solution at t = 0 (mg/L), t is time (s), and t_e is response time for the probe (s).

In order to study the influence of ethanol on k_La, four different concentrations were used: 0, 1, 3 and 8 g/L. Also, four different impeller speeds (135, 300, 450 and 600 rpm) were studied for their effects on the oxygen mass transfer coefficient. The best fitting mass transfer coefficients obtained with different impeller speeds and ethanol concentrations are shown in Figure 4-3. The overall oxygen mass transfer coefficient increases from 0.0020 to 0.0025 s^{-1} and from 0.0095 to 0.027 s^{-1} with increasing ethanol concentration from 0 to 1 g/L at 135 and 300 rpm, respectively, but remains at the same level with further increases of ethanol concentration. When the ethanol concentration was increased from 0 to 8 g/L, k_La increased from 0.015 to 0.049 and from 0.017 to 0.076 s^{-1} when impeller speeds of 450 and 600 rpm, respectively, were applied. This demonstrates that these low ethanol concentrations can increase the mass transfer coefficients by as much as a factor of four. This is a considerable improvement

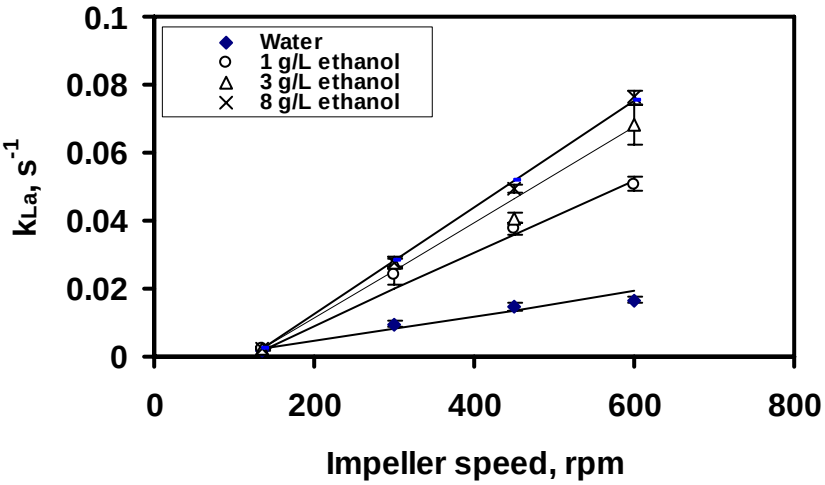

Figure 4-3. Effects of ethanol concentration and impeller speed on oxygen mass transfer coefficients (error bars are standard deviations)

compared to increases of 2.4 times observed by Benedek and Heideger (1971) using 11.7 g/L of sodium chloride. Voigt and Schugerl (1979) reported that k_La increased by a factor of three with ethanol addition in a bubble column.

The overall oxygen transfer coefficient increases with increasing impeller speed over the range of 135 to 600 rpm as shown in Figure 4-3. This trend agrees with k_La measurements in stirred tanks reported by others (Benedek and Heideger, 1971; Robinson and Wilke, 1973, 1974; Hassan and Robinson, 1980).

The gas holdup was also measured for each operating condition. After the bioreactor was filled initially with the ethanol solution, the gas volume was determined by measuring the amount of liquid that overflowed with the introduction of air at a constant flow rate of 3.5 L/min at each impeller speed. The gas holdup was then

calculated by dividing the gas volume by total bioreactor volume, and the results are given in Table 4-1. The experimental data show that the gas holdup increases with increasing ethanol concentration and with increasing impeller speed.

Table 4-1. Gas Holdup

	Gas holdup (ε, %)				
	135 rpm	300 rpm	450 rpm	600	rpm
Distilled Water	1.76	2.49	2.96	3.51	
1 g/L Ethanol Solution	1.78	2.48	3.42	4.76	
3 g/L Ethanol Solution	1.82	2.54	3.56	5.35	
8 g/L Ethanol Solution	1.85	2.66	3.77	5.91	
20 g/L Ethanol Solution	-	-	-	7.76	

Determination of Average Bubble Diameter

The interfacial area, a in Equation (4-4), can be calculated from the experimental data of k_La using a constant k_L value of 0.000135 m/s in distilled water (Calderbank and Moo-Young, 1961). The other parameter needed to evaluate bubble diameter is gas holdup. The increase in gas holdup is due to the decrease in surface tension, which was measured with a Du Noüy ring – tensiometer (model K10ST, Tekmar Company). The surface tension was determined to be 71.7, 71.4, 70.2 and 67.7 mN/m for ethanol concentrations in distilled water of 0, 1, 3, and 8 g/L, respectively. With gas holdup data measured, the average bubble diameter can then be calculated from (Hill *et al.*, 1996):

$$d_b = \frac{6 \times \varepsilon}{a} \qquad (4\text{-}5)$$

The results of the average bubble diameter are shown in Figure 4-4. At lower impeller speeds, reducing the speed increased the bubble size. For example, in the distilled water, the average bubble diameter decreased from 7 to 2 mm with an increase of impeller speed from 135 to 300 rpm. At 1 g/L ethanol, bubble size decreased from 6 to 0.8 mm with this same increase of impeller speeds. At 135 rpm, the average bubble diameter decreased from 7 to 6 mm with the addition of ethanol. The bubble diameter decreased from 2 to 0.8 mm at 300 rpm and from 1.7 to 0.7 mm at impeller speeds of 450 and 600 rpm, respectively. This indicates that both the addition of ethanol and the increase in impeller speed decrease bubble diameters. There was no significant further decrease in bubble diameter with increase of impeller speed beyond about 400 rpm, which is consistent with the results visually observed using a digital camera. It was also observed that beyond ethanol concentration of 1 g/L there was no further decrease in the bubble size. The decrease in bubble size by addition of ethanol is also due to the decrease in surface tension. These observations of average bubble diameter were similar to those in the stirred tanks reported by others using electrolytes as a mean of enhancing mass transfer (Lee and Meyrick, 1970; Benedek and Heideger, 1971; Robinson and Wilke, 1974).

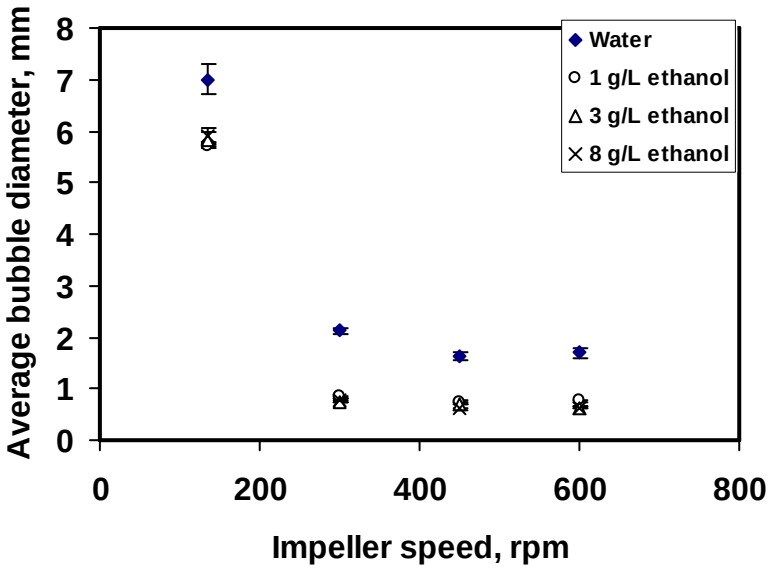

Figure 4-4. Experimentally measured bubble diameters in the well-mixed bioreactor (error bars are standard deviations).

Correlation of Oxygen Mass Transfer Coefficient

It was observed in this study that the gas holdup did not vary when the impeller speeds were less than 135 rpm. Therefore, the value of k_La was assumed to remain constant below 135 rpm. Commercial software, Tablecurve (Jandel Scientific, San Rafael, California), was used to help formulate an empirical model for the overall mass transfer coefficients. The lines in Figure 4-3 represent the following best-fit, empirical equation for ethanol concentrations over the range of 0 to 8 g/L and impeller speeds over the range of 135 to 600 rpm:

$$k_La\ (s^{-1}) = 0.002 \qquad \text{for } N \le 135 \text{ rpm}, 0 \le [E] \le 8 \text{ g/L} \qquad (4\text{-}6)$$

k_La=-0.00285+0.00214[E]-0.0118[E]$^{0.5}$+3.595x10^{-5}N-1.587x10^{-5}[E]N

+8.741x10^{-5}[E]$^{0.5}$N for 135 ≤ N ≤ 600 rpm, 0≤ [E] ≤ 8 g/L (4-7)

where [E] is ethanol liquid concentration (g/L), N is agitation speed (rpm). It is apparent from Equation (4-7) that both individual and interacting effects are significant for stirring speed and ethanol concentration.

The smaller bubble diameters generated at high impeller speeds and with the addition of a small quantity of ethanol increase both the gas holdup and the gas-liquid interfacial area. Both features improve the mass transfer rate of oxygen into the liquid phase. Thus it is clear that the addition of a small amount of ethanol to an actual fermentation process has the potential to enhance the rate of biomass build-up and even the total amount of biomass produced inside the bioreactor.

The volumetric mass transfer coefficient, average bubble diameter and gas holdup in a well-mixed fermentor were found to be dependent on impeller speed and ethanol concentration. Both k_La and gas holdup increased with increasing impeller speed and ethanol concentration in pure water. The average bubble diameter decreased with increasing impeller speed and ethanol concentration in the distilled water. The oxygen mass transfer coefficients have been successfully modeled using empirical correlations.

4.2 Air Stripping

The air stripping parameters (β values as per Singh and Hill, 1987) were determined by performing a brief experiment with no microbial inoculation using the

Bioflow III bioreactor. Equation (4-8) describes the relation between substrate concentration in the liquid phase and time (Singh and Hill, 1987):

$$\ln(\frac{S_0}{S}) = \beta \cdot t \qquad (4\text{-}8)$$

where S_o and S represent the substrate concentrations at time zero and time t. By plotting $\ln(S_0/S)$ versus t, the slope of the straight line will give the air stripping parameter (β).

The ethanol air stripping studies were conducted at an initial liquid ethanol concentration of 8.6 g/L, impeller speed of 450 RPM, and temperature of 25.0 $^{\circ}$C, while varying air flow rates through the well–mixed bioreactor. The ethanol air stripping parameters (β values) were determined (See Figures 4-5) to be 0.002 and 0.007 h^{-1} for air flow rates of 0.4 L/min (0.3 vvm) and 1.4 L/min (1 vvm), respectively. The toluene air stripping rates (See Figure 4-6), at initial liquid toluene concentration of 440 mg/L, were found to be 2.2, 5.3, 10.4, and 12.6 h^{-1} for air flow rates of 0.4, 0.9, 1.4, 2.1 L/min, respectively. The results show that the air stripping parameter increases with the increase of air flow rates as predicted by Singh and Hill (1987), and stripping rates obtained in this study for ethanol were much lower than those for toluene. It was also observed that benzyl alcohol was not stripped to any detectable level at any of the operating conditions used in this study.

In order to minimize the air stripping effects during batch and continuous bioremediation studies, the air flow rate was maintained at a low value of 0.4 L/min (0.3 vvm) during all bioremediation studies.

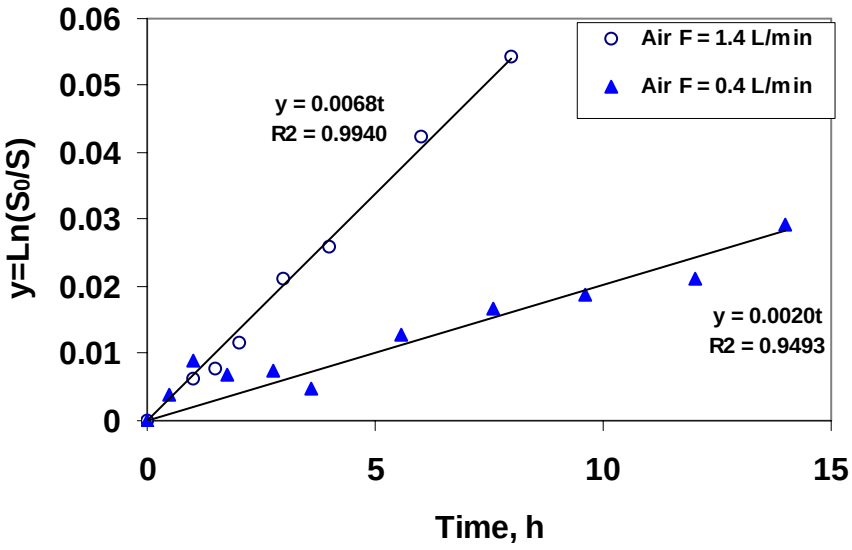

Figure 4-5. Ethanol air stripping coefficients at ethanol concentration of 8.6 g/L

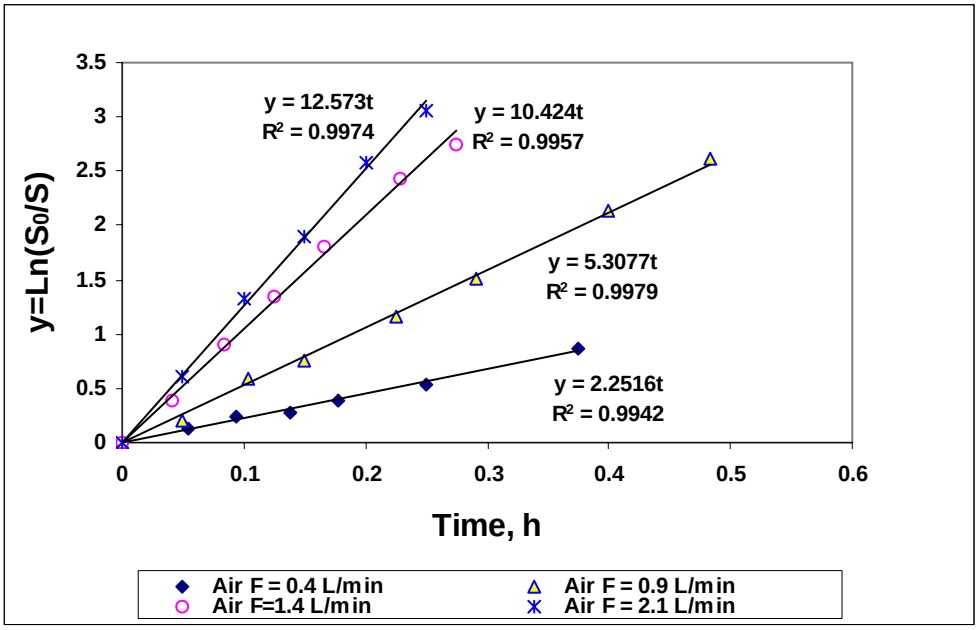

Figure 4-6 Toluene air stripping coefficients at toluene liquid concentration of 440 mg/L

4.3 Batch Growth on Ethanol and Benzyl Alcohol

4.3.1 Batch Growth on Ethanol

One of the ethanol batch growth experiments is shown in Figure 4-7 (S_0 = 2.3 g/L). Growth started after a 5 h lag phase and was reflected exactly by ethanol consumption in the bioreactor. The initial concentration of 2.3 g/L of ethanol was completely consumed in less than 12 hours. At low initial ethanol concentrations no byproduct was detected in the media and the Monod model was used to describe the growth kinetics:

$$\mu = \frac{1}{X}\frac{dX}{dt} = \frac{\mu_{\max} S}{K_s + S} \qquad (4\text{-}9)$$

μ_{max} is the maximum specific growth rate and K_s is the Monod saturation constant. The specific growth rate on ethanol during the log phase was determined by plotting ln(X) versus time. The dissolved oxygen values were found to be higher than the critical value (0.35 mg/L, Shuler and Kargi, 2002) for growth on ethanol at initial concentrations up to 5.8 g/L, which indicated that oxygen mass transfer is not a rate-limiting step under these conditions. For the batch growth experiments at ethanol initial concentrations up to 5.8 g/L, the specific growth rates were within the range of $0.37 \pm 0.03\,h^{-1}$. This rate of growth on ethanol is much greater than the maximum specific growth rate (0.046 h^{-1}) of *Acetobacter aceti* on ethanol reported earlier by Wei *et al*., 1999. *Pseudomonas putida* (ATCC 23973) will therefore be much more effective in removing ethanol from contaminated air compared to that earlier work. The growth process is reproducible, and Figure 4-8 shows the results for two different batch runs.

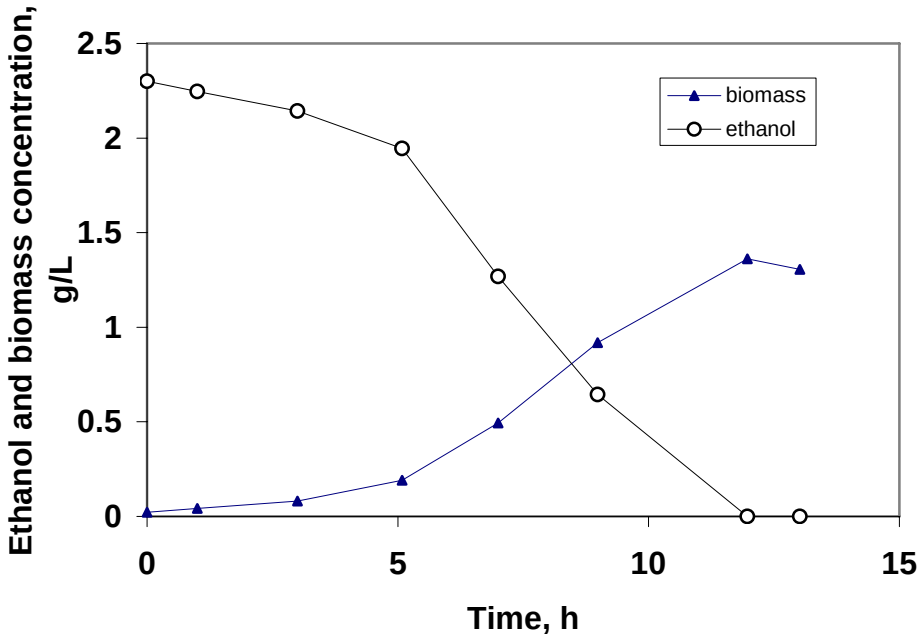

Figure 4-7. Batch growth of *Pseudomonas putida* on ethanol at initial concentration of 2.3 g/L, air flow rate of 0.4 L/min, 450 rpm and 25.0^{o}C

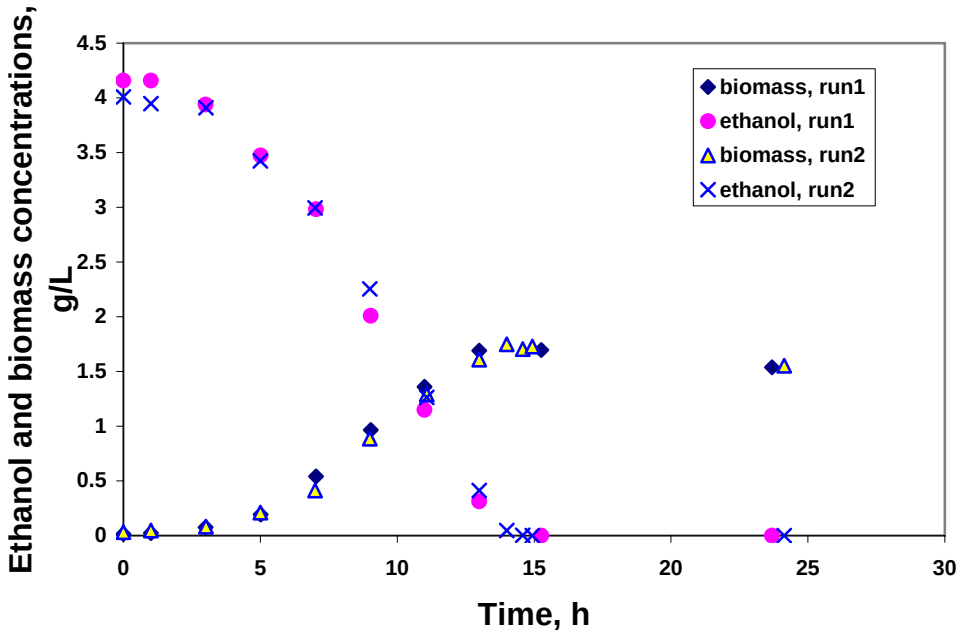

Figure 4-8 Comparison of results from two different runs of batch growth of *P. putida* on ethanol using the same reactor

4.3.2 Batch Growth on Benzyl Alcohol

The results of batch growth with benzyl alcohol at different initial concentrations are shown in Figures 4-9a-b. The results indicate that the higher the initial concentration, the longer the lag phase, i.e., it takes longer time for bacteria to adapt to the environment. For instance, the lag phase is around 3 hours at an initial benzyl alcohol concentration of 0.7 g/L, while it took the bacteria 5 and 18 hours to adapt to the environment at initial concentrations of 2.0 and 2.8 g/L, respectively. This is a typical indication of substrate inhibition. Figure 4-10 gives the results of the specific growth rates with respect to benzyl alcohol concentrations. The specific growth rate decreases dramatically at benzyl alcohol concentrations above 1.0 g/L indicating that benzyl alcohol inhibited the growth of *Pseudomonas putida (*ATCC 23973). An empirical relationship (Luong, 1987) was used to correlate benzyl alcohol inhibition:

$$\mu = \frac{\mu_m S}{K_s + S}(1 - \frac{S}{S_m})^n \qquad (4\text{-}10)$$

where S_m is the maximum substrate concentration above which growth is completely inhibited . Since it is known that *Pseudomonas putida* has a low Monod saturation constant when growing on aromatic substrates (Hill and Robinson, 1975), K_s can be set to as low as 1 mg/L. The value of S_m was found to be 2.9 ± 0.05 g/L (i.e., 0.19 C-mol/L) by best fitting experimental results using Equation 4-10 (See Figure 4-10). This was further proved by the experimental results, i.e., when benzyl alcohol initial concentration is higher than 3.0 g/L, benzyl alcohol concentration remains the same level as the initial concentration and no biomass growth was detected within 48 hours, such as the results shown in Figure 4-9b at an initial concentration of 4.0 g/L.

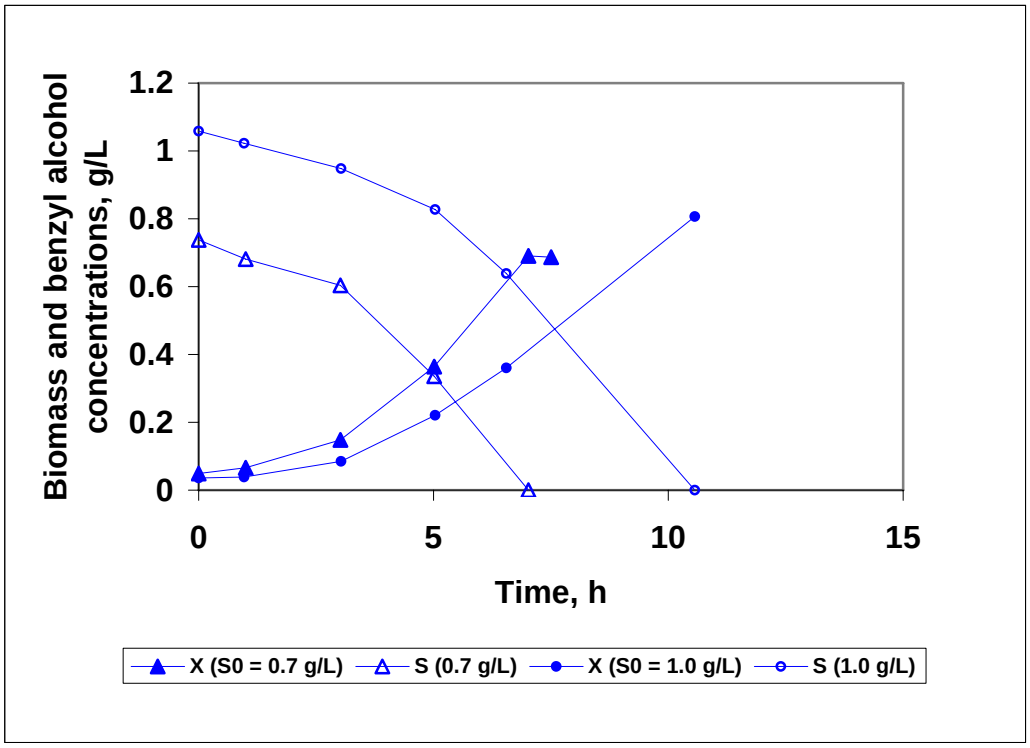

Figure 4-9a. Batch growth on benzyl alcohol at different initial concentrations of 0.7 and 1.0 g/L

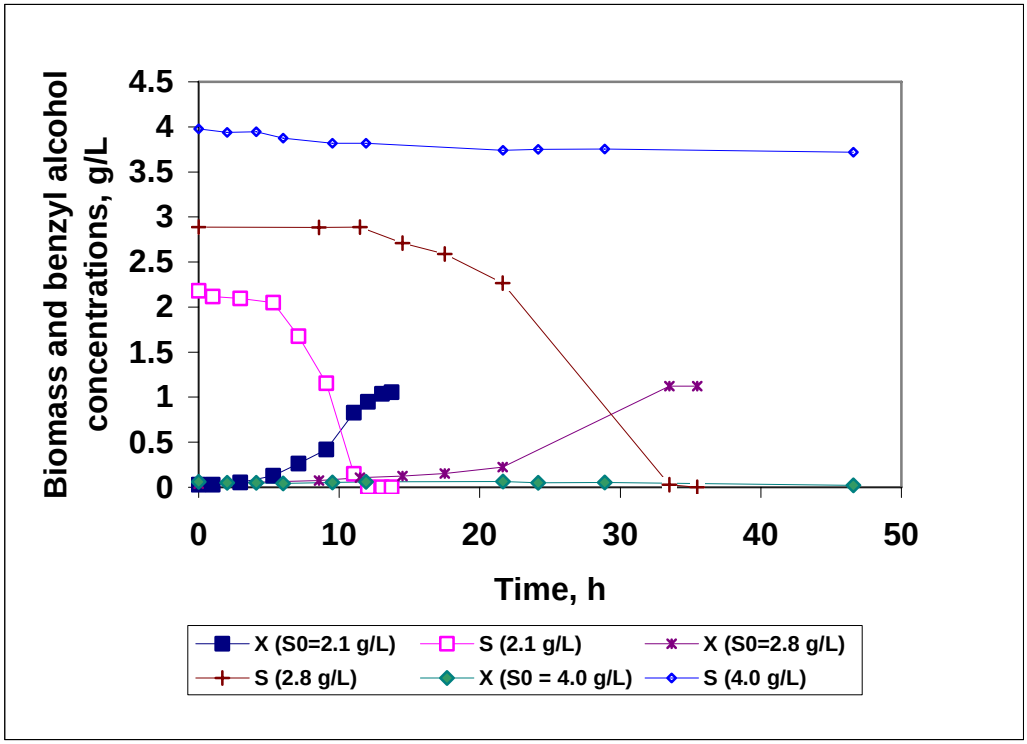

Figure 4-9b. Batch growth on benzyl alcohol at different initial concentrations of 2.1 g/L to 4.0 g/L

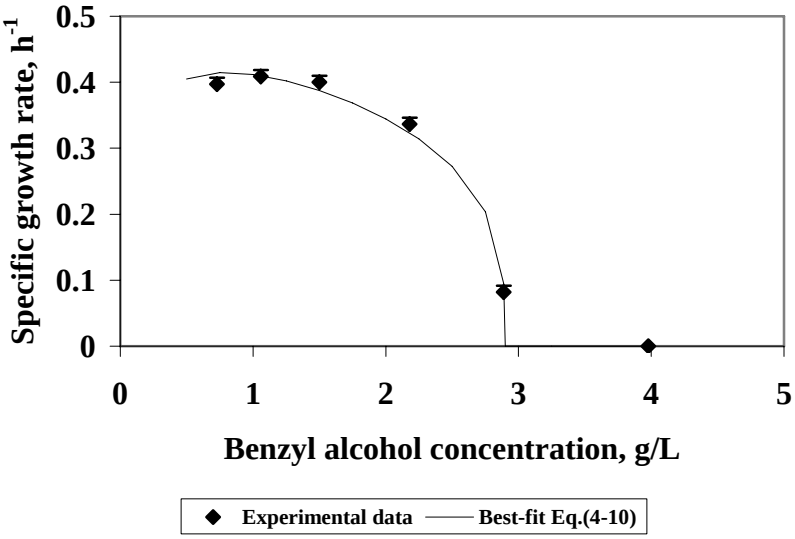

Figure 4-10 Inhibitory Effect of benzyl alcohol on growth of *P. putida* (ATCC23973)

4.4 Continuous Bioremediation

4.4.1 Ethanol Bioremediation

Pseudomonas putida was initially grown in a batch culture which contained an initial dissolved ethanol concentration of 2.6 g/L. After 11 hours, when the ethanol was completely consumed and the biomass concentration reached a certain level, the medium pump was started at a flow rate of 150 mL/h (dilution rate of 0.1 h^{-1}) and ethanol was continuously added at an air inlet concentration of 15.9 mg/L and flow rate of 0.37 L/min (ethanol loading of 235 mg/L-h). Figure 4-11 demonstrates that the ethanol transferred from the polluted air stream was continuously utilized by *Pseudomonas putida*. After operating for 25 hours, the inlet ethanol concentration was increased to 19.5 mg/L (air flow rate to 0.39 L/min accordingly; ethanol loading of 304 mg/L-h). The bioreactor was again operated at steady state for another 25 hours before shutting down the bioreactor in order to study other operating conditions. During the steady state operations, there was no ethanol detected from the outlet gas stream.

Figure 4-12 shows the results for another independent continuous run. After operating for 38 hours at an inlet ethanol concentration of 15.9 mg/L and air flow rate of 0.37 L/min (ethanol loading of 235 mg/L-h), the ethanol inlet concentration was increased to 25.0 mg/L and the air flow rate was increased to 0.42 L/min (ethanol loading of 420 mg/L-h). The biomass concentration and the media pH started to decrease while acetic acid was detected in the liquid phase (identified by GC-MS, Model VG70VSE, VG Analytical). Dissolved oxygen indicated a value of 0 mg/L at this condition. Instead of being completely converted to biomass, ethanol was only partially converted to acetic acid and then excreted into the media when the inlet

ethanol loading was beyond the maximum uptake rate of the cells due to oxygen limitation. There was no detectable ethanol bypassing the reactor in gas phase under all the above operating conditions.

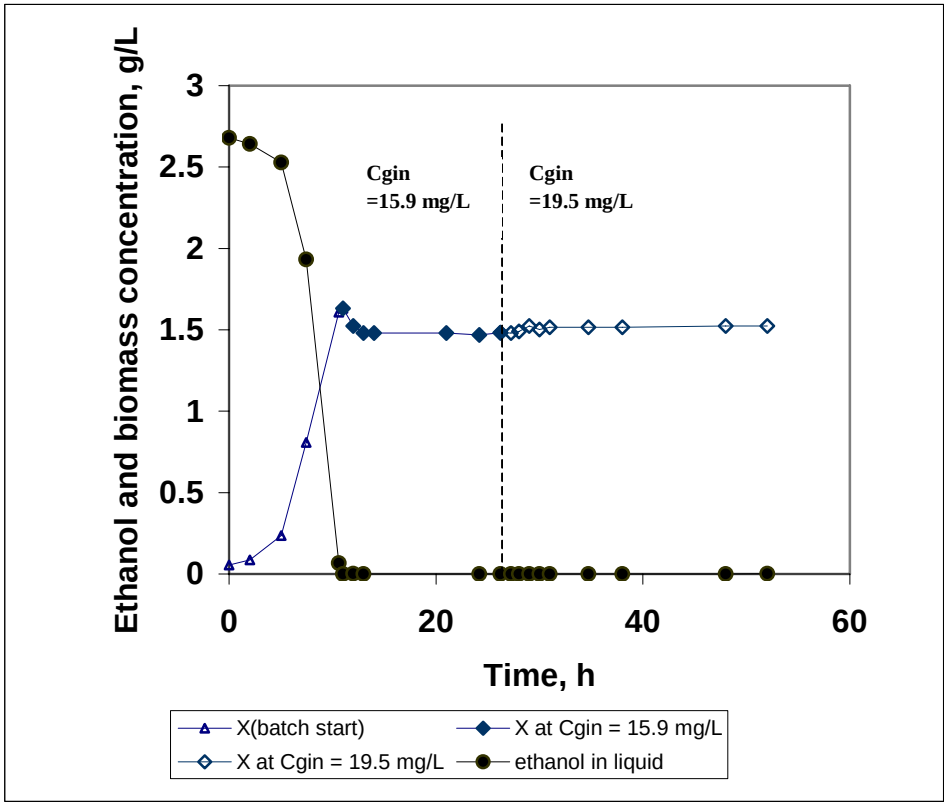

Figure 4-11. Continuous removal of ethanol from a polluted gas stream by *Pseudomonas putida* at a dilution rate of $0.1h^{-1}$ and 25.0°C, and at inlet ethanol concentrations of 15.9 and 19.5 mg/L (no detectable ethanol or acetic acid in the liquid)

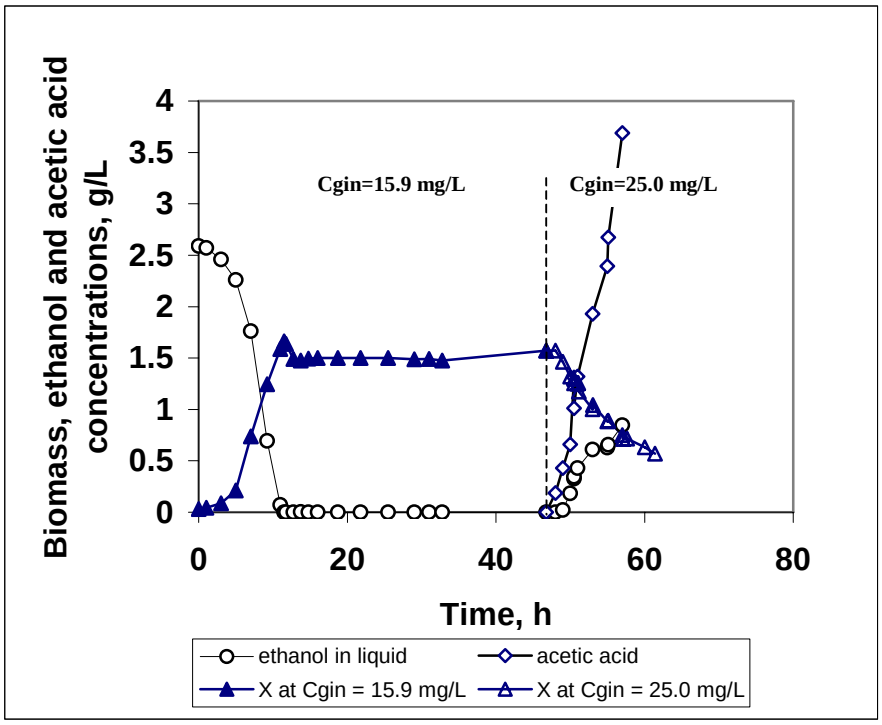

Figure 4-12. Continuous removal of ethanol from a polluted air stream by *Pseudomonas putida* at dilution rate of $0.1h^{-1}$ and 25.0°C, and inlet ethanol concentrations of 15.9 and 25.0 mg/L

Ethanol removal efficiency of 100% was reached in this study using a well-mixed bioreactor at loadings up to 304 mg/L-h without detectable ethanol bypassing the reactor in gas phase. This is superior to ethanol bioremediation using biofilters reported by other authors (see Table 4.2 for some examples). This reveals that the use of a well-mixed bioreactor represents an effective method for removal of water soluble VOCs from contaminated air streams, and it can handle transient loading changes as long as other nutrients, such as ammonium and oxygen, are supplied in sufficient quantities, which will be further discussed in Section 5.6.

Table 4-2. Comparison of bioremediation of air streams contaminated with ethanol using a CSTR against using a biofilter

Pollutant	Inlet Conc.& Loading (g/m^3, g/m^3-h)	Removal Efficiency
Ethanol[1]	1.89, 120	89%
Ethanol[2]	3.0, 90	100%
Ethanol[2]	10.0, 300	68%
Ethanol	19.5, 304	100% (this work)

1. Kiared et al., 1996.
2. Arulneyam et al., 2000.

4.4.2 Toluene Bioremediation

The bioremediation of toluene as the sole carbon source in the contaminated air was attempted in continuous mode. Different conditions were studied by varying the dilution rates from 0.01 to 0.1 h^{-1}, the toluene air inlet concentrations from 4.5 to 23.0 mg/L and air flow rates of 0.25 to 0.37 L/min (resulting in inlet toluene loadings from 70 to 386 mg/L-h). At toluene inlet concentration of 4.5 mg/L, it was observed that 96 % of the inlet toluene was initially captured within the liquid phase. However, toluene concentration in the liquid phase steadily increased to 30 mg/L over a 30 minute interval, resulting in the complete inhibition of *Pseudomonas putida* with no biomass growth. Figures 4-13 and 4-14 demonstrate the results at toluene inlet concentrations of 23.0 and 11.0 mg/L, respectively.

Figure 4-13 illustrates continuous removal of toluene at a gas inlet concentration of 23.0 mg/L and dilution rates of 0.01 and 0.027 h^{-1}. As shown in Figure 4-13 at dilution rate of 0.01 h^{-1}, biomass could use toluene as carbon source for growth, but the

operation could not reach steady state. At the dilution rate of 0.027 h^{-1}, biomass concentrations declined, which in turn caused toluene gas outlet concentrations to increase. Both cases failed to reach steady state operation. Figure 4-14 shows the results of toluene removal at a toluene gas inlet concentration of 11.0 mg/L and at dilution rates of 0.027 and 0.005 h^{-1}. Under both conditions, 70% of the inlet toluene bypassed the reactor through gas phase, and benzyl alcohol accumulated in the liquid phase with concentrations up to 0.4 g/L. Under all the above conditions, toluene concentrations in the outlet gas consistently increased with respect to time while benzyl alcohol accumulated in the liquid phase, which in turn failed to reach steady state. It was concluded that toluene, as the sole carbon source, could not be effectively utilized by *Pseudomonas putida,* and thus only bioremediation of the mixtures of co-substrates and toluene were further investigated.

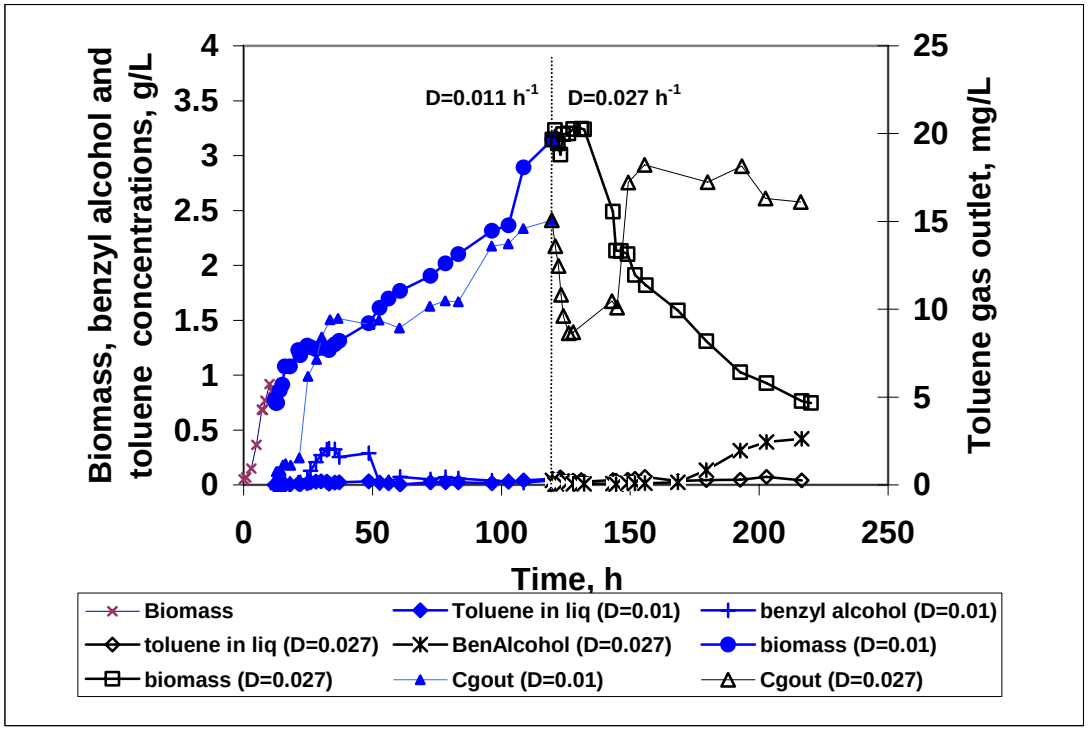

Figure 4-13. Continuous removal of toluene at gas inlet of 23.0 mg/L and dilution rates of 0.01 and 0.027 h^{-1}

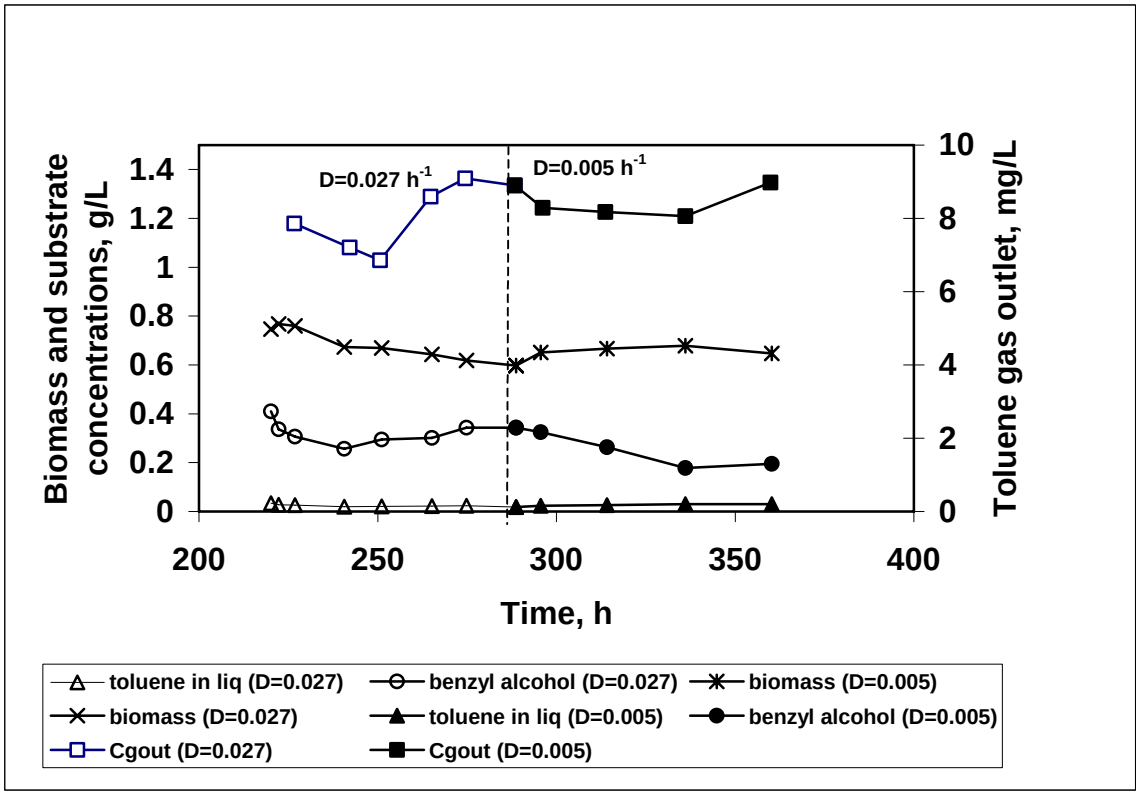

Figure 4-14. Continuous removal of toluene at gas inlet concentration of 11.0 mg/L

4.4.3 Toluene-ethanol Bioremediation

For this set of experiments, the aqueous nutrients were added to the bioreactor at 150 mL/h (dilution rate of 0.1 h^{-1}), ethanol was introduced through an air stream at an inlet concentration of 15.9 mg/L and at an air flow rate of 0.4 L/min (loading of 254 mg/L-h, see Figure 4-15). Figure 4-15 shows a continuation of a previous operation. When the operation reached steady state, toluene was introduced into the bioreactor at an air inlet concentration of 4.5 mg/L (loading of 72 mg/L-h, total loading of 326 mg/L-h). Ethanol removal efficiency remained at 100% and toluene removal efficiency reached 89% at steady state conditions. The liquid concentrations of toluene and benzyl alcohol were below 10 and 70 mg/L (results are not presented in the Figure 4-15), respectively. After maintaining steady state conditions for 20 hours, the toluene inlet concentration was increased to 5.8 mg/L while the ethanol inlet concentration was maintained at 15.9 mg/L and the air flow rate was maintained at 0.4 L/min (toluene loading of 93 mg/L-h, total loading of 347 mg/L-h). Over the next 20 hours, toluene concentration in the outlet air stream increased almost three-fold and reached 1.2 mg/L which represented a gas removal efficiency of 79 % (See Figure 4-16). However, the liquid phase ethanol concentration increased to 0.47 g/L and the benzyl alcohol concentration steadily climbed to 0.12 g/L. This was due to oxygen depletion since dissolved oxygen reading fell to zero. This will be further discussed in Section 5.6. Since ethanol is volatile and therefore difficult to supply as a co-substrate, benzyl alcohol was next introduced in the liquid feed as another potential co-substrate.

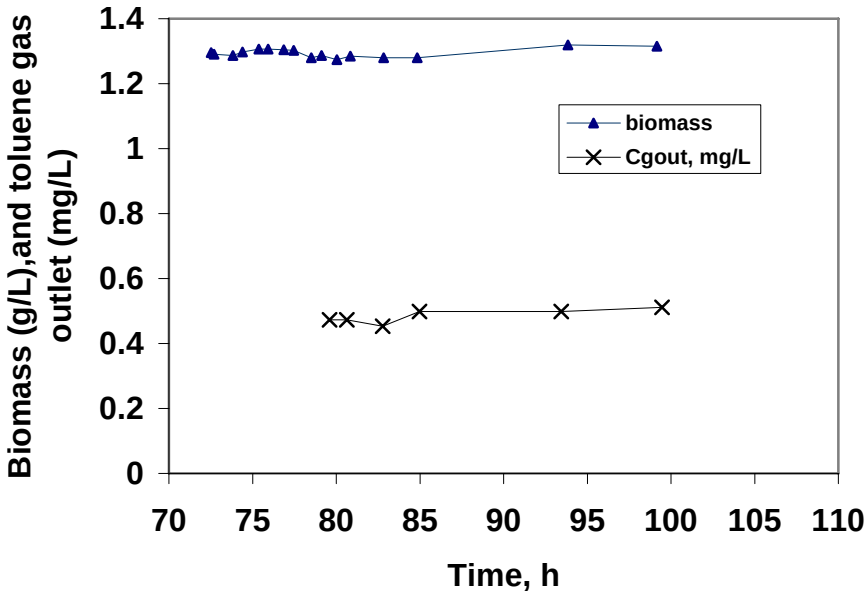

Figure 4-15. Continuous removal of toluene-ethanol mixture from a polluted air stream by *Pseudomonas putida* at a dilution rate of $0.1h^{-1}$, 25.0°C, air flow rate of 0.4 L/min, and at ethanol inlet concentration of 15.9 mg/L and toluene inlet concentration of 4.5 mg/L

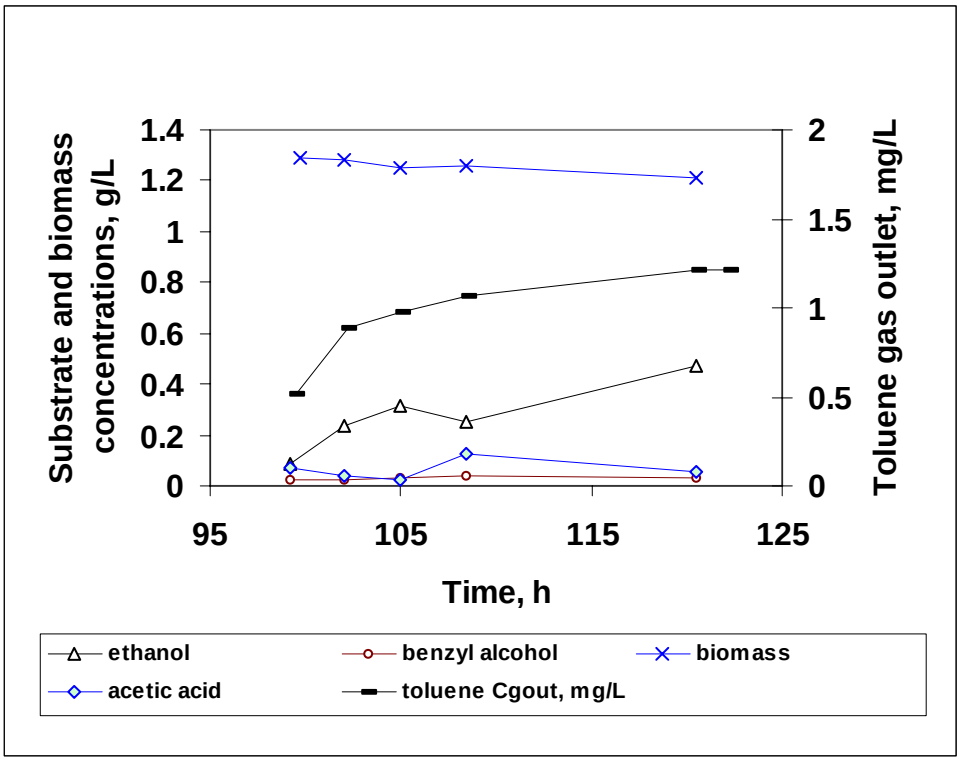

Figure 4-16. Continuous removal of toluene-ethanol mixture from a polluted air stream at a dilution rate of 0.1 h^{-1} and ethanol inlet concentration of 15.9 mg/L with toluene inlet concentration of 5.8 mg/L

4.4.4 Toluene-benzyl alcohol Bioremediation

Prior to continuous bioremediation of benzyl alcohol and toluene, cultures were started in batch mode with an initial benzyl alcohol concentration of 1.0 g/L to obtain an initial high population of biomass for the continuous bioremediation studies.

The medium was added to the reactor at 150 mL/h (dilution rate of 0.1 h^{-1}), benzyl alcohol was added at a feed rate of 0.12 g/h using a syringe pump, and the air flow rate was set at 0.4 L/min. When the benzyl alcohol feed rate was 0.12 g/h and toluene inlet concentrations were 4.5 and 5.7 mg/L (toluene loadings of 72 and 91 mg/L-h, total loadings of 152 and 171 mg/L-h), conditions reached steady state and the

toluene removal efficiencies were above 97 % (Figures 4-17 and 4-18). With a toluene gas inlet concentration of 4.5 mg/L, there was no detectable toluene in the liquid phase. With a toluene gas inlet concentration of 5.7 mg/L, the toluene concentration in the liquid phase was below 4.0 mg/L, and no other metabolites were detected in the liquid phase in both cases.

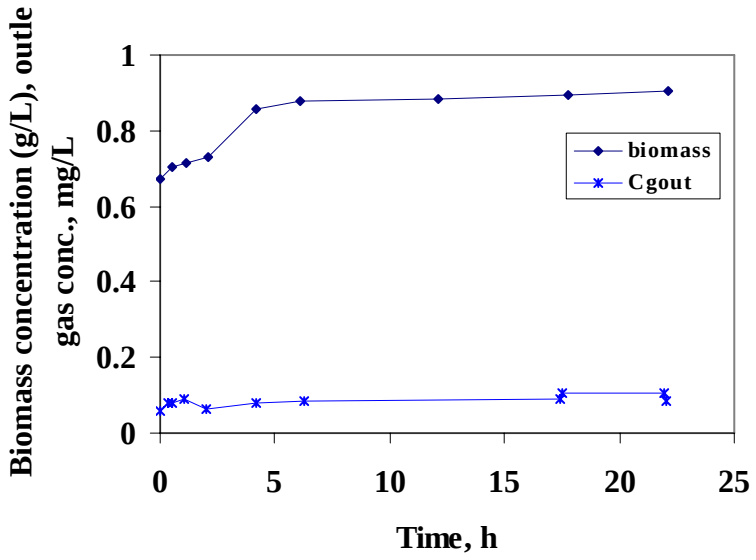

Figure 4-17. Bioremediation of toluene-benzyl alcohol mixtures by *Pseudomonas putida* in a continuous mode at a dilution rate of 0.1 h^{-1}, 25.0°C, air flow rate of 0.4 L/min, and at a benzyl alcohol inlet concentration of 0.12 g/h and toluene inlet concentration of 4.5 mg/L

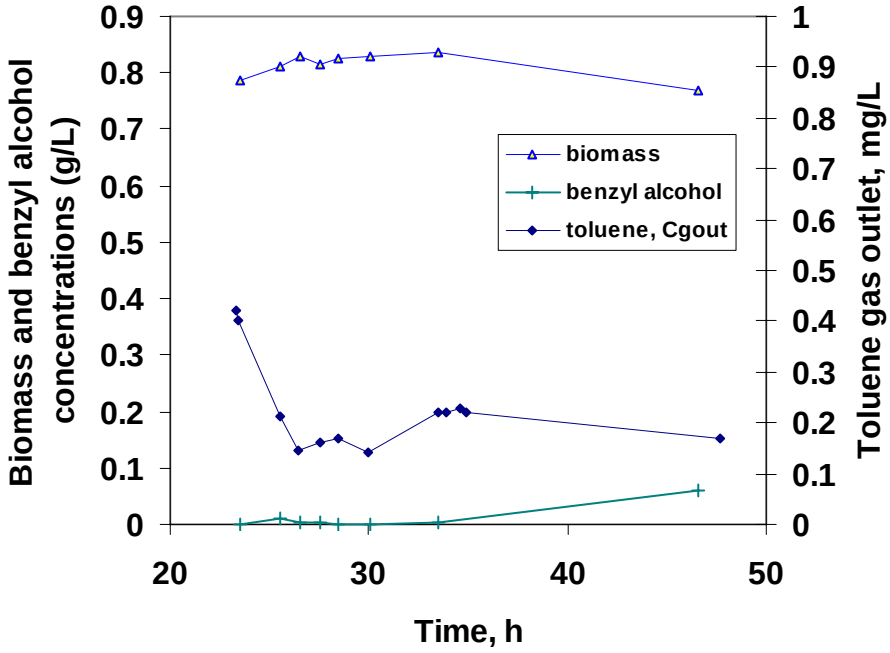

Figure 4-18. Bioremediation of toluene-benzyl alcohol mixture by *Pseudomonas putida* in a continuous mode at dilution rate of 0.1 h^{-1}, 25.0°C, air flow rate of 0.4 L/min, and at a benzyl alcohol inlet concentration of 0.12 g/h and toluene inlet concentration of 5.7 mg/L

Two more independent experiments were conducted at different benzyl alcohol feed rates of 0.34 and 0.46 g/h (See Figures 4-19 and 4-20). When benzyl alcohol was added at feed rates of 0.34 and 0.46 g/h at an inlet toluene concentration of 4.5 mg/L, the toluene concentrations in the outlet gas increased to 0.21 and 0.45 mg/L, which resulted in toluene removal efficiencies of 95 % and 90 %, respectively. There was no detectable benzyl alcohol in the liquid, and the toluene liquid concentration remained at 15 mg/L for these two cases. However, benzoic acid was detected in the liquid phase (identified by GC-MS, Model VG70VSE, VG Analytical). Benzoic acid in the liquid phase reached concentrations up to 0.6 and 1.6 g/L for benzyl alcohol feed rates of 0.34 and 0.46 g/h, respectively. In these cases, benzyl alcohol was partially oxidized to benzoic acid instead of being completely converted to biomass due to oxygen depletion when benzyl alcohol feed rates reached 0.34 g/h. Dissolved oxygen measurements indicated a value of 0 mg/L. When the benzyl alcohol feed rates were increased (e.g, 0.34 g/h), the bacteria in the reactor required more dissolved oxygen for their growth. Oxygen depletion caused this change of bioremediation mechanism in the toluene/benzyl alcohol pathways, which will be further discussed in Section 5.6. This demonstrates that a benzyl alcohol feed rate above 0.34 g/h represents too high of a metabolic load for *Pseudomonas putida* due to oxygen limitation and no new steady-state operating condition could be achieved.

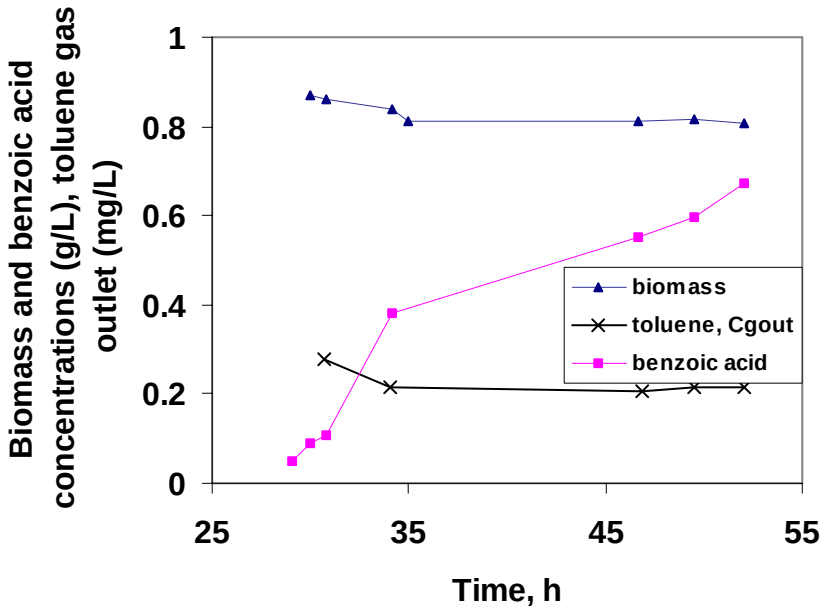

Figure 4-19. Biodegradation of benzyl alcohol and toluene in a continuous mode (dilution rate of 0.1 h^{-1}, benzene alcohol feed rate = 0.34 g/h; toluene inlet concentration of 4.5 mg/L)

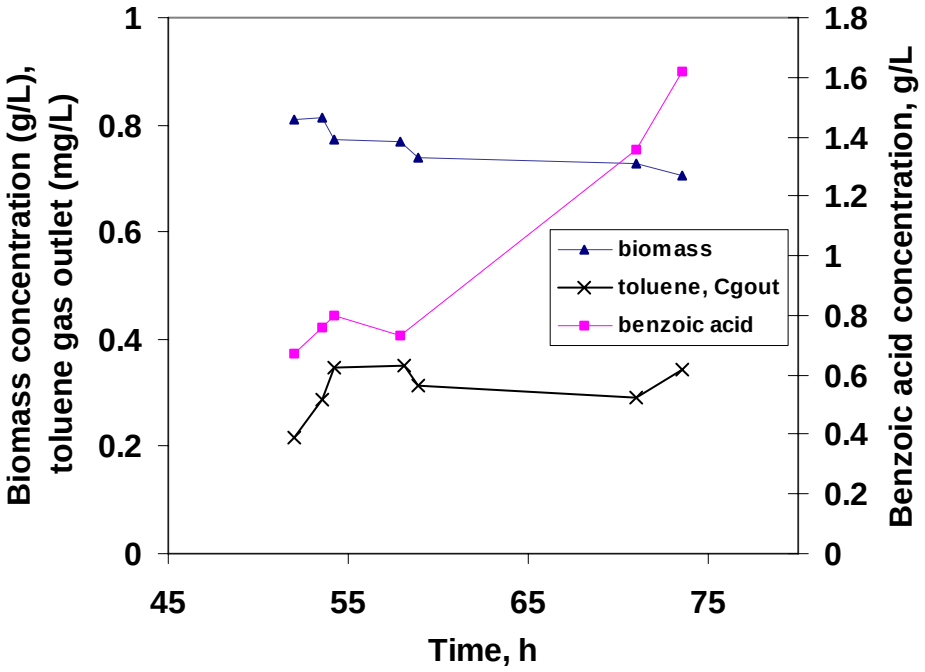

Figure 4-20. Biodegradation of benzyl alcohol and toluene in a continuous mode (dilution rate of 0.1 h^{-1}, benzene alcohol feed rate = 0.46 g/h; toluene inlet concentration of 4.5 mg/L)

4.5 Conclusions of Experimental Studies

Ethanol and toluene contaminated air streams have been successfully bioremediated in a well-mixed bioreactor. Ethanol was completely absorbed into the growth media, while toluene was absorbed with mass transfer coefficients up to $1.0x10^{-3}s^{-1}$. Furthermore, it was observed that toluene was stripped from the fermentation media at rates approximately 1000 times higher than those observed for

ethanol. These results clearly indicate the volatile, hydrophobic nature of toluene, relative to that of ethanol.

In this study, it was found that unless ethanol or benzyl alcohol was added to the reaction mixture, *Pseudomonas putida* could not oxidize toluene continuously. This agrees with the results of Gibson et al. (1968). They discovered that the crude cell extracts of *Pseudomonas putida* that grow on benzyl alcohol contained an active dehydrogenase which permits benzyl alcohol to produce $NADH_2$. This reduced NAD is required in the initial reaction of toluene.

Appreciable bioremediation rates of both ethanol and toluene from contaminated air streams using a traditional, well-mixed bioreactor were achieved. By operating the bioreactor in a continuous mode, ethanol removal efficiencies reached 100% with inlet loadings up to 304 mg/L-h. Using ethanol as co-substrate, the removal efficiency reached 100% for ethanol and 89% for toluene at ethanol inlet concentration of 15.9 mg/L and toluene inlet concentration of 4.5 mg/L. With the presence of benzyl alcohol as co-substrate at inlet toluene concentrations and total loadings up to 5.7 mg/L and 171 mg/L-h, toluene removal efficiencies were as high as 97 %. A summary of the bioremediation results for ethanol and toluene removal in this study is provided in Table 4-3. These results compare favorably to biofiltration units for the removal of either ethanol or toluene from contaminated air streams, and bode well for commercial implementation since well-mixed bioreactors are much easier to operate than biofilters.

Table 4-3. Bioremediation results of air contaminated with ethanol and toluene as single substrates or as mixtures using a well-mixed bioreactor in this study compared with biofilter results

	Inlet concentration (C_{gin}) (g/m^3)	Total Inlet Loading[1] (g/m^3-h)	Removal Efficiency
Toluene[2]	2.63	102	93%
Toluene[2]	2.64	121	90%
Toluene[3]	3.7	70	70%
Ethanol	15.9	235	100%
	19.5	304	100%
	25.0	420	Unstable[4]
Toluene	23.0	386	Unstable
	11.0	176	Unstable
	4.5	70	Unstable
Ethanol &Toluene	15.9 (ethanol) & 4.5 (toluene)	326	100%(ethanol) 89% (toluene)
	15.9 (ethanol) & 5.8 (toluene)	347	Unstable
Toluene & Benzyl Alcohol (BA)	4.5 (toluene) & 0.12 g/h BA	152	97% (toluene) 100% (BA)
(toluene)	5.7 (toluene) & 0.12 g/h BA	171	97% 100% (BA)
	4.5 (toluene) & BA>0.34g/h	>299	Unstable

Note:
1. Inlet loading = $Q*C_{gin}/V$
2. Jorio et al., 1998.
3. Kiared et al., 1996.
4. There were pollutants accumulated in the liquid phase in all these cases.

CHAPTER FIVE - MATHEMATICAL MODELING

In order to understand the metabolic activities for ethanol or benzyl alcohol bioremediation by *Pseudomonas putida* (ATCC 23973), a metabolic model was established based on biochemical theories and experimental observations.

5.1 Model for Ethanol Bioremediation

5.1.1 Metabolic Equations

The metabolic reactions for the aerobic metabolism of ethanol can be separated into two groups: 1) the energy consuming reactions and 2) the energy generating reactions. The energy consuming reactions are due to the production of biomass while the energy producing reactions include ethanol catabolism and oxidative phosphorylation. The major metabolic activities taking place in ethanol bioremediation are described as follows[2] and are shown in Figure 5.1 (developed in this work).

(1) Biomass Formation from Ethanol

In the synthesis of biomass, it is assumed that 0.27 mol CO_2 is produced per C-mole biomass synthesized (Gornmers, et al., 1988). Once the precursors have been made, the following stoichiometry for the synthesis of biomass from precursors can be assumed to apply (Roels, 1983; Stouthamer, 1979):

[2] In order to simplify the Equations, phosphate balance and charge balance are not included in the Equations. For instance, the charge on NAD and the inorganic form of phosphate P_i will not be included in the Equations.

1 C-mole precursors + K ATP ⟶ 1 C-mole biomass (5-1)

in which adenosine triphosphate (ATP), an energy-rich compound, acts as a phosphate carrier and transfers energy between reactions. Thus, the amount of ATP needed for the formation of 1 C-mol biomass from precursors is represented by the variable K.

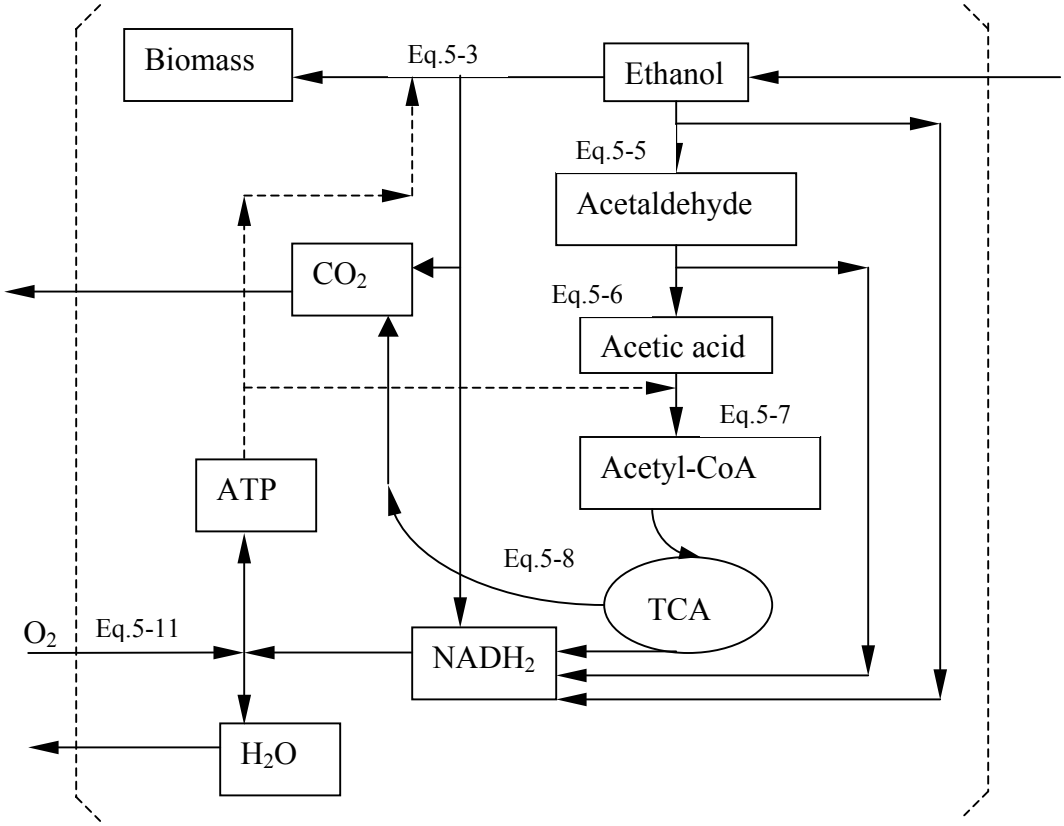

Figure 5.1 Hypothesized Metabolic Pathways for Ethanol Bioremediation
("⟶" indicates the conversion or transport of compounds; "⇢" indicates the transport of energy ATP)

A quantity of ATP is also required for biomass maintenance. This process will be assumed to be first order (Roels, 1983) with respect to biomass. The term, m_{ATP}, is the specific ATP consumption (mol-ATP/C-mol.h) due to the maintenance activities:

$$r^{m}_{ATP} = m_{ATP} C_x \quad (5\text{-}2)$$

The stoichiometry of the biomass synthesis from ethanol can be expressed in 1 C-mol of biomass formed as:

$$-1.27CH_3O_{0.5} - 0.2NH_3 - \alpha_{1E}ATP - 0.305H_2O - 1.81NAD$$
$$+ CH_{1.4}O_{0.4}N_{0.2} + 0.27CO_2 + 1.81NADH_2 + \alpha_{1E}ADP = 0 \qquad (5\text{-}3)$$

Where $CH_3O_{0.5}$ is the expression of 1-C-mol of ethanol (C_2H_6O), while $CH_{1.4}O_{0.4}N_{0.2}$ is the expression of 1 C-mol of biomass ($C_5H_7O_2N$). The biomass composition ($C_5H_7O_2N$) is based on the formula proposed by McCarty (1975) and was used by Brown (2000) for the composition of *Pseudomonas putida* (ATCC 23973). In Equation 5-3, α_{1E} represents the amount of ATP used in the biomass synthesis reactions and is given by:

$$\alpha_{1E} = K + \frac{m_{ATP}}{\mu} \qquad \text{when } \mu > 0 \qquad (5\text{-}4)$$

in which μ is the specific biomass growth rate (h^{-1}) and m_{ATP}/μ is the amount of ATP consumed by the biomass maintenance processes (Roels, 1983). In this equation, $NADH_2$ stands for reducing equivalents in the form of $NADH_2$ or any other equivalent form of metabolic reductant.

(2) Catabolism of Ethanol

The catabolic pathways supply the required ATP and NADH for biomass synthesis. Reactions (5-5) – (5-10) summarize the overall stoichiometry for the catabolic pathways. Initially, ethanol is oxidized by dehydrogenases to form an aldehyde (Equation 5-5), then to acetic acid (Equation 5-6), which can be metabolized to acetyl-CoA through the beta-oxidation pathway with consumption of ATP (Equation

5-7) (Gaudy, 1980, See Appendix A-I). Acetyl-CoA is oxidized through the TCA pathway that generates $NADH_2$ (Equation 5-8).

$$CH_3CH_2OH + NAD \rightarrow NADH_2 + CH_3CHO \quad (5\text{-}5)$$

$$CH_3CHO + NAD + H_2O \rightarrow CH_3COOH + NADH_2 \quad (5\text{-}6)$$

$$CH_3COOH + ATP + CoASH \rightarrow CH_3COSCoA + H_2O + ADP \quad (5\text{-}7)$$

Acetyl-CoA

In the TCA cycle (See Appendix A-II),

$$CH_3COSCoA + 4NAD + 3H_2O \rightarrow 4NADH_2 + 2CO_2 + CoASH \quad (5\text{-}8)$$

The overall, general catabolic equation of ethanol oxidation can be derived based on the above pathways (Geurts et al., 1980; Roels, 1983; see also Appendix A-I):

$$C_2H_6O + ATP + 3H_2O + 6NAD \rightarrow 2CO_2 + 6NADH_2 \quad (5\text{-}9)$$

This equation can be written in terms of 1 C-mol of ethanol as:

$$-CH_3O_{0.5} - \tfrac{1}{2}\ ATP - \frac{3}{2}\ H_2O - 3NAD + CO_2 + 3\ NADH_2 = 0 \quad (5\text{-}10)$$

(3) Oxidative Phosphorylation

In the oxidative phosphorylation reaction, ATP is produced from the oxidation of $NADH_2$. The amount of ATP produced per electron pair is represented by δ, the so-called P/O ratio, which represents the efficiency of oxidative phosphorylation. This process can be represented by:

$$-NADH_2 - \tfrac{1}{2}\ O_2 - \delta ADP + H_2O + \delta\ ATP + NAD = 0 \quad (5\text{-}11)$$

Please note that the phosphorus molecules are not included in the equations as stated in note 1 on page 80. The net amount of $NADH_2$ produced during biomass precursor

synthesis and in the ethanol catabolism reaction is assumed to yield ATP according to Equation (5-11).

5.1.2 Mathematical Modeling

The reaction network (5-3), (5-10) and (5-11) can be written in condensed form using the stoichiometric matrix θ_e, where the first compound is taken to be 1 C-mol of ethanol, followed by biomass, oxygen, carbon dioxide, ATP, and $NADH_2$. The stoichiometric matrix θ_e for reactions (5-3), (5-10) and (5-11) can be written as:

$$\theta_e = \begin{bmatrix} r_e \\ r_x \\ r_{o_2} \\ r_{co_2} \\ r_{ATP} \\ r_{NADH_2} \end{bmatrix} = \begin{bmatrix} -1.27 & -1 & 0 \\ 1 & 0 & 0 \\ 0 & 0 & -0.5 \\ 0.27 & 1 & 0 \\ -\alpha_{1E} & -0.5 & \delta \\ 1.81 & 3 & -1 \end{bmatrix} \qquad (5\text{-}12)$$

The reaction rate vector ν for the three reactions (5-3), (5-10) and (5-11) can be written as:

$$\vec{\nu} = \begin{bmatrix} \nu_1 \\ \nu_2 \\ \nu_3 \end{bmatrix} \qquad (5\text{-}13)$$

where ν_1, ν_2, ν_3 are the rates of reactions according to Equations (5-3), (5-10), and (5-11), respectively.

The following set of six linear relations is obtained, by writing out the compound balances for each of the six compounds (ethanol, biomass, oxygen, carbon dioxide, ATP and $NADH_2$):

$$\vec{r} = \theta_e \cdot \vec{\nu} + \vec{\phi} \qquad (5\text{-}14)$$

where $\vec{\phi}$ is the vector of flow into the system (=In – Out), and $\vec{r}$ is the vector of the overall conversion rates.

If the well-known assumption (Roels, 1983) is made that no net accumulation of $NADH_2$ and ATP takes place, except as an integral part of the biomass ($r_5 = r_6 = 0$), the overall conversion rates of the key compounds can be obtained:

$$r_e = -1.27\nu_1 - \nu_2 \tag{5-14a}$$

$$r_x = \nu_1 \tag{5-14b}$$

$$r_{o_2} = -0.5\nu_3 \tag{5-14c}$$

$$r_{co_2} = 0.27\nu_1 + \nu_2 \tag{5-14d}$$

$$-\alpha_{1E} \cdot \nu_1 - 0.5 \cdot \nu_2 + \delta \cdot \nu_3 = 0 \tag{5-14e}$$

$$1.81 \cdot \nu_1 + 3\nu_2 - \nu_3 = 0 \tag{5-14f}$$

From the above equations, it is possible to express the overall conversion rates of ethanol, oxygen, and carbon dioxide in terms of r_x (overall conversion rate of biomass). For instance, coupling Equations (5-14a), (5-14b), (5-4) and (5-2) with Equations (5-14e) and (5-14f), the overall conversion rate of ethanol becomes (See Appendix D for detailed mathematical derivations):

$$-r_e = \left(\frac{-0.635 + 2\delta + K}{3\delta - 0.5}\right) r_x + \left(\frac{m_{ATP}}{3\delta - 0.5}\right) \cdot C_x = \frac{1}{Y_{ex}^{\max}} r_x + m_e C_x \tag{5-15}$$

Equation (5-15) describes the amount of ethanol required for the production of biomass and maintenance. The following equations relate the maximal yields and maintenance to the metabolic model parameters (K, δ, m_{ATP}) based on Equation (5-15):

$$\frac{1}{Y_{ex}^{\max}} = \frac{-0.635 + 2\delta + K}{3\delta - 0.5} \tag{5-15a}$$

$$m_e = \frac{m_{atp}}{3\delta - 0.5} \tag{5-15b}$$

Equations (5-15a) and (5-15b) provide relations between the three energetic parameters: K, δ, m_{ATP}. If we assume that these three parameters are fundamental parameters for the strain, then a similar model as derived above can be derived for other substrates, and in this model the yield coefficients will be different functions of the three energetic parameters. If the yield coefficients are experimentally determined for growth on different substrates the energetic parameters can be estimated (Nielsen and Villadsen, 2001). An important assumption in this approach is that the values of parameters do not change with the carbon source, even though the functions change with different carbon sources.

For continuous operation, at steady state, $\vec{r} = 0$, thus the following equations can be obtained from Equation (5-14):

$$\vec{\phi} = -\theta_e \cdot \vec{\nu} \tag{5-16}$$

$$\phi_e = 1.27\nu_1 + \nu_2 \tag{5-16a}$$

$$\phi_x = -\nu_1 \tag{5-16b}$$

where ϕ_e and ϕ_x are the flow of ethanol and biomass into the system (C-mol/L-h), respectively. Therefore, by coupling Equations (5-14e), (5-14f) with Equations (5-16a) and (5-16b), the relation between the flows of ethanol and biomass at steady state in continuous mode can be expressed by (see Appendix D for detailed mathematical derivations):

$$\phi_e = \frac{1}{Y_{ex}^{\max}}(-\phi_x) + m_e C_x \qquad (5\text{-}17)$$

where the relations for the defined maximal yields and maintenance, and the metabolic model parameters (K,δ, m_{ATP}) are the same forms as indicated in Equations (5-15a) and (5-15b).

5.2 Model for Benzyl Alcohol Bioremediation

5.2.1 Metabolic Equations

The major metabolic activities taking place in benzyl alcohol bioremediation are shown in Figure 5-2 (developed in this work) and are described below.

(1) Biomass Synthesis from Benzyl Alcohol

It is assumed that in the synthesis of biomass, 0.27 mol CO_2 is produced per C-mole biomass synthesized (Gornmers *et al*., 1988). The stoichiometry of the biomass formation reaction from benzyl alcohol is as follows (expressed as 1 C-mol of benzyl alcohol and 1 C-mol of biomass):

$$-1.27CH_{8/7}O_{1/7} - 0.2NH_3 - \alpha_{1B}ATP - 0.758H_2O - 1.084NAD + CH_{7/5}O_{2/5}N_{1/5} + 1.084NADH_2 + 0.27CO_2 + \alpha_{1B}ADP = 0 \qquad (5\text{-}18)$$

where $\alpha_{1B} = K + \frac{m_{ATP}}{\mu}$ (when μ>0) is assumed to be the same form as described in Equation (5-4).

(2) Catabolism of Benzyl Alcohol

For benzyl alcohol, based on its pathway (See Appendix A-III), the catabolism is represented by the following reactions:

$$\underset{\text{Benzyl alcohol}}{C_7H_8O} + 2NAD + 3H_2O + 2O_2 \longrightarrow C_3H_4O_3 + C_2H_4O + CH_2O_2 + CO_2 + 2NADH_2 \qquad (5\text{-}19)$$

Pyruvate Acetaldehyde Formate

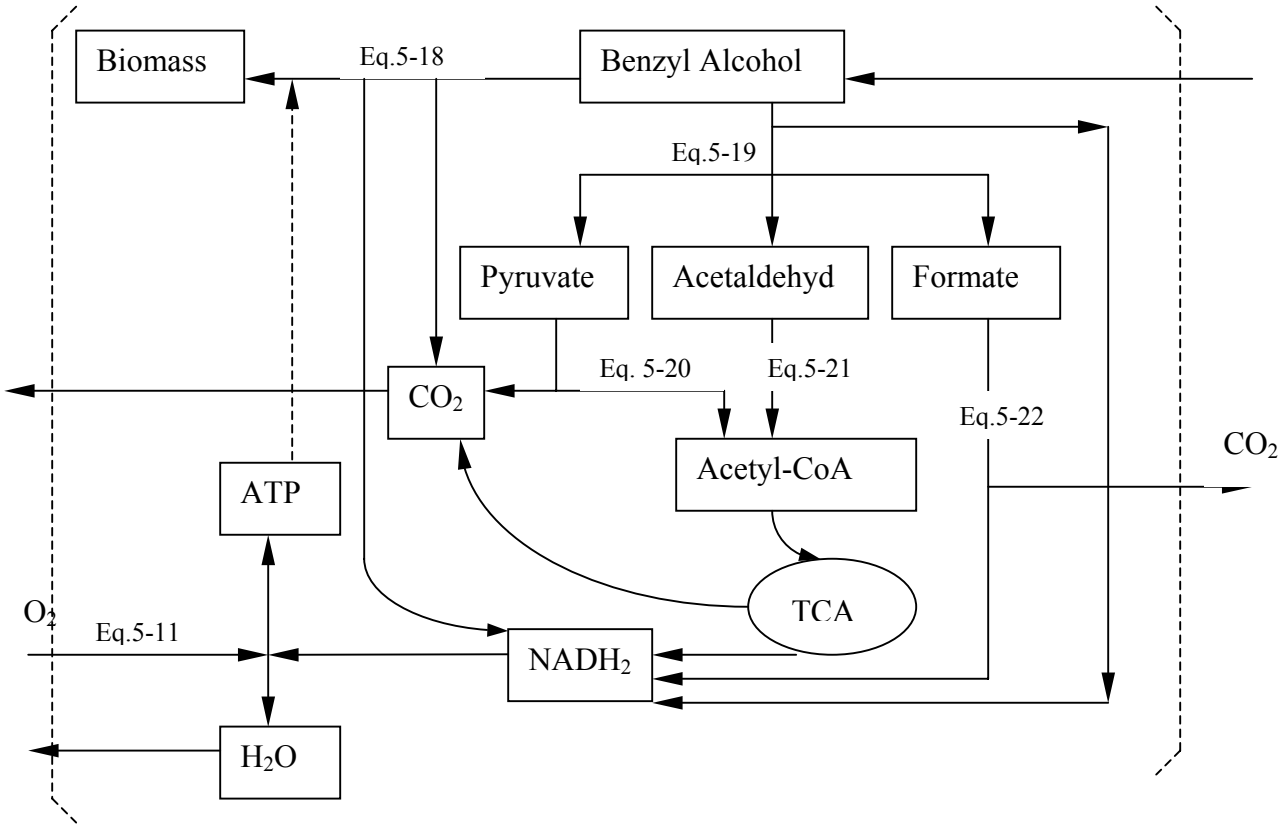

Figure 5-2 Hypothesized Metabolic Pathways for Benzyl Alcohol Bioremediation ("⟶ " indicates the conversion or transport of compounds; " ---▶" indicates the transport of energy ATP)

$$C_3H_4O_3 + NAD + CoASH \longrightarrow CH_3COSCoA + CO_2 + NADH_2 \quad (5\text{-}20)$$

$$C_2H_4O + NAD + CoASH \longrightarrow CH_3COSCoA + NADH_2 \quad (5\text{-}21)$$

$$CH_2O_2 + NAD \longrightarrow CO_2 + NADH_2 \quad (5\text{-}22)$$

In the TCA cycle,

$$2CH_3COSCoA + 6H_2O + 8\ NAD \longrightarrow 8NADH_2 + 4CO_2 + 2CoASH \quad (5\text{-}23)$$

Coupling the metabolic Equations (5-19) – (5-23), the overall catabolism of benzyl alcohol can then be represented by:

$$C_7H_8O + 13\ NAD + 9\ H_2O + 2O_2 \longrightarrow 13\ NADH_2 + 7\ CO_2 \qquad (5\text{-}24)$$

Equation (5-24) can be rearranged based on 1 C-mol benzyl alcohol as:

$$-CH_{8/7}O_{1/7} - \frac{9}{7}H_2O - \frac{2}{7}O_2 - \frac{13}{7}NAD + \frac{13}{7}NADH_2 + CO_2 = 0 \qquad (5\text{-}25)$$

(3) Oxidative Phosphorylation

The net amount of $NADH_2$ produced in the biomass precursor synthesis and in the benzyl alcohol catabolism reaction is consumed to yield ATP according to equation (5-11):

$$-NADH_2 - \frac{1}{2}O_2 - \delta ADP + H_2O + \delta ATP + NAD = 0 \qquad (5\text{-}11)$$

5.2.2 Mathematical Modeling

Similar to the procedure used in Section 5.1.2, the reaction Equations (5-18), (5-25) and (5-11) can be written in condensed form using the stoichiometric matrix θ_b, where the first compound is taken to be benzyl alcohol, followed by biomass, ammonia, oxygen, carbon dioxide, water, ATP, and $NADH_2$.

The conversion rates can be expressed as a function of the reaction rates by a set of linear equations with parameters composed of the stoichiometric coefficients (Roels, 1983). The stoichiometric matrix θ_b for three reactions (5-18), (5-25) and (5-11) can be written with 1 C-mol basis as:

$$\theta_b = \begin{bmatrix} r_b \\ r_x \\ r_N \\ r_{o_2} \\ r_{co_2} \\ r_w \\ r_{ATP} \\ r_{NADH} \end{bmatrix} = \begin{bmatrix} -1.27 & -1 & 0 \\ 1 & 0 & 0 \\ -0.2 & 0 & 0 \\ 0 & -\frac{2}{7} & -0.5 \\ 0.27 & 1 & 0 \\ -0.758 & -\frac{9}{7} & 1 \\ -\alpha_{11} & 0 & \delta \\ 1.084 & \frac{13}{7} & -1 \end{bmatrix} \quad (5\text{-}26)$$

The rates of reactions (5-18), (5-25) and (5-11) are ν_1 to ν_3, and can be expressed by the rate vector $\vec{\nu}$:

$$\vec{\nu} = \begin{bmatrix} \nu_1 \\ \nu_2 \\ \nu_3 \end{bmatrix} \quad (5\text{-}27)$$

The following set of eight linear relations is obtained, by writing out the balances for each of the 8 species (benzyl alcohol, biomass, ammonia, oxygen, carbon dioxide, water, ATP and $NADH_2$):

$$\vec{r} = \theta_b \cdot \vec{\nu} + \vec{\phi} \quad (5\text{-}28)$$

Where $\vec{\phi}$ is the vector of flow, and $\vec{r}$ is the vector of the overall conversion rates of the compounds.

For batch bioremediations, there was no flow into or out of the system, i.e., $\phi_b = 0$ and $\phi_x = 0$. Thus the overall conversion rates of benzyl alcohol and biomass based on 1 C-mol can be obtained as:

$$-r_b = 1.27\nu_1 + \nu_2 \quad (5\text{-}28a)$$

$$r_x = \nu_1 \tag{5-28b}$$

Again, if the well-known assumption (Roels, 1983) is made that no net accumulation of $NADH_2$ and ATP takes place, except as an integral part of biomass, Equations (5-28c) and (5-28d) can be obtained:

$$-\alpha_{1b} \cdot \nu_1 + \delta \cdot \nu_3 = 0 \tag{5-28c}$$

$$1.084 \cdot \nu_1 + \frac{13}{7}\nu_2 - \nu_3 = 0 \tag{5-28d}$$

Coupling Equations (5-28a) to (5-28d), the overall equation for the conversion of benzyl alcohol becomes (see Appendix D-2 for detailed mathematical derivations):

$$-r_b = \frac{(K + 1.274\delta)}{(13/7)\delta} r_x + [\frac{m_{ATP}}{(13/7)\delta}] \cdot C_x \tag{5-29}$$

If Equation (5-29) is re-written by introducing the defined maximal yields and maintenance terms, Equation (5-30) can be formed:

$$-r_b = \frac{1}{Y_{bx}^{\max}} r_x + m_b C_x \tag{5-30}$$

Equation (5-30) describes the amount of benzyl alcohol required for the production of biomass and maintenance. By coupling Equations (5-29) and (5-30), the following relations for the defined maximal yields and maintenance, and the metabolic model parameters (K, δ, m_{ATP}) can be obtained:

$$\frac{1}{Y_{bx}^{\max}} = \frac{(K + 1.274\delta)}{(13/7)\delta} \tag{5-30a}$$

$$m_b = \frac{m_{atp}}{(13/7)\delta} \tag{5-30b}$$

For continuous operation, at steady state, $\vec{r} = 0$, thus the following equations can be obtained from Equation (5-28):

$$\vec{\phi} = -\theta_b \cdot \vec{\nu} \tag{5-31}$$

$$\phi_b = 1.27\nu_1 + \nu_2 \tag{5-31a}$$

$$\phi_x = -\nu_1 \tag{5-31b}$$

where ϕ_b and ϕ_x represent the flow of ethanol and biomass into the system (C-mol/L h), respectively. Therefore, by coupling Equations (5-28c), (5-28d) with Equations (5-31a) and (5-31b), the relationship between the flows of benzyl alcohol and biomass under steady state and continuous mode conditions can be expressed by:

$$\phi_b = \frac{1}{Y_{bx}^{\max}}(-\phi_x) + m_b C_x \tag{5-32}$$

where the relations for the defined maximal yields and maintenance and the metabolic model parameters (K, δ, m_{ATP}) are the same forms as indicated in Equations (5-30a) and (5-30b).

5.3 Estimation of Parameters

5.3.1 Estimation of Parameters from Batch Growth Results

In this work, it is assumed that the substrate concentration in the media is rate controlling according to simplistic non-structured models. Thus, for experiments conducted in a batch reactor, the overall conversion rates of the controlled components can be represented by

$$r = \frac{dC}{dt} \tag{5-33}$$

where r is the overall conversion rate of the key metabolic component (C-mol/L-h), C is the concentration of the key metabolic component (C-mol/L).

For the kinetic model of ethanol as sole substrate, the Monod model was used as the rate controlling equation for growth metabolism:

$$r_x = \mu C_x = \frac{\mu_{e,\max} C_e}{K_e + C_e} C_x \tag{5-34}$$

To allow for maintenance requirements, Equation (5-34) is coupled with Equation (5-15), and the expression for ethanol conversion rate becomes:

$$-\frac{dC_e}{dt} = (\frac{1}{Y_{xe}^{\max}})(\frac{\mu_{e,\max} C_e}{K_e + C_e})C_x + m_e C_x \tag{5-35}$$

Similarly, for the kinetic modeling of benzyl alcohol as sole substrate, the following substrate inhibition model is assumed to apply (Luong, 1987):

$$r_x = \mu C_x = \frac{\mu_{b,\max} C_b}{K_b + C_b}(1 - \frac{C_b}{C_{b,\max}})^n \cdot C_x \tag{5-36}$$

The benzyl alcohol conversion rate is obtained by coupling Equations (5-30) and (5-36):

$$-\frac{dC_b}{dt} = (\frac{1}{Y_{xb}^{\max}})(\frac{\mu_{b,\max} C_b}{K_b + C_b})(1 - \frac{C_b}{C_{b,\max}})^n \cdot C_x + m_b C_x \tag{5-37}$$

For parameter estimation purposes, nine independent sets of batch experiments were conducted with different initial ethanol concentrations (0.10, 0.12, 0.17, 0.18 and 0.26 C-mol/L), and with differential initial benzyl alcohol concentrations (0.048, 0.069, 0.14, and 0.18 C-mol/L) added into the reactor at time zero. Measurements of the concentrations of ethanol and biomass were obtained in the first five sets of experiments, and concentration measurements were performed for benzyl alcohol and biomass in the last four sets of experiments at certain time intervals throughout the reactions.

The data sets used to evaluate the kinetic parameters through a least squares, nonlinear regression technique. The concentration profiles of the key components were calculated and the parameters were adjusted to minimize the sum of square of differences between the experimental results and the simulated results from the derived model. The ordinary differential equations were solved for the concentration profiles of the key components by applying the Runge-Kutta, 4^{th} order numerical procedure using the spreadsheet: EXCEL. The least squares of the differences between the experimental results and the simulated results were solved by the SOLVER function in the EXCEL program to obtain the optimum parameters. The optimum parameters for ethanol and benzyl alcohol bioremediation obtained as such are given in Tables 5.1 and 5.2, respectively. The uncertainty was estimated using Monte Carlo method (See Section 5.3.2). Applying the yield coefficients of ethanol and benzyl alcohol of 0.59 and 0.45 to Equations (5-15a) and (5-30a), one can obtain:

$$\delta = 0.91 \pm 0.03 \tag{5-38}$$

$$K = 2.61 \pm 0.13 \tag{5-39}$$

The error analysis for these two parameters (δ and K) is given in Appendix E.

Table 5.1 Optimum Parameters for Ethanol Bioremediation

Parameters (units)	Symbol	Value	Units
The Maximum Yield	$Y_{xe}^{\max}$	0.59 ± 0.002	
The Maximum Specific Rate of Biomass Synthesis	$\mu_{xe}^{\max}$	0.56 ± 0.01	1/h
The Half Saturation Constant of Biomass Synthesis	K_e	0.026 ± 0.008	C-mol/L
The Specific Maintenance Rate	$m_{s,e}$	0.053 ± 0.006	C-mol/C-mol-h

Table 5.2 Optimum Parameters for Benzyl Alcohol Bioremediation

Parameters	Symbol	Value	Units
The Maximum Yield	$Y_{xb}^{\max}$	0.45 ± 0.01	
The Maximum Specific Rate of Biomass Synthesis	$\mu_{xb}^{\max}$	0.42 ± 0.01	1/h
The Half Saturation Constant of Biomass Synthesis	K_b	0.022 ± 0.007	C-mol/L
The Specific Maintenance Rate	[1] $m_{s,b}$	0.030-0.072	C-mol/C-mol h
The Maximum Substrate Conc.	$C_{b,\max}$	0.19 ± 0.01	C-mol/L
Inhibition Power	n	0.3 ± 0.07	

[1] Due to the inhibition of benzyl alcohol, the maintenance for growth varied from 0.014 to 0.072 C-mol/C-mol h for benzyl alcohol initial concentrations ranging from 0.05 to 0.19 C-mol/L.

Figures 5.3(a-e) show the simulation results for five individual runs of ethanol bioremediation using the optimum parameters in Table 5.1. The parity plots presented in Figures 5.4 (a-b) compare the simulation results with the batch experimental results of ethanol bioremediation at different initial ethanol concentrations. The dash lines in

Figures 5.4a and 5.4b present 95% confidence intervals: error = $\pm t_{0.025,N} * S$ (Kennedy and Neville, 1974), where $t_{0.025,53} = 2.009$, s is the standard deviation (for biomass s_x = 0.0057 C-mol/L; for ethanol s_e = 0.0089 C-mol/L). The results reveal that most of the predicted values for both ethanol and biomass fall within 95% confidence level.

Figure 5-4c shows the determination of specific growth rates of *Pseudomonas putida* (ATCC 23973) on ethanol by plotting ln(X) versus time for the batch runs. The slope of the straight line gives the specific growth rate of bacteria during the exponential growth phase, which is found to be $0.37 \pm 0.03\ h^{-1}$ for ethanol initial concentrations between 2.3 to 5.8 g/L. This result shows that there is no inhibition effect for ethanol growing on *P. putida* within the range of this investigation, which verifies the use of the Monod model for growth on ethanol.

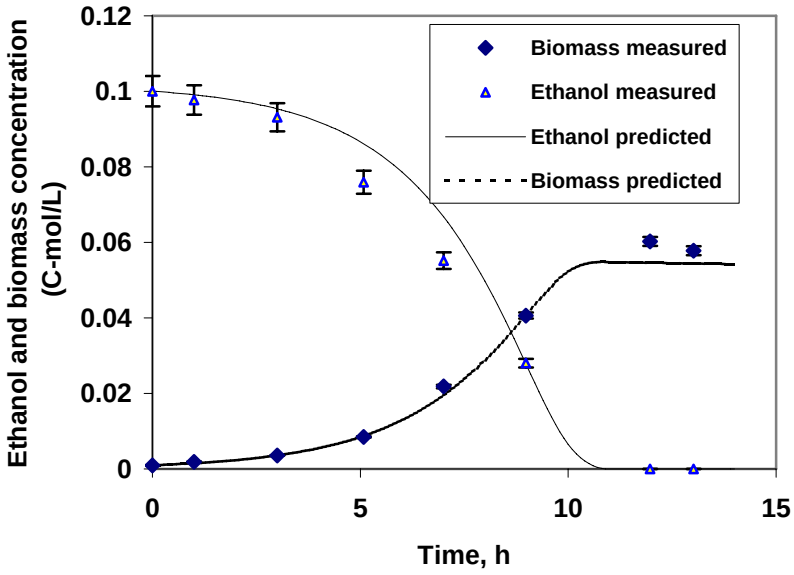

Figure 5.3 (a) Simulation of ethanol bioremediation at initial ethanol concentration of 0.10 C-mol/L.

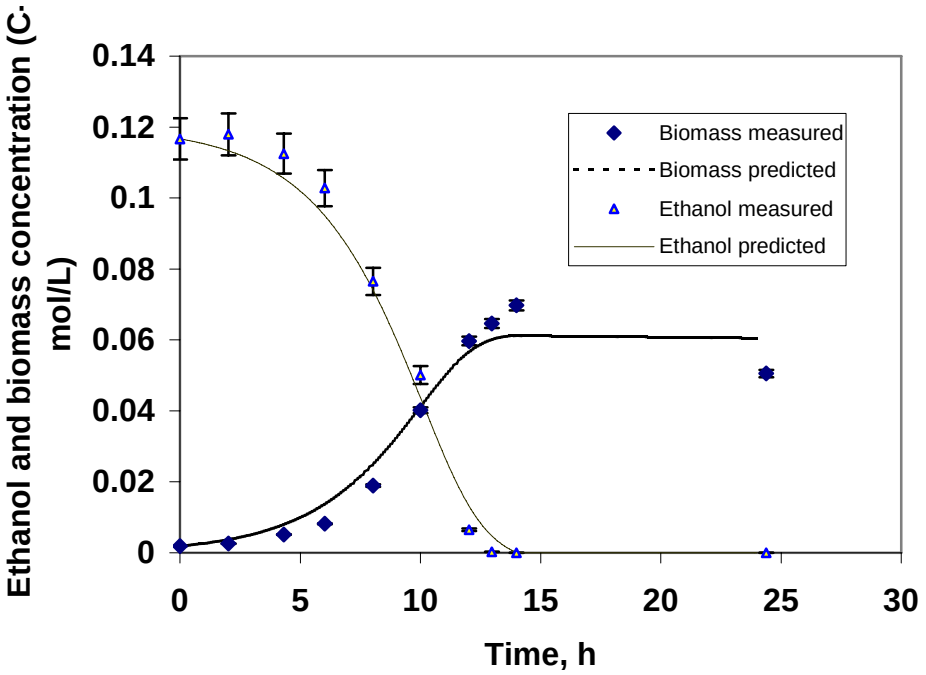

Figure 5.3 (b) Simulation of ethanol bioremediation at initial ethanol concentration of 0.12 C-mol/L.

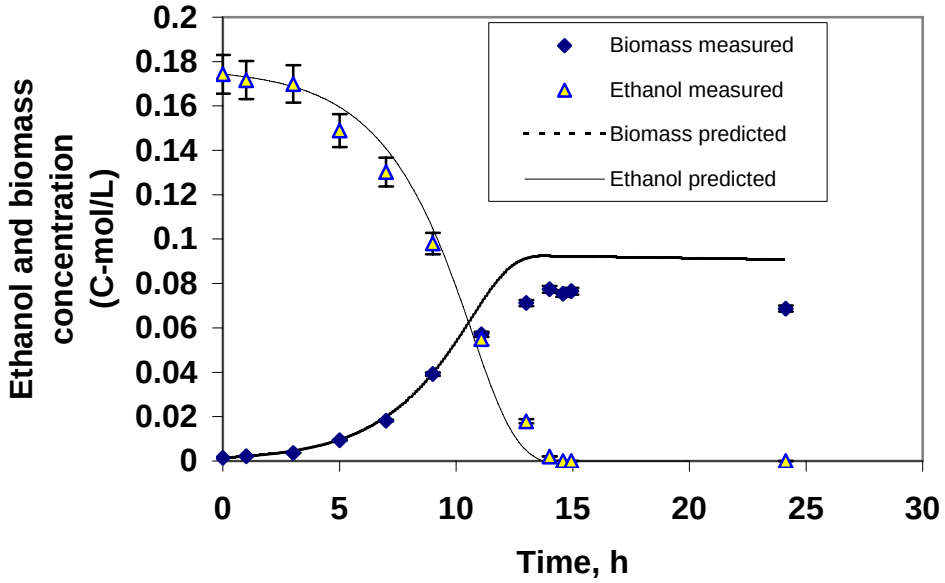

Figure 5.3 (c) Simulation of ethanol bioremediation at initial ethanol concentration of 0.17 C-mol/L.

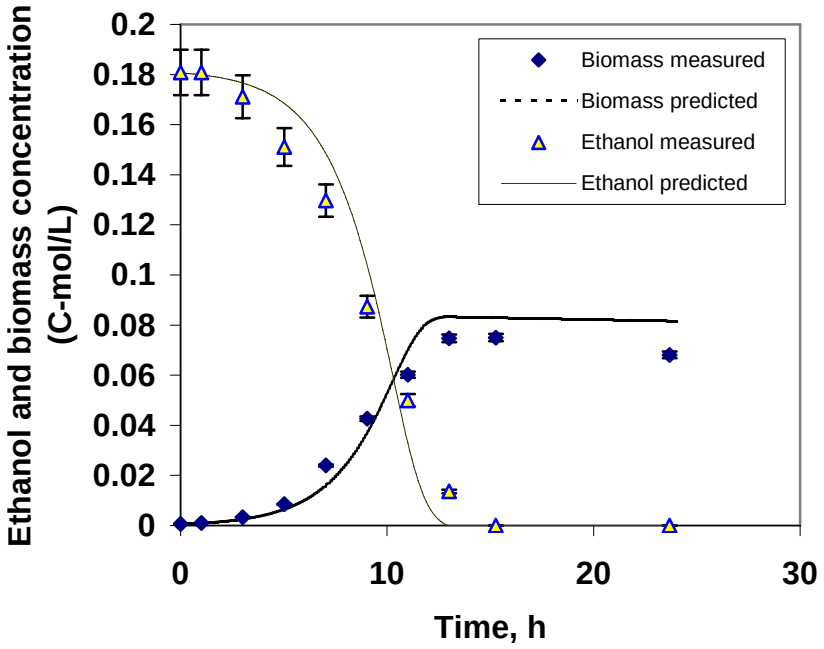

Figure 5.3 (d) Simulation of ethanol bioremediation at initial ethanol concentration of 0.18 C-mol/L.

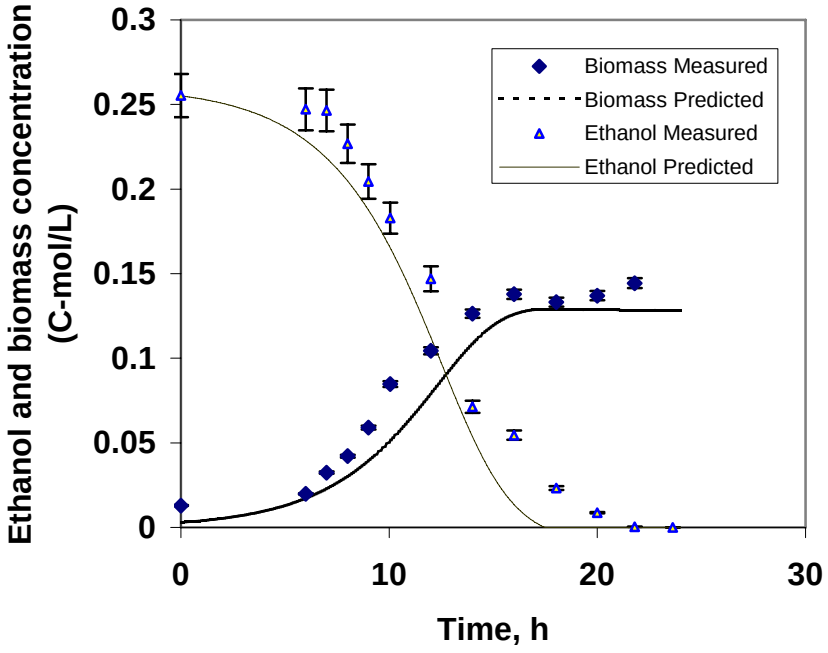

Figure 5.3 (e) Simulation of ethanol bioremediation at initial ethanol concentration of 0.25 C-mol/L.

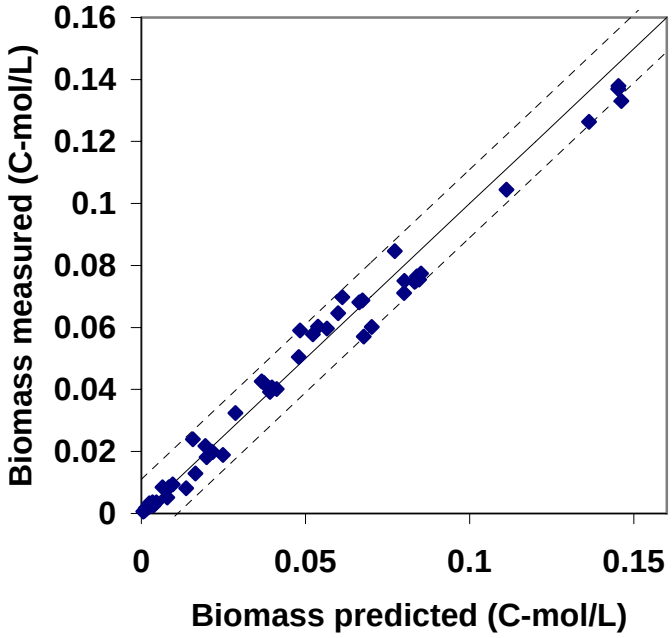

Figure 5.4a Comparison of the simulation results and the experimental results of biomass at different initial ethanol concentrations (--- 95% confidence interval: $\hat{y} \pm t_{0.025} * s$)

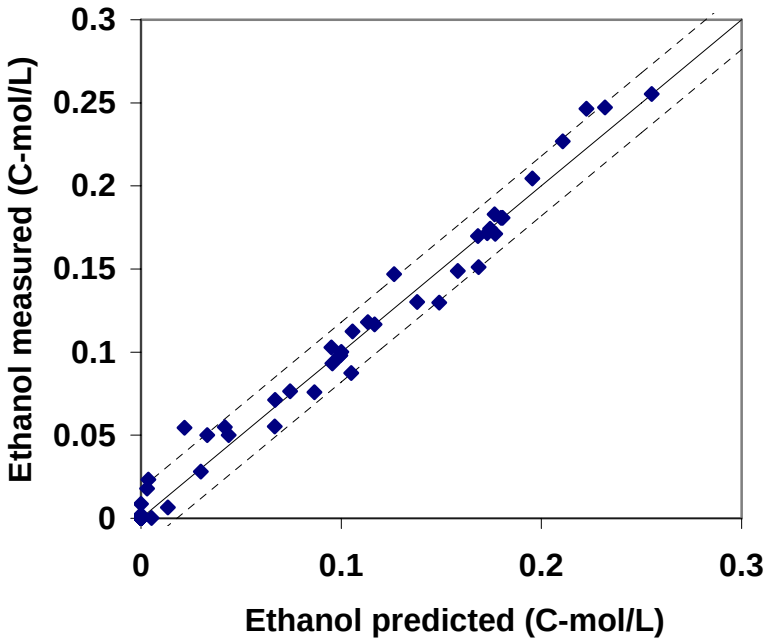

Figure 5.4b Comparison of the simulation results and the experimental results of ethanol at different initial ethanol concentrations (---95% confidence interval: $\hat{y} \pm t_{0.025} * s$)

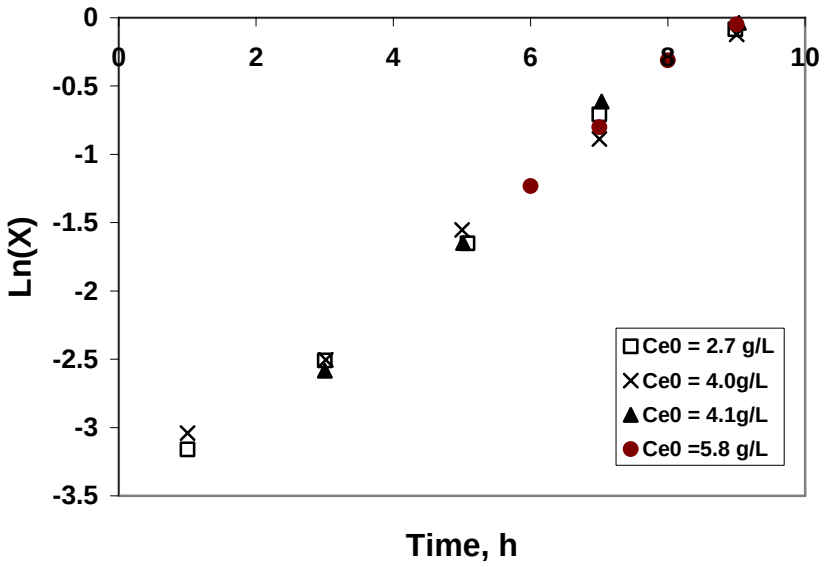

Figure 5.4c Determination of the specific growth rates of *P.putida* on ethanol

Figures 5.5 (a-d) demonstrate the simulation results using the optimum parameters in Table 5.2 for benzyl alcohol bioremediation. The parity plots presented in Figures 5.6 (a-b) compare the simulation results with the batch experimental results of benzyl alcohol bioremediation at different initial benzyl alcohol concentrations. The dash lines in Figures 5.6a and 5.6b present 95% confidence interval: error $= \pm t_{0.025,N} * s$ (Kennedy and Neville, 1974), where $t_{0.025,30}$ =2.042, s is the standard error: for biomass s_x =0.0019 , for benzyl alcohol s_b=0.0031. The results reveal that most of the predicted values for both biomass and benzyl alcohol fall within 95% confidence level.

Figure 5-6c shows the determination of the specific growth rates of *Pseudomonas putida* (ATCC 23973) on benzyl alcohol by plotting ln (*X*) versus time for the batch runs. The slopes of the straight lines determined as such are shown on the graph, which indicates that benzyl alcohol inhibits the growth of *P. putida*. The μ_{max} value was found to be $0.41h^{-1}$ using Equation (4-10), which agrees with the result obtained by using non-linear fitting (see Table 5.2). From the comparison of the simulated results and the experimental results, the simulation models for both ethanol and benzyl alcohol bioremediation are capable of accurately predicting the growth data.

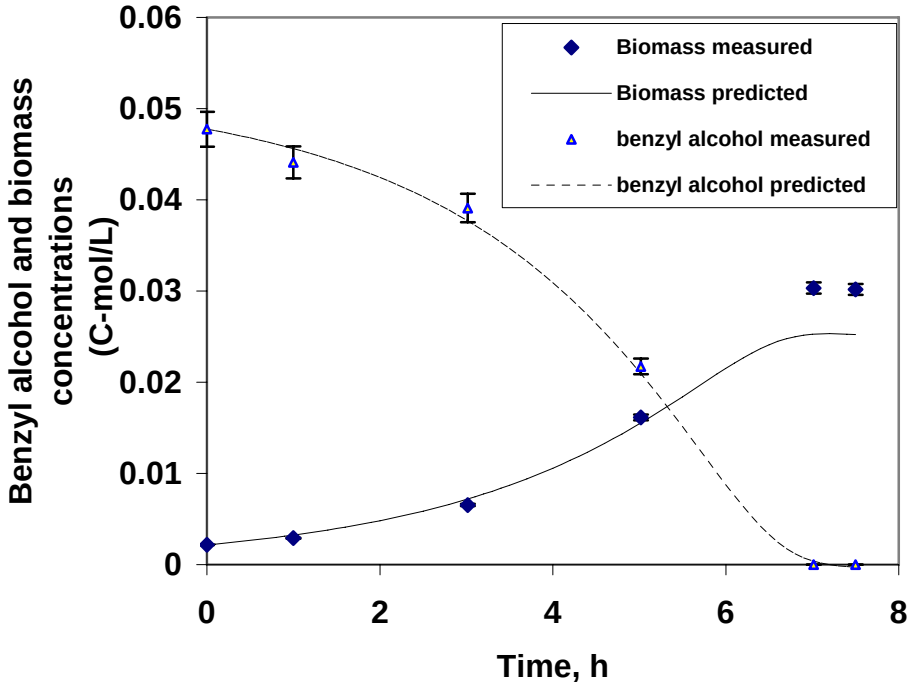

Figure 5.5(a). Simulation of benzyl alcohol bioremediation at initial benzyl alcohol concentration of 0.048 C-mol/L.

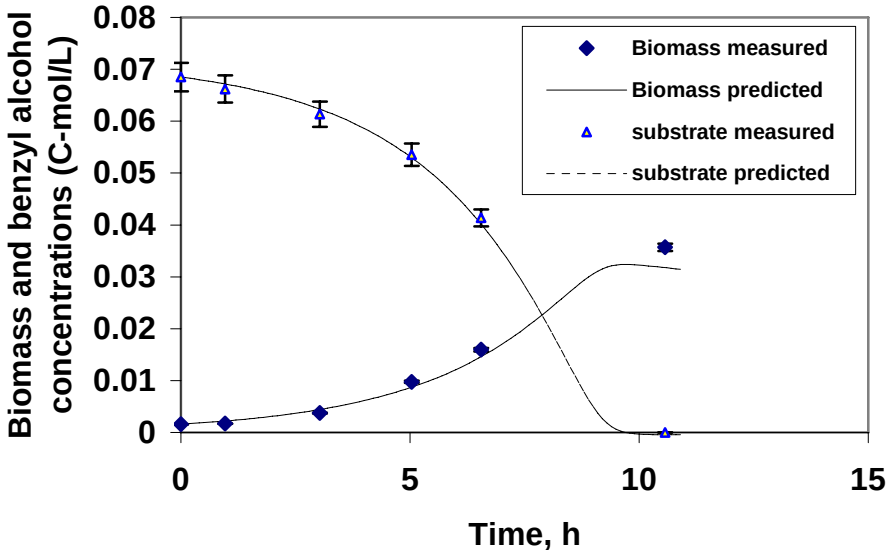

Figure 5.5(b). Simulation of benzyl alcohol bioremediation at initial benzyl alcohol concentration of 0.068 C-mol/L.

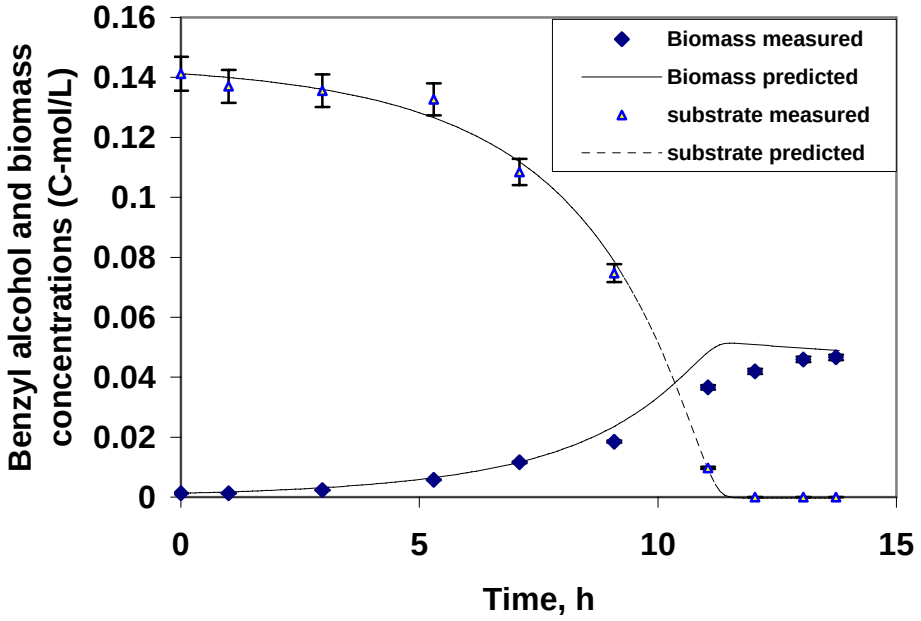

Figure 5.5(c). Simulation of benzyl alcohol bioremediation at initial benzyl alcohol concentration of 0.14 C-mol/L.

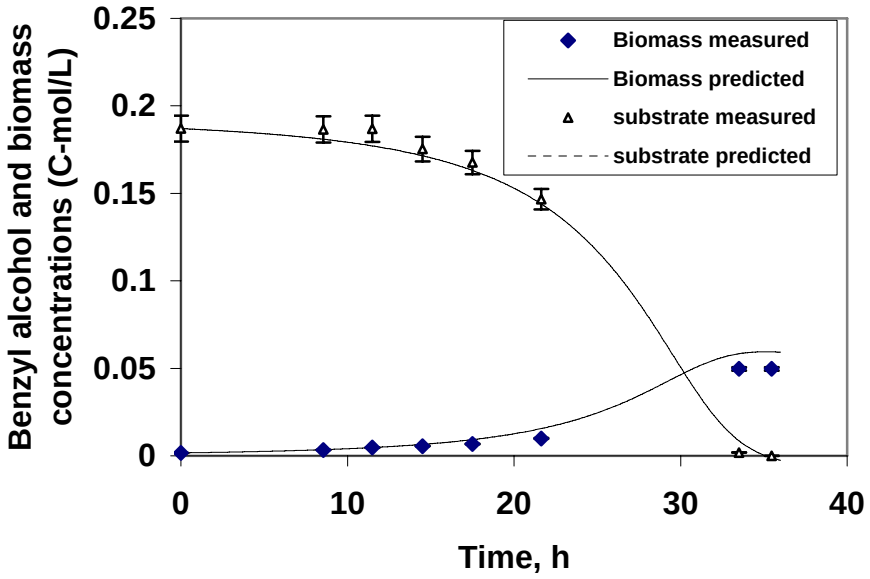

Figure 5.5(d). Simulation of benzyl alcohol bioremediation at initial benzyl alcohol concentration of 0.18 C-mol/L.

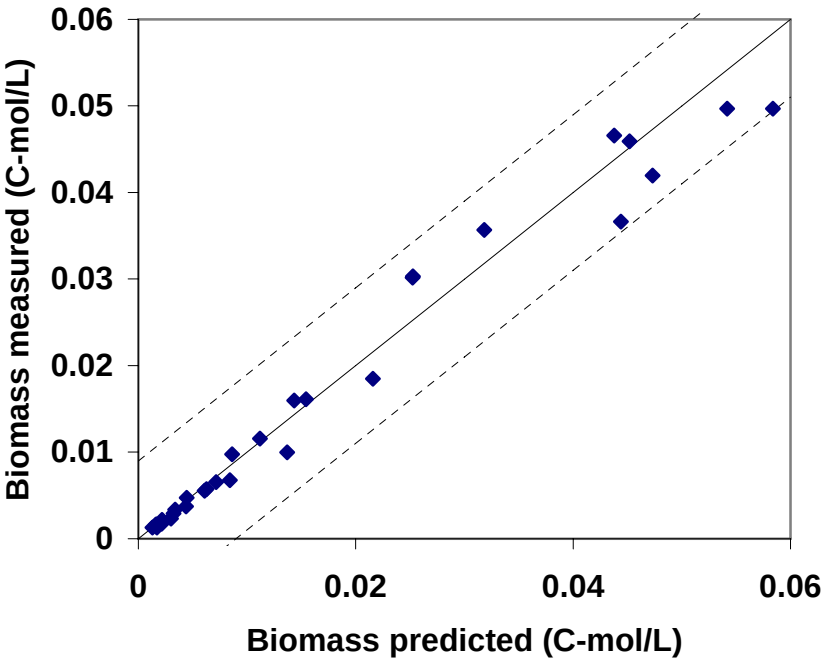

Figure 5.6a Comparison of the simulation results and the experimental results of biomass at different initial benzyl alcohol concentrations (--- 95% confidence interval)

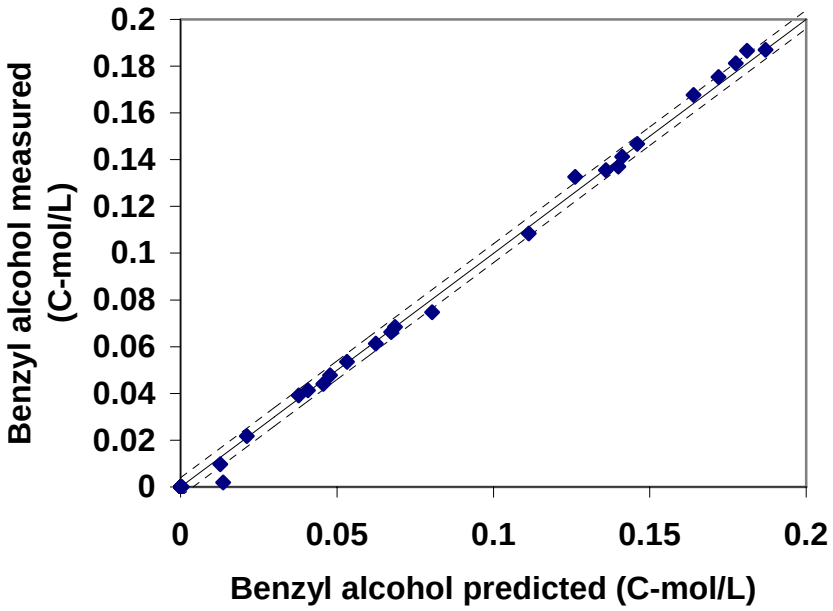

Figure 5.6b Comparison of the simulation results and the experimental results of benzyl alcohol at different initial benzyl alcohol concentrations (---95% confidence interval)

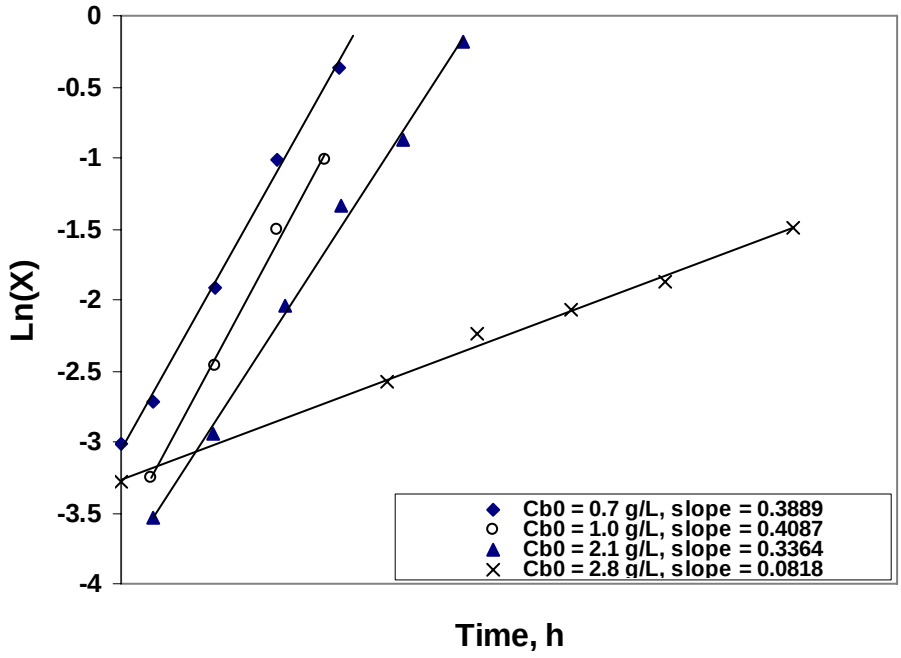

Figure 5.6c Determination of the specific growth rates of *P.putida* on benzyl alcohol

5.3.2 Parameters Uncertainty Analysis

The Monte Carlo method consists of "sampling" to create artificial data sets that are analyzed statistically to learn how well a model performs. The Monte Carlo method has been applied to determine the uncertainty of parameters using a non-linear model fitting technique (Feller and Blaich, 2001; Wang, 2001; Purwaningsih, 2002). The evaluation of the mathematical model with Monte Carlo "sampling" is carried out by the following procedure.

1) Determining the mean and error estimate (equal to standard deviation) of experimental data based on experimental replication.

   The mean at a specific measuring time is calculated by Equation (5-40):

$$\bar{x} = \frac{\sum_{i=1}^{5} x_i}{N} \qquad (5\text{-}40)$$

where x_i is the ith measurement for a controlled component, and N is the number of replication experimental runs.

The normalized deviation for a controlled component at a specific measuring time is calculated by Equation (5-40a):

$$error = \sqrt{\frac{\sum_{1}^{n} (x_i - \bar{x})^2}{(N-1)}} / \bar{x} \qquad (5\text{-}40a)$$

2) Generating data sets of synthetic experimental results as:

$$\text{Simulated data} = (1\text{-error}) \cdot \bar{x} + t_{0.025,20} \cdot \text{error} \cdot \bar{x} \cdot Rand() \qquad (5\text{-}41)$$

where $t_{0.025,20} \approx 2$, and *Rand()* (a function in EXCEL) returns an evenly distributed random number greater than or equal to 0 and less than or equal to 1. A new random number is returned every time the worksheet is calculated.

3) Performing a non-linear fitting procedure on the synthetic data sets to obtain the kinetic parameter value(s).

4) Repeating the Monte Carlo "Sampling" 20 times to generate 20 sets of "artificial experimental data", thereby creating 20 sets of the kinetic parameter value(s) (Wang, 2001; Purwaningsih, 2002).

5) The distribution of kinetic parameter values is used to calculate the uncertainty range associated with the fit parameters.

The uncertainty values of parameters obtained above are shown in Tables 5-1 and 5-2 for the parameters of ethanol and benzyl alcohol as sole substrate, respectively.

5.4 Modeling of Continuous Bioremediation

5.4.1 Modeling of Continuous Ethanol Bioremediation at Steady State

The relationship between the flows of ethanol and biomass under the continuous steady state conditions, can be derived from Equation (5-17):

$$\phi_e \cdot Y_{ex}^{\max} = (-\phi_x) + m_{e,c} C_x \qquad (5\text{-}42)$$

where $m_{e,c}$ is the maintenance factor at steady state conditions for ethanol bioremediation. The flows of ethanol and biomass are represented by Equation (5-42a) and (5-42b):

$$\phi_e = \frac{Q(y_{in} - y_{out})}{V} + \frac{F(C_{e0} - C_e)}{V} \qquad (5\text{-}42a)$$

$$-\phi_x = \frac{F(C_x - C_{x0})}{V} = \mu C_x \qquad (5\text{-}42b)$$

The biomass concentration in the reactor operating under steady state continuous conditions, can then be obtained by coupling Equation (5-42) with Equations (5-42a) and (5-42b):

$$C_x = \frac{\phi_e \cdot Y_{ex}^{\max}}{(\mu + m_{e,c})} \qquad (5\text{-}43)$$

In Equation (5-43) ϕ_e, C_x and μ were directly measured during the continuous bioremediation of ethanol. By applying these experimental results (Figure 5-7), $m_{e,c}$ was found to be 0.010 ± 0.001 (C-mol/C-mol-h). The maintenance required for growth on

ethanol in a steady state mode is lower than the amount required in a batch mode. Therefore, biomass growth is more efficient when conducted under steady state continuous conditions than the growth in batch condition. This is believed caused by different environmental conditions such as pH level.

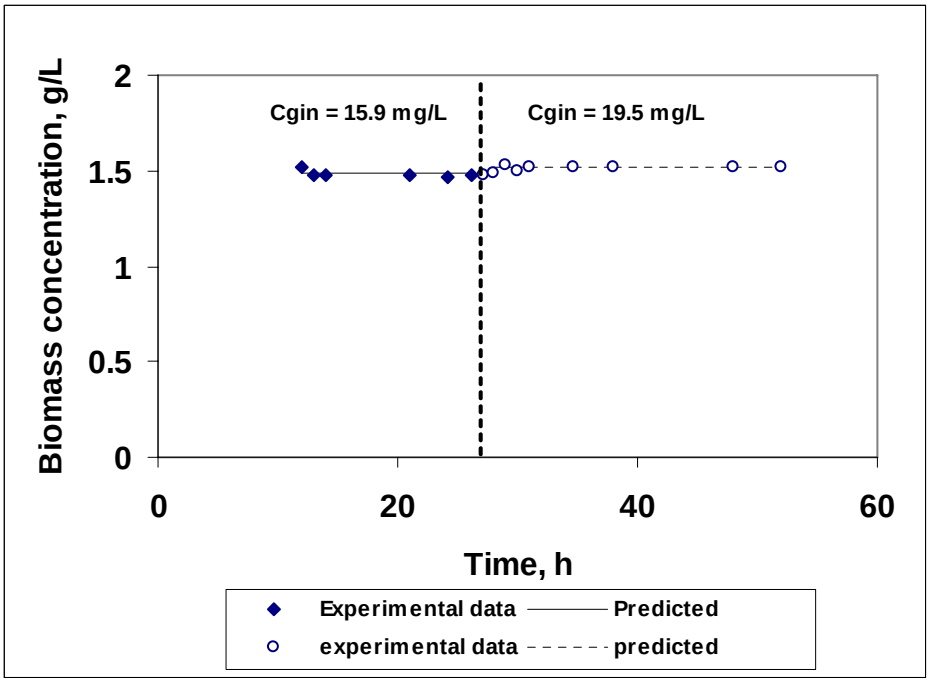

Figure 5-7 Simulation of ethanol bioremediation at steady state (ethanol inlet concentration of 15.9 and 19.5 mg/L)

5.4.2 Modeling of Continuous Bioremediation of Ethanol and Toluene Mixtures at Steady State

Because toluene, as the sole carbon and energy source, did not lead to steady state conditions, the acquired data is insufficient for verifying the models, i.e., from the results of the experimental studies, toluene by itself cannot be oxidized by *Pseudomonas putida*. Therefore, all further toluene-related models will deal with bioremediation of a mixture of toluene and benzyl alcohol and/or ethanol.

When the concept of inhibited co-metabolism is applied to bioremediation of mixtures of toluene and ethanol, it is assumed that biomass formed from ethanol and toluene acts as an inhibitor (Bailey and Ollis, 1986; Chang *et al*, 1993; Bielefeldt and Stensel, 1999). In addition to the reaction Equations (5-3), (5-10) and (5-11) for ethanol bioremediation, toluene catabolism is represented by Equation (5-44) on a 1 C-mol basis, which was derived from the toluene pathway (Davey and Gibson, 1974; Wackett, 2004, see Appendix A-III):

$$CH_{8/7} + \frac{8}{7}H_2O + \frac{3}{7}O_2 + \frac{12}{7}NAD \xrightarrow{r_4} \frac{12}{7}NADH_2 + CO_2 \qquad (5\text{-}44)$$

The stoichiometric matrix, θ_{et}, for four reactions (5-3), (5-10), (5-11) and (5-44) can be written as

$$\theta_{et} = \begin{bmatrix} r_e \\ r_t \\ r_x \\ r_{o_2} \\ r_{co_2} \\ r_{ATP} \\ r_{NADH} \end{bmatrix} = \begin{bmatrix} -1.27 & -1 & 0 & 0 \\ 0 & 0 & 0 & -1 \\ 1 & 0 & 0 & 0 \\ 0 & 0 & -0.5 & -\frac{3}{7} \\ 0.27 & 1 & 0 & 1 \\ -\alpha_{1E} & -0.5 & \delta & 0 \\ 1.81 & 3 & -1 & \frac{12}{7} \end{bmatrix} \qquad (5\text{-}45)$$

The reaction rate vector ν for four reactions (5-3), (5-10), (5-11), and (5-44) can be written as:

$$\vec{\nu} = \begin{bmatrix} \nu_1 \\ \nu_2 \\ \nu_3 \\ \nu_4 \end{bmatrix} \qquad (5\text{-}46)$$

where ν_1, ν_2, ν_3, ν_4 are the rates of reactions according to Equations (5-3), (5-10), (5-11), and (5-44) respectively. The following set of seven linear relations is obtained, by writing out the compound balances for each of the seven compounds (ethanol, toluene, biomass, oxygen, carbon dioxide, ATP and $NADH_2$):

$$\vec{r} = \theta_{et} \cdot \vec{\nu} + \vec{\phi} \tag{5-14}$$

where $\vec{\phi}$ is the vector of flows, and $\vec{r}$ is the vector of the overall conversion rates.

For continuous operation at steady state, $\vec{r} = 0$, the following equations can be obtained from Equation (5-14):

$$\vec{\phi} = -\theta_{et} \cdot \vec{\nu} \tag{5-47}$$

Again, if the well-known assumption (Roels, 1983) is made that no net accumulation of $NADH_2$ and ATP takes place, i.e., Equations (5-47a) and (5-47b) are obtained:

$$-\alpha_{1b} \cdot \nu_1 - 0.5\nu_2 + \delta \cdot \nu_3 = 0 \tag{5-47a}$$

$$1.81 \cdot \nu_1 + 3\nu_2 - \nu_3 + \frac{12}{7}\nu_4 = 0 \tag{5-47b}$$

The following equations can be obtained from Equations 5-47:

$$\phi_e = 1.27\nu_1 + \nu_2 \tag{5-47c}$$

$$\phi_T = \nu_4 \tag{5-47d}$$

$$\phi_x = -\nu_1 \tag{5-47e}$$

where ϕ_e, ϕ_T and ϕ_x represent the flow of ethanol, toluene, and biomass into the system (C-mol/L h), respectively. Therefore, by coupling Equations (5-47c) to (5-47e) with Equations (5-47a) and (5-47b), the relation between the flows of ethanol, toluene and biomass with steady state, continuous mode operation can be expressed by:

$$\phi_e \cdot Y_{ex}^{\max} + \phi_T \cdot Y_{tx}^{\max} = (-\phi_x) + m_{et} C_x \quad (5\text{-}48)$$

Coupling with the parameters obtained from Equations (5-38) and (5-39), the maximal yield coefficients of ethanol and toluene were found to be 0.59 and 0.41, respectively:

$$Y_{ex}^{\max} = \frac{3\delta - 0.5}{K + 2\delta - 0.635} = 0.59 \quad (5\text{-}48a)$$

$$\text{and } Y_{tx}^{\max} = \frac{12\delta}{7(K + 2\delta - 0.635)} = 0.41 \quad (5\text{-}48b)$$

In Equation (5-48), $(-\phi_x) = \frac{F(C_x - C_{x0})}{V} = \mu C_x$, thus the concentration of biomass can be determined as:

$$C_x = \frac{1}{(\mu + m_{et})} \cdot (\phi_e \cdot Y_{ex}^{\max} + \phi_T \cdot Y_{tx}^{\max}) \quad (5\text{-}49)$$

In Equation (5-49), $\phi_e = \frac{Q(y_{in} - y_{out})}{V} + \frac{F(C_{e0} - C_e)}{V}$, (5-49a)

$$\phi_T = \frac{Q(y_{in,T} - y_{out,T})}{V} + \frac{F(C_{T0} - C_T)}{V} , \quad (5\text{-}49b)$$

ϕ_e and ϕ_T can be then calculated from the measured data in the experimental studies. Coupling Equations (5-49), (5-49a) to (5-49b) with Equation (5-48a) and (5-48b), the maintenance for biomass growth in steady state bioremediation of mixed toluene and ethanol was then predicted as 0.027 ± 0.001 (C-mol/L/C-mol h) by applying the experimental data at steady state (Figure 5-8). This maintenance term is higher than that (0.010 ± 0.001 C-mol/C-mol h) for bioremediation of ethanol as sole carbon source in a continuous operation. This is caused by the stress of metabolizing toluene, a more toxic substrate.

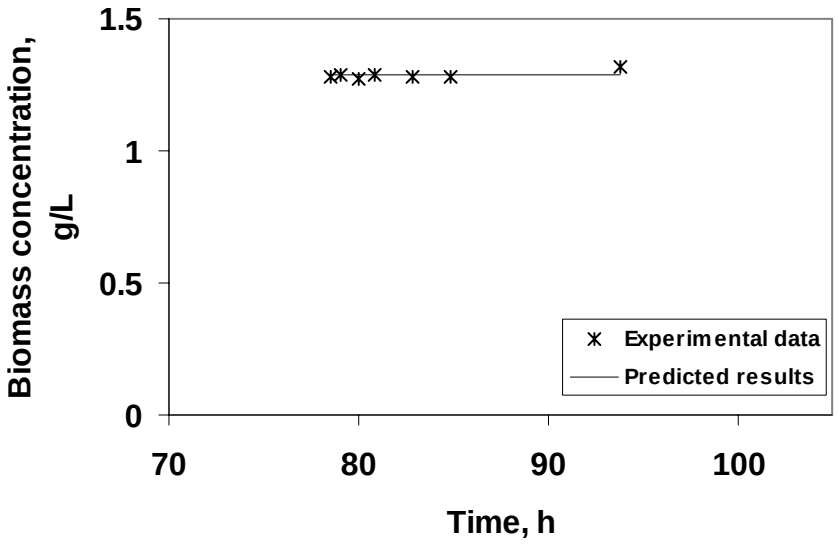

Figure 5-8 Simulation of mixed toluene and ethanol bioremediation at steady state (ethanol inlet of 15.9 mg/L and toluene inlet of 4.5 mg/L)

5.4.3 Modeling of Mixed Toluene Benzyl Alcohol Bioremediation at Steady State

Based on the toluene pathway (Davey and Gibson, 1974; Wackett, 2004, see Appendix A-III), toluene is first converted to benzyl alcohol with the consumption of $NADH_2$:

$$CH_{8/7} + \frac{1}{7} NADH_2 + \frac{1}{7} O_2 \xrightarrow{r_4} CH_{8/7}O_{1/7} + \frac{1}{7} H_2O + NAD \qquad (5\text{-}50)$$

An assumption is made that biomass is formed from only benzyl alcohol, and is not generated by this first metabolic step. The stoichiometric matrix θ_{bt} for the four reactions (5-18), (5-25), (5-11) and (5-50) can be written as:

$$\theta_{bt} = \begin{bmatrix} r_b \\ r_t \\ r_x \\ r_N \\ r_{o_2} \\ r_{co_2} \\ r_{ATP} \\ r_{NADH} \end{bmatrix} = \begin{bmatrix} -1.27 & -1 & 0 & 1 \\ 0 & 0 & 0 & -1 \\ 1 & 0 & 0 & 0 \\ -0.2 & 0 & 0 & 0 \\ 0 & -\frac{2}{7} & -0.5 & -\frac{1}{7} \\ 0.27 & 1 & 0 & 0 \\ -\alpha_{11} & 0 & \delta & 0 \\ 1.084 & \frac{13}{7} & -1 & -\frac{1}{7} \end{bmatrix} \quad (5\text{-}51)$$

The rates of reactions (5-18), (5-25), (5-11) and (5-50) are ν_1 to ν_4, and can be expressed by the rate vector $\vec{\nu}$:

$$\vec{\nu} = \begin{bmatrix} \nu_1 \\ \nu_2 \\ \nu_3 \\ \nu_4 \end{bmatrix} \quad (5\text{-}51a)$$

By writing out the compound balances for each of the eight compounds (benzyl alcohol, toluene, biomass, ammonia, oxygen, carbon dioxide, ATP and $NADH_2$), the following nine linear relations are obtained:

$$\vec{r} = \theta_{bt} \cdot \vec{\nu} + \vec{\phi} \quad (5\text{-}52)$$

where $\vec{\phi}$ is the vector of flow, and $\vec{r}$ is the vector of the overall conversion rates of the compounds.

For continuous operation at steady state, $\vec{r} = 0$, thus the following equations can be obtained from Equation (5-52):

$$\vec{\phi} = -\theta_{bt} \cdot \vec{\nu} \quad (5\text{-}53)$$

$$\phi_b = 1.27\nu_1 + \nu_2 - \nu_4 \quad (5\text{-}53a)$$

$$\phi_T = \nu_4 \tag{5-53b}$$

$$\phi_x = -\nu_1 \tag{5-53c}$$

where ϕ_b , ϕ_t and ϕ_x are the flow of benzyl alcohol, toluene, and biomass into the system (C-mol/L h), respectively.

Again, if the well-known assumption (Roels, 1983) is made that no net accumulation of $NADH_2$ and ATP takes place, the Equations (5-47a) and (5-47b) can be obtained:

$$-\alpha_{1b} \cdot \nu_1 + \delta \cdot \nu_4 = 0 \tag{5-53d}$$

$$1.084 \cdot \nu + \frac{13}{7}\nu_2 - \nu_3 - \frac{1}{7}\nu_4 = 0 \tag{5-53e}$$

Therefore, by coupling Equations (5-53a) to (5-53e), the relation between the flows of benzyl alcohol, toluene and biomass in steady state continuous mode can be expressed by:

$$\phi_b \cdot Y_{bx}^{\max} + \phi_T \cdot Y_{tx}^{\max} = (-\phi_x) + m_{bt} C_x \tag{5-54}$$

Coupling with the parameters obtained from Equations (5-38) and (5-39), the following results can be obtained:

$$\frac{1}{Y_{bx}^{\max}} = \frac{7(K + 1.274\delta)}{(13\delta)} \qquad = 0.44 \tag{5-54a}$$

$$\text{and } Y_{tx}^{\max} = \frac{12\delta}{7(K + 1.274\delta)} \qquad = 0.414 \tag{5-54b}$$

In Equation (5-54), $(-\phi_x) = \mu C_x$, therefore, the concentration of biomass can be acquired by Equation (5-55):

$$C_x = \frac{1}{(\mu + m_{bt})} \cdot (\phi_b \cdot Y_{bx}^{\max} + \phi_T \cdot Y_{tx}^{\max}) \tag{5-55}$$

in which $\phi_b = \frac{F(C_{b0} - C_b)}{V}$, (5-55a)

$$\phi_T = \frac{Q(y_{in,T} - y_{out,T})}{V} + \frac{F(C_{T0} - C_T)}{V} \quad (5\text{-}49b)$$

that can be determined by the measured variables from the experimental studies. Therefore, the maintenance for biomass growth in steady state bioremediation of mixed toluene and benzyl alcohol can be predicted as 0.069 ± 0.001 C-mol/C-mol-h by applying the experimental data. This value is much higher than that for ethanol as sole substrate (0.010 ± 0.001 C-mol/C-mol h), which is due to the toxicity and inhibition of both toluene and benzyl alcohol.

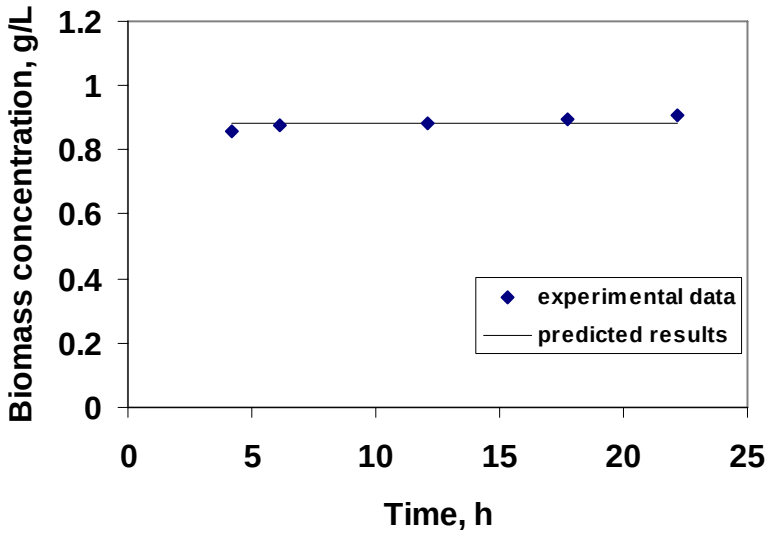

Figure 5-9 Simulation results of toluene-benzyl alcohol bioremediation at steady state (*Cgin,t* = 5.7 mg/L, BA feed rate of 0.12 g/h)

In this study, a metabolic model has been developed to simulate ethanol and benzyl alcohol bioremediation. The development of the stoichiometric coefficients for the reactions was based on the fundamental biochemical principles and mass balances, which allow the resulting model to be applicable to a wide range of operating conditions. From the comparison of the simulated results and the experimental data, the models of ethanol and benzyl alcohol bioremediation were found to predict both batch and continuous bioremediation with 95% confidence level. The results also show that the biomass maintenance term varies with the operating conditions, i.e. for same substrate, biomass maintenance needs are less for continuous steady state conditions than that for batch conditions. This is likely due to the transient nutrient and environmental (pH) conditions during the batch reactions. For continuous steady state operations, the more readily degradable substrate, ethanol, requires less maintenance for biomass growth than when ethanol is bioremediated in the presence of toluene. The presence of toluene in the mixture requires more ethanol for biomass maintenance. Additional consumption of ethanol for maintenance purposes was observed (0.027 compared to 0.010 C-mol/C-mol.h) when the toluene substrate concentration is high in the media.

5.5 Theoretical Prediction of Batch Growth

5.5.1 Batch Growth on Ethanol

As mentioned earlier (see Equation 5-34), the Monod equation has been used by many researchers to empirically fit a wide range of microbial growth data. It is the

most commonly applied, unstructured model for microbial growth. We have assumed that the growth kinetics on ethanol is described by the Monod equation:

$$\mu = \frac{\mu_{e,\max} S_e}{K_s + S_e} \qquad (5\text{-}56)$$

where $\mu_{e,\max}$ is the maximum specific growth rate when $S_e >> K_s$. Figure 5-10 shows the variation of μ as a function of S_e (ethanol mass concentration). In the Monod model, K_s is the empirical value which represents the limiting substrate concentration at which the specific growth rate is half of its maximum value. That is, it separates the plot of μ versus S_e into a low-substrate-concentration range where the specific growth rate is strongly dependent on S_e, and a high-substrate-concentration range where μ is more or less independent of S_e. In general, $\mu = \mu_m$ for $S_e >> K_s$ and $\mu = \frac{\mu_{e,\max}}{K_s} S_e$ for $S_e << K_s$.

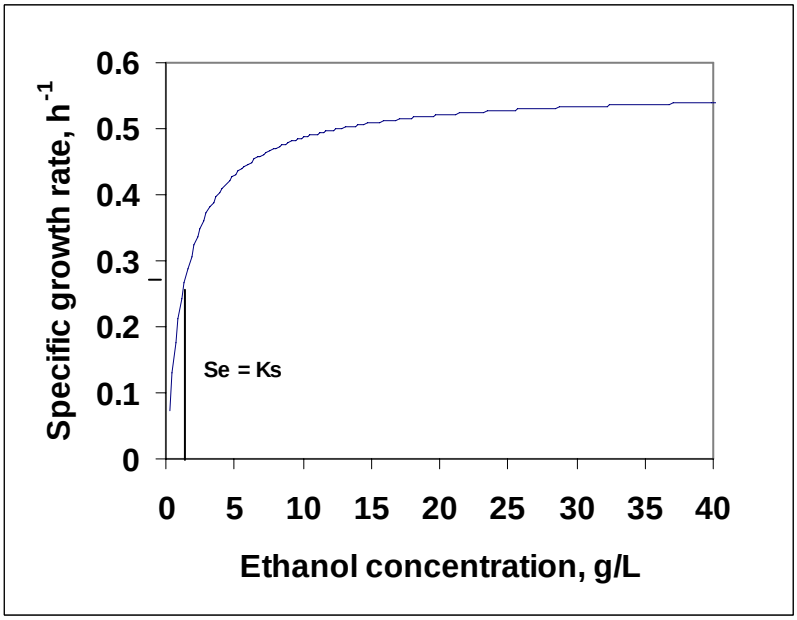

Figure 5-10. Effect of ethanol concentrations on the specific growth rate of *P. putida* according to the Monod model

Equations (5-34) and (5-35) and the values of parameters in Table 5-1 are applied in the prediction of batch growth on ethanol.

$$r_x = \mu C_x = \frac{\mu_{e,\max} C_e}{K_e + C_e} C_x \tag{5-34}$$

$$-\frac{dC_e}{dt} = (\frac{1}{Y_{xe}^{\max}})(\frac{\mu_{e,\max} C_e}{K_e + C_e})C_x + m_e C_x \tag{5-35}$$

Figure 5-11(a) illustrates the typical profiles of ethanol (*S (g/L)* =23.02(g/C-mol)*C_e(C-mol/L)) and biomass mass concentrations (*X(g/L)* = 22.6 (g/C-mol)*C_x (C-mol/L)) during batch growth at different ethanol initial concentrations. The results show that after a "lag phase" (caused by the initial low concentration of biomass) of about 5 hours, there is a long exponential growth phase (log phase) where the biomass concentration increases exponentially with time. At the end, where the substrate is consumed completely, growth stops. This is a typical behaviour when the growth follows Monod kinetics.

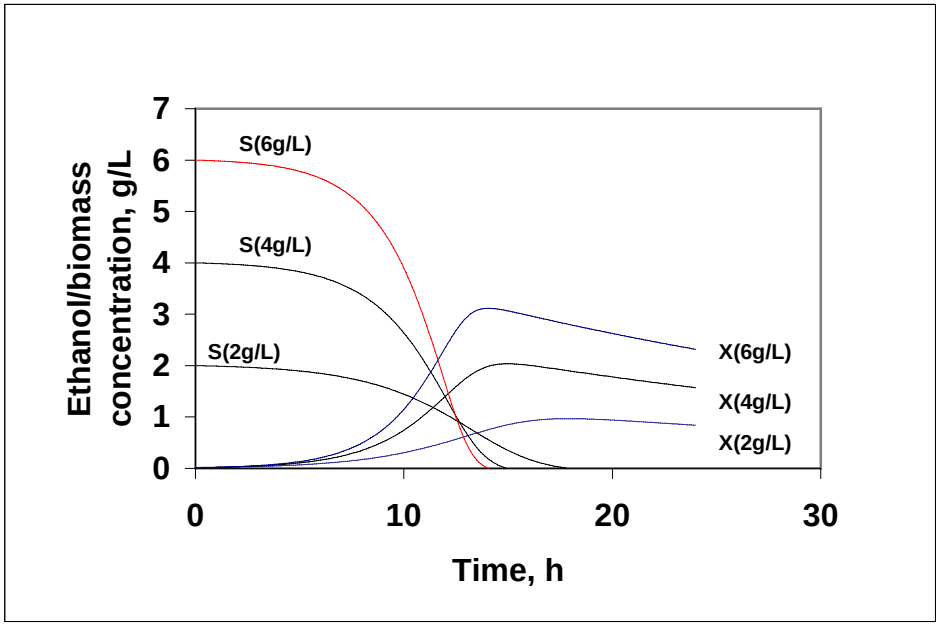

Figure 5-11(a). Theoretical prediction of batch growth on ethanol (2, 4, 6 g/L)

Figures 5-11 (b)-(c) demonstrate the concentration predictions for biomass (X), ethanol (S), ammonia ($(NH_4)_2SO_4$, C_n), along with oxygen consumption (Q_o), carbon dioxide formation (Qc) and ATP consumption (r_{ATP}) during a batch growth with ethanol at initial concentrations of 4 and 6 g/L, respectively. The calculations are described below:

(1) Biomass and ethanol mass concentrations are calculated from the mole concentrations obtained by Equations (5-34) and (5-35) as mentioned above.

(2) Ammonia concentration is calculated by:

$$C_n = C_{n0} - 0.2 r_x * (132/2) \quad \text{(g/L)} \qquad (5\text{-}57)$$

where C_{n0} is the initial $(NH_4)_2SO_4$ concentration used in the medium, is 2.0 g/L.

(3) The amount of ATP consumed for the formation of biomass including maintenance term can be described by (Roels, 1980):

$$r_{ATP} = \frac{1}{Y_{ATP}^{\max}} r_x + m_{ATP} \cdot C_x \qquad (5\text{-}58)$$

where r_{ATP} is the ATP consumption rate (mol/L-h); the parameter Y_{ATP} is the reciprocal of parameter K in Equation (5-4), which has been determined in Section 5.3.1.

(4) The following equations (Equations (5-59a) and 5-59b) are applied in the prediction of oxygen uptake rates and mass transfer rates. Oxygen consumption rate is calculated as:

$$Q_{O_2} = \mu C_x / Y_{O_2} * 32 \qquad \text{(g/L-h)} \qquad (5\text{-}59a)$$

Oxygen mass transfer rate is described by:

$$Q_{o_2\_mass} = k_L a \cdot (C_{o_2}^* - C_{o_2}) \qquad (5\text{-}59b)$$

Figures (5-11b) and (5-11c) indicate that oxygen consumption reaches higher rates when the log phase starts. A peak in the product of μC_x, and thus the total oxygen demand, occurs near the end of the exponential phase and the approach to the stationary phase. The results also indicate that a higher initial concentration of ethanol results in a higher biomass level, and thus a higher oxygen demand for cell growth. For instance, the maximum oxygen demand of 1.6 g/L-h for 6 g/L initial concentration is higher than that of 0.9 g/L-h for initial concentration of 4 g/L. In the cases of an ethanol initial concentrations below 6 g/L, the maximum oxygen supply ($k_L a \cdot C_{o_2}^*$) is always higher than the maximum oxygen demand ($\mu_{\max} C_x / Y_{O_2}$). Thus the main resistance to increased oxygen consumption is microbial metabolism and the reaction appears to be always growth rate limited, not oxygen mass transfer limited. This agrees with the

observations from the experimental studies that the DO levels were higher than the critical value ($(C_{cr} = 5\% * 7mg/L = 0.35mg/L)$,Shuler and Kargi, 2002) for growth at ethanol initial concentrations up to 5.8 g/L (See Section 4.3.1). The ATP consumption rate demonstrates the same trend as the oxygen consumption rate. It also reaches higher rates when the log phase starts, i.e. when the cells start to grow, they consume more ATP. The results also show that the initial nitrogen source ((2.0 grams/litre of $NH_4)_2SO_4$ in this study) was sufficient for growth when the ethanol initial concentrations are below 6 g/L.

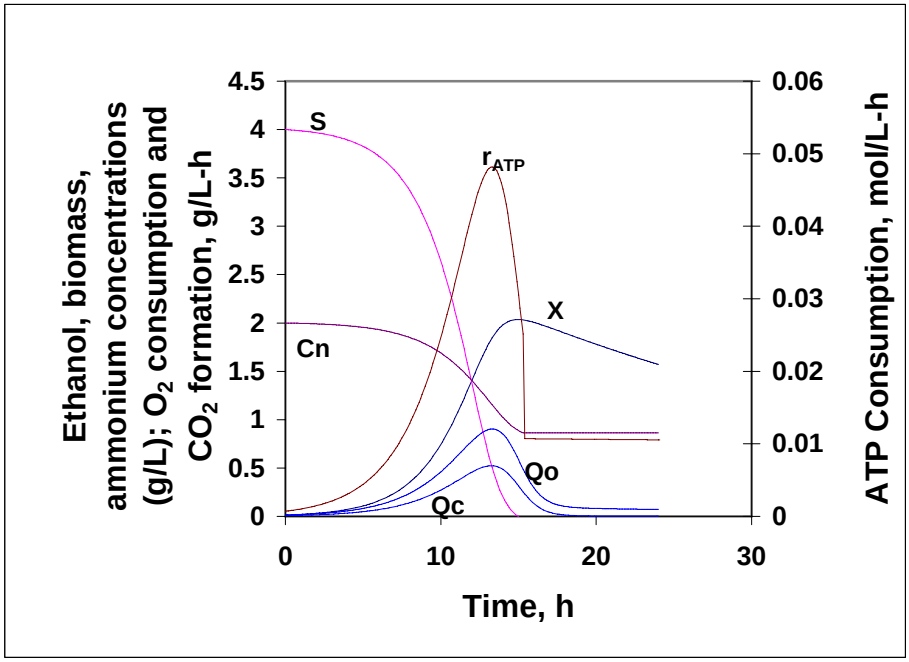

Figure 5-11(b). Prediction of batch growth on ethanol at initial concentration of 4 g/L

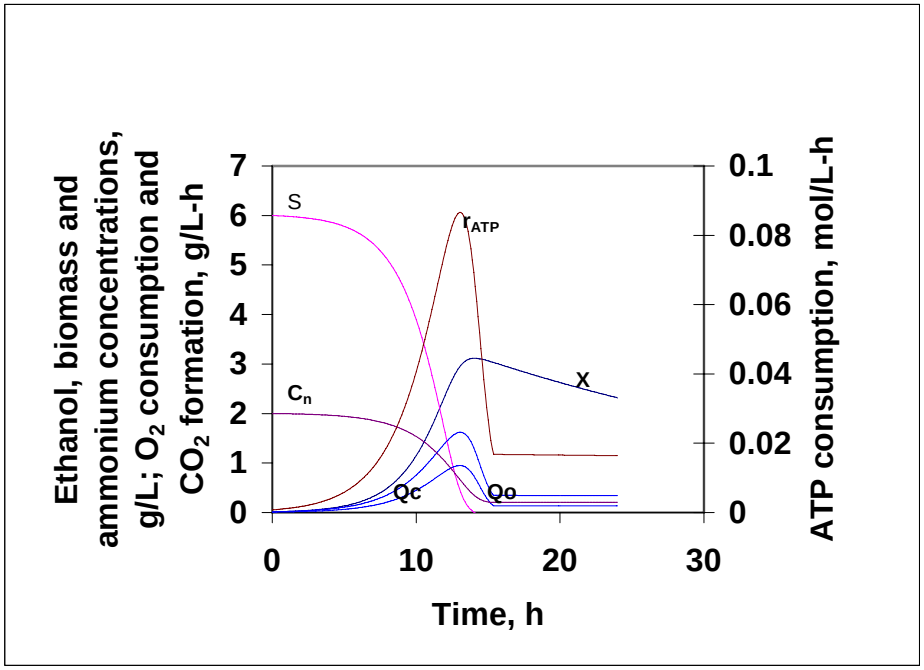

Figure 5-11(c). Prediction of batch growth on ethanol at initial concentration of 6 g/L

5.5.2 Batch Growth on Benzyl Alcohol

The specific growth rate of *Pseudomonas putida* on benzyl alcohol was assumed to follow the following substrate inhibition equation (4-10):

$$\mu = \frac{\mu_{b,\max} C_b}{K_b + C_b}\left(1 - \frac{C_b}{C_{b,\max}}\right)^n \qquad (4\text{-}10)$$

The values of parameters in Table 5-2 are applied in Equation (4-10). Figure 5-12 shows the effect of benzyl alcohol concentration on the specific growth rate. The results demonstrate that at low concentration, the specific growth rate increases with increase of benzyl alcohol concentrations. However, after the concentration of benzyl alcohol reaches 1.2 g/L, the specific growth rate starts decreasing with further increase of benzyl alcohol concentration. When the benzyl alcohol concentration reaches $C_{b,max}$ (2.9 g/L), the cells cease to grow, and the specific growth rate equals zero.

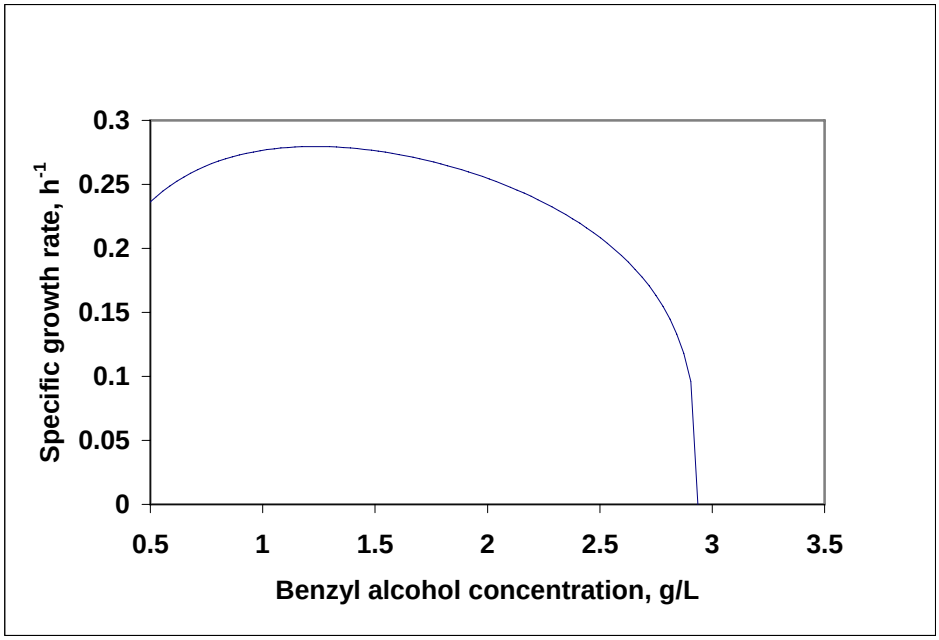

Figure 5-12. Effect of benzyl alcohol concentration on the specific growth rate of *P. Putida*

Equations (5-36), (5-37) and the values of parameters in Tables 5-2 are applied for the calculations of biomass and benzyl alcohol concentrations in batch growth at different initial benzyl alcohol concentrations.

$$r_x = \mu C_x = \frac{\mu_{b,\max} C_b}{K_b + C_b}\left(1 - \frac{C_b}{C_{b,\max}}\right)^n C_x \qquad (5\text{-}36)$$

$$-\frac{dC_b}{dt} = \left(\frac{1}{Y_{xb}^{\max}}\right)\left(\frac{\mu_{b,\max} C_b}{K_b + C_b}\right)\left(1 - \frac{C_b}{C_{b,\max}}\right)^n C_x + m_b C_x \qquad (5\text{-}37)$$

The predicted results are shown in Figures 5-13a-c. The mass concentrations are calculated from the mole concentrations obtained from Equations (5-36) and (5-37).

Figure 5-13a shows that the lower the initial benzyl alcohol concentration, the shorter the lag phase. This is caused by the inhibition effect of benzyl alcohol. The results also indicate that the closer the initial concentration is to the maximum inhibition concentration ($C_{b,max}$), the lower the specific growth rate until it reaches zero, where the substrate concentration stays unchanged. At the initial concentration of 2.5 g/L, the lag phase is around 10 hours, i.e. the cells need a much longer time to overcome the high inhibitory concentration of substrate.

Figure 5-13b shows the oxygen consumption rate (*Qo)*, calculated from Equation (5-59a)) and carbon dioxide formation rate (*Qc*), along with the ammonia (C_n), substrate (benzyl alcohol, *S)* and biomass (*X*) concentrations at an initial concentration of benzyl alcohol of 1.0 g/L. Similar to batch growth on ethanol, the peak oxygen demand appears near the end of the log phase. The maximum oxygen supply is higher than the maximum oxygen demand of 0.35 g/L-h. Thus, oxygen is not rate-limiting substrate for this case. The results also indicate that after the benzyl alcohol was completely consumed (S=0), there is still sufficient ammonia in the medium (C_n = 0.2 g/L after S=0). Figure 5-13c shows that the ATP consumption (r_ATP) reaches a higher value when the log phase starts. A peak in the production of μC_x, and thus the ATP consumption, occurs near the end of the exponential phase and the approach to the stationary phase.

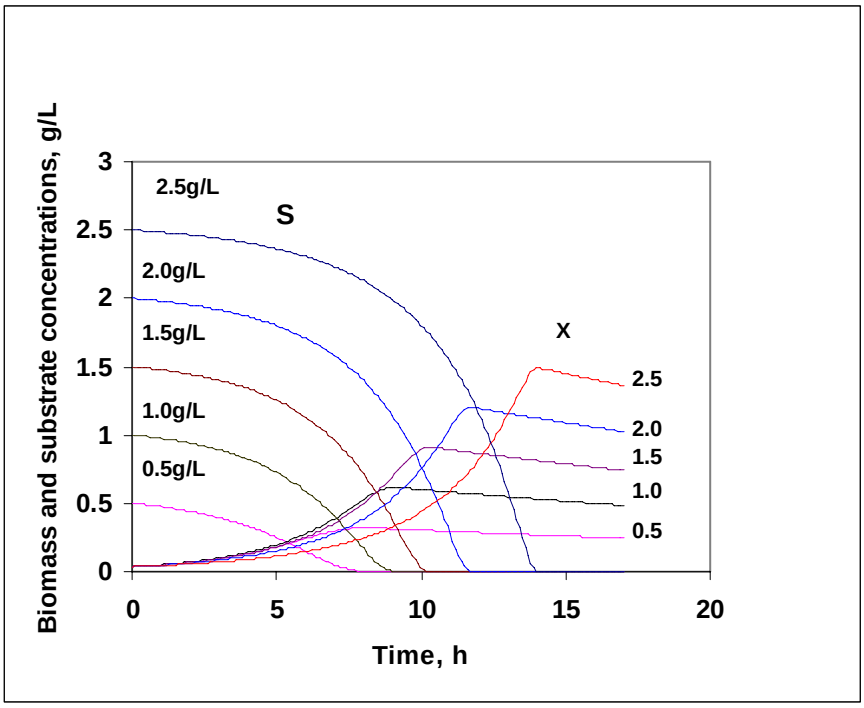

Figure 5-13(a). Prediction of batch growth on benzyl alcohol at different initial concentrations

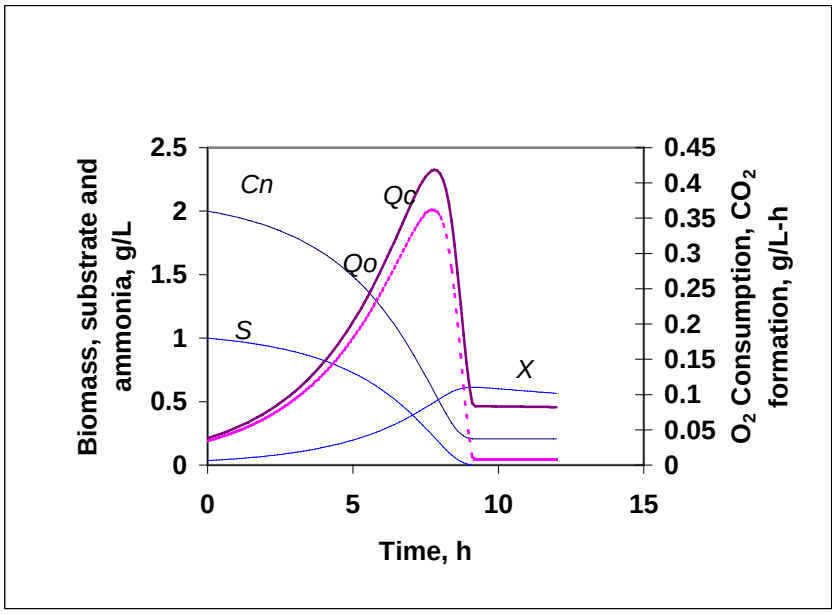

Figure 5-13(b). Prediction of batch growth on benzyl alcohol at initial concentration of 1g/L

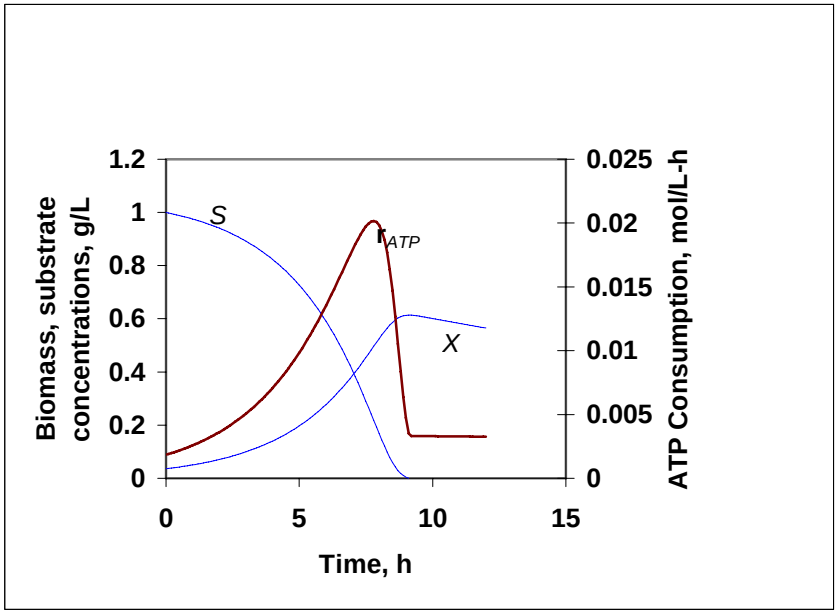

Figure 5-13(c). Prediction of ATP consumption rate for batch growth on benzyl alcohol at initial concentration of 1g/L

The carbon nutrient affects oxygen demand in a major way, i.e. the oxygen demand varies with different carbon sources. For instance, the oxygen demand for growth on benzyl alcohol is higher than that for growth on ethanol due to the magnitude of the theoretical yield term Y_{o_2} (0.644 for ethanol, 0.585 for benzyl alcohol, derivation of the equations are given in Appendix D).

5.6 Theoretical Prediction of Continuous Operation

5.6.1 Theoretical Prediction of Steady State Continuous Removal of Ethanol

In continuous operation, the biomass concentration can be represented by:

$$\frac{dC_x}{dt} = D(C_{x,0} - C_x) + \mu C_x \qquad (5\text{-}60)$$

where D is dilution rate (= F/V_R), which is the reciprocal of the residence time. μ is the specific growth rate (h^{-1}).

Because the feed media are sterile, $C_{x0} = 0$. When the system is at steady state ($dC_x/dt = 0$), then:

$$\mu = D \tag{5-61}$$

In a continuous stirred tank bioreactor (CSTR), cells are removed at a rate equal to their growth rate, and the growth rate of cells is equal to the dilution rate during steady state operations. This phenomenon allows us to manipulate growth rate as an independent parameter. Since growth rate is limited by at least one substrate in the CSTR, a simple description of its performance can be made by substituting the Monod equation for μ in Equation (5-61):

$$\mu = D = \frac{\mu_m C_e}{K_s + C_e} \tag{5-62}$$

If D is set at a value greater than μ_m, the culture cannot reproduce quickly enough to maintain itself and is washed out. That is, when $\mu < D$, $\frac{dX}{dt} = (\mu - D)C_x < 0$, then biomass would be washed out. Moreover, when the dissolved oxygen (DO) is higher than the critical value (DO> C_{cr}), the growth rate is independent of the DO value. When the DO is lower than C_{cr}, the growth approaches a first-order rate dependence on the dissolved-oxygen concentration (Shuler and Kargi, 2002). The oxygen limitation results in $\mu < D$, thus biomass will also be washed out, and the operation will no longer be steady state.

Using Equation (5-62) at steady state, when other nutrients are in excess, the ethanol concentration can be described as a function of the dilution rate for $D < \mu_m$ and $C_{O_2} > C_{cr}$:

$$C_e = \frac{DK_e}{\mu_m - D} \tag{5-63}$$

Equation (5-63) shows that at steady state, the ethanol concentration in the reactor is independent of the substrate feed concentration. This is true for any functional relationship $\mu = \mu(C_e)$. However, if μ depends on the concentration of one of the metabolic products, then C_e will also depend on the feed concentration, C_{e0}.

The following equations are applied in the prediction of continuous removal of ethanol.

$$\phi_e = \frac{Q(y_{in} - y_{out})}{V} + \frac{F(C_{e0} - C_e)}{V} \tag{5-42a}$$

$$-\phi_x = \frac{F(C_x - C_{x0})}{V} = \mu C_x \tag{5-42b}$$

$$C_x = \frac{\phi_e \cdot Y_{ex}^{\max}}{(\mu + m_{e,c})} \tag{5-43}$$

Considering Equations (5-42a), (5-42b) and (5-43) at steady state, the biomass concentration is a function of dilution rate and can be represented by:

$$C_x = \frac{[\frac{Q}{V}(y_{in} - y_{out}) + D(C_{e,0} - C_e)] \cdot Y_{ex}^{\max}}{(m_{e,c} + D)} \tag{5-64}$$

Since ethanol was introduced into the reactor by the gas stream not the liquid stream ($C_{e0} = 0$), and ethanol in the effluent gas stream is negligible ($y_{out} = 0$), then Equation (5-64) becomes:

$$C_{x,ss} = \frac{[\frac{Q}{V}(y_{in}) - DC_e] \cdot Y_{ex}^{\max}}{(m_{e,c} + D)} \tag{5-65}$$

Equation (5-65) indicates that the biomass concentration always depends on the substrate feed concentration (y_{in}), and the higher the feed concentration the higher will be the biomass concentration.

If ethanol gas inlet concentration were kept constant with all dilution rates, biomass levels would be too high at low dilution rates and they will be too low for the higher dilution rates. Therefore, we can increase ethanol gas inlet concentrations as the dilution rate increases.

$$y_{e,in} = f(D*V/Q) \qquad (5\text{-}66)$$

The prediction of continuous removal of ethanol was based on varying gas inlet concentrations (Equation (5-66)), i.e. $y_{e,in}$ proportionally increases with increasing dilution rates. Using the values of parameters obtained for ethanol bioremediation listed in Table 5.1, and operating under steady state continuous conditions ($m_{e,c} = 0.010 C-mol/C-mol.h^{-1}$) using the typical levels employed in this study ($Q = 24L/h, V_R = 1.5L$), the ethanol removal in a CSTR at steady state can be predicted by Equations (5-63) and (5-65) as a function of dilution rate and inlet ethanol concentration.

Figure 5-14a shows the results of biomass (X), substrate (ethanol, C_e), ammonia (C_n), and dissolved oxygen (DO) concentrations for different values of ethanol addition rates. In Figure 5-14a, the term $m_{e,c}$ is significant at low dilution rates, and the biomass concentration (X) becomes smaller than if maintenance is neglected; i.e. at low dilution rates, the substrate is consumed for maintenance of the biomass. At very high dilution rates (close to μ_m), the cells are washed out (X=0), and the ethanol concentration (C_e)

corresponds with the value associated with 100% of the ethanol from gas stream being dissolved in the liquid phase, i.e. maximum addition of ethanol through the gas phase.

The ammonia concentration in the liquid phase is calculated by:

$$C_N = C_{N0} - 0.2C_x \cdot (132/2) \quad \text{(g/L)} \tag{5-67}$$

This is derived from $D(C_{N0}-C_N) = 0.2\,\mu\, C_x$ at steady state. At steady state, oxygen consumption equals oxygen mass transfer rates, then the DO level is determined by coupling Equations (5-59a) and (5-59b):

$$DO = C_{o_2} = C^*_{o_2} - Q_{O_2}/k_L a \tag{5-68}$$

The ammonia concentration remains higher than 1.7 g/L for all dilution rates up to 0.32 h^{-1} due to the continual addition of the fresh medium at a level (C_{n0} = 2.0 g/L) which is sufficient for the cells' growth. The DO values are higher than 4 mg/L for steady state operations ($\mu < 0.32h^{-1}$). When the dilution rate is higher than 0.32 h^{-1}, the cells are washed out and the DO is the same as the maximum dissolved oxygen in the medium solution (7.0 mg/L).

The results in Figure 5-14a predict that both the ammonia and oxygen are sufficient to support the steady state operations at all dilution rates up to 0.32 h^{-1}. When the dilution rate is greater than 0.32 h^{-1}, the cells are washed out so there is no demand for oxygen and ammonia. We can conclude that the dilution rate should not be set too low or too high for steady state operation in the continuous removal of ethanol from polluted air. Figure 5-14b shows the predicted results of biomass (X) and substrate (ethanol, C_e) concentrations, and dissolved oxygen level (DO) at higher ethanol addition rates, i.e. $y_{e,in} = 0.14D(V/Q)$. The DO level decreases as dilution rates increase. When the dilution rate is higher than 0.1 h^{-1}, DO declines to a level that is below the

critical value. This condition results in cells being washed out. The system can only be operated at steady state at dilution rates below 0.1 h^{-1}.

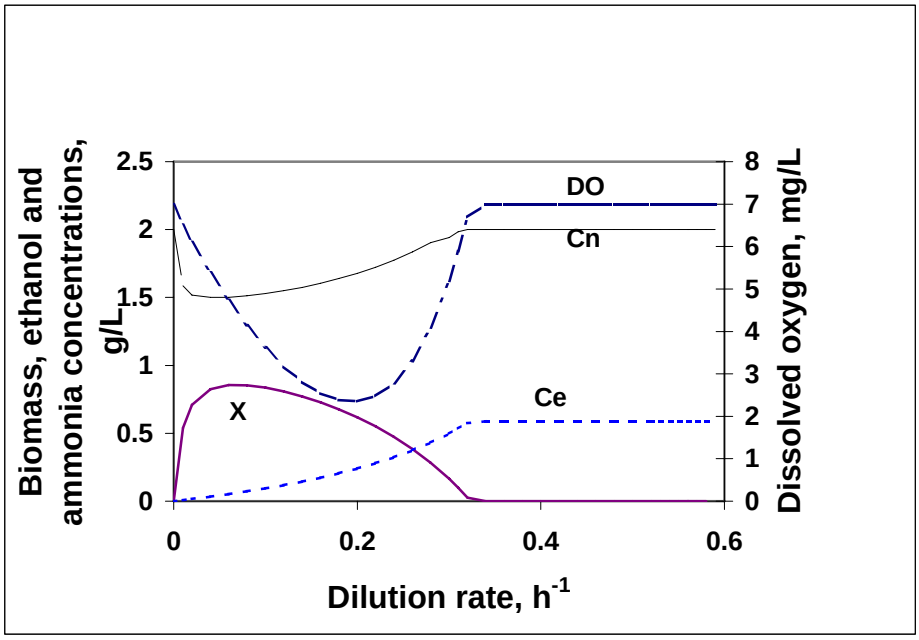

Figure 5-14(a). Prediction of continuous removal of ethanol ($y_{e,in} = 0.082D(V/Q)$)

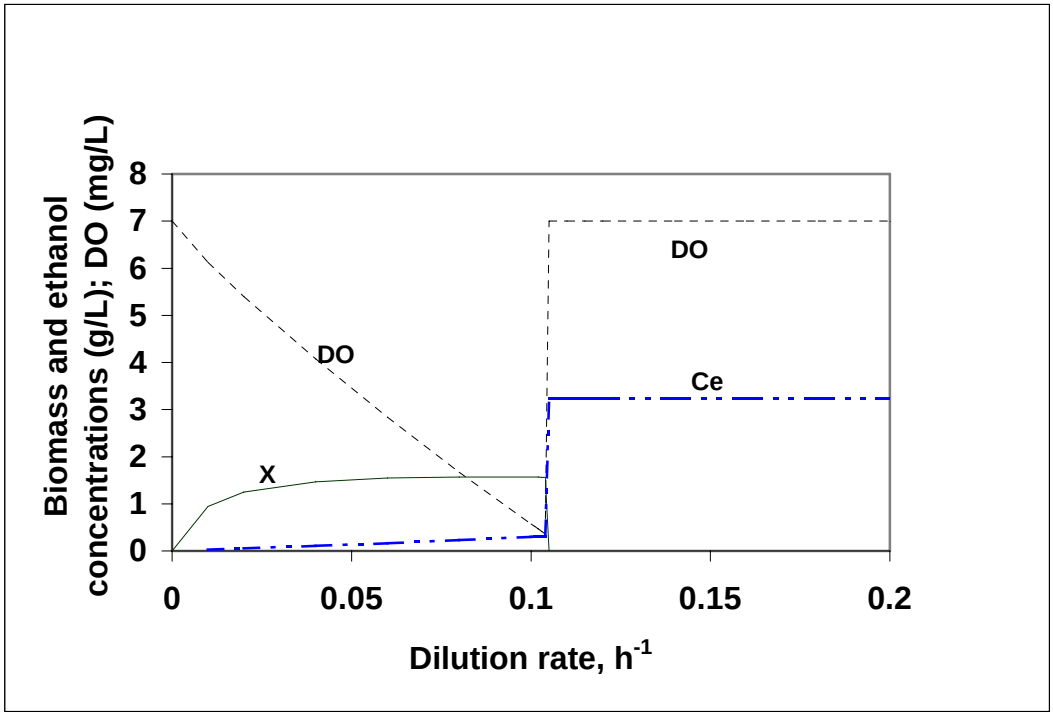

Figure 5-14(b). Prediction of continuous removal of ethanol ($y_{e,in} = 0.14D(V/Q)$)

There are a range of CSTR dilution rates for which stable operation can be achieved. It cannot be set too low or too high. In conclusion, the predictions of continuous removal of ethanol from contaminated air have demonstrated the following points:

1. At ethanol gas inlet concentrations of $y_{e,in} = 0.082D(V/Q)$, the system can be operated at steady state conditions with dilution rates up to 0.32 h^{-1}.
2. At ethanol gas inlet concentrations of $y_{e,in} = 0.14D(V/Q)$, the system can be operated at steady state conditions with dilution rates up to 0.10 h^{-1}.
3. When ethanol gas inlet concentrations are higher than 0.14 *D(V/Q)*, limitations with respect to oxygen supply appear, i.e. unless oxygen enriched air or pure

oxygen is supplied, the system cannot be operated at steady state under these conditions.

4. Low dilution rates generate low biomass concentrations because ethanol is consumed for maintenance requirements.

5.6.2 Theoretical Predictions of Steady State Continuous Removal of Benzyl Alcohol

The relation between the specific growth rate and benzyl alcohol concentration was given by:

$$\mu = \frac{\mu_{b,\max} C_b}{K_b + C_b}(1 - \frac{C_b}{C_{b,\max}})^n \qquad (4\text{-}3)$$

The biomass concentration can be predicted by combining $-\phi_x = \mu C_x$ and $\phi_b = D(C_{b0} - C_b)$ with Equation (5-32):

$$C_x = \frac{D(C_{b0} - C_b)}{(\mu / Y_{xb} + m_b)} \qquad (5\text{-}69)$$

Using the values of parameters obtained for benzyl alcohol bioremediation listed in Table 5.2 with the operating conditions of the reactor used in this study $(Q = 24L/h;\ V_R = 1.5L)$, benzyl alcohol removal in a CSTR at steady state can be predicted by Equations (4-3) and (5-69) as a function of dilution rate and feed rate. Results are shown in Figures 5-15a-c. Figure 5-15a reveals that the system can be maintained at steady state for dilution rates up to 0.25 h^{-1}. When the dilution rate is higher than 0.25 h^{-1}, the cells are washed out (X=0) and the substrate concentration reaches the same as the feed ($C_b = C_{b0}$). The results also indicate that DO level is higher

than 4.0 mg/L at all dilution rates up to 0.25 h^{-1}, i.e. oxygen is not a rate-limiting factor for these operations.

Figure 5-15b shows biomass (X), benzyl alcohol (C_b), ammonia (C_n) and dissolved oxygen (DO) at a benzyl alcohol feed concentration of 1.2 g/L. When the dilution rate is higher than 0.27 h^{-1}, the cells are washed out (X=0). Since no microbial consumption happens, the substrate concentration is the same as the feed ($C_b = C_{b0}$). This figure also reveals that the DO level is above 0.75 mg/L for all dilution rates up to 0.27h^{-1}, which is higher than the critical oxygen value. Thus, the system can be maintained at steady state for all dilution rates up to 0.27h^{-1} at feed concentration of 1.2g/L.

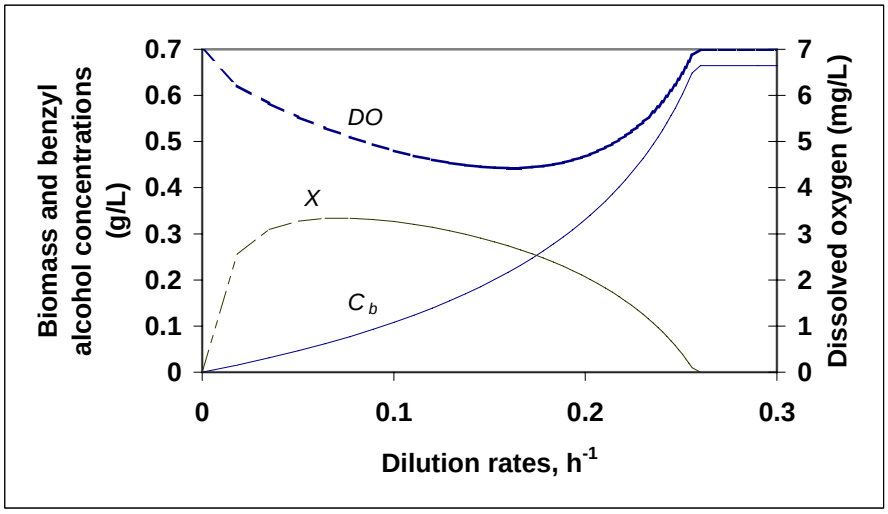

Figure 5-15(a). Prediction of continuous removal of benzyl alcohol (C_{b0} = 0.66 g/L)

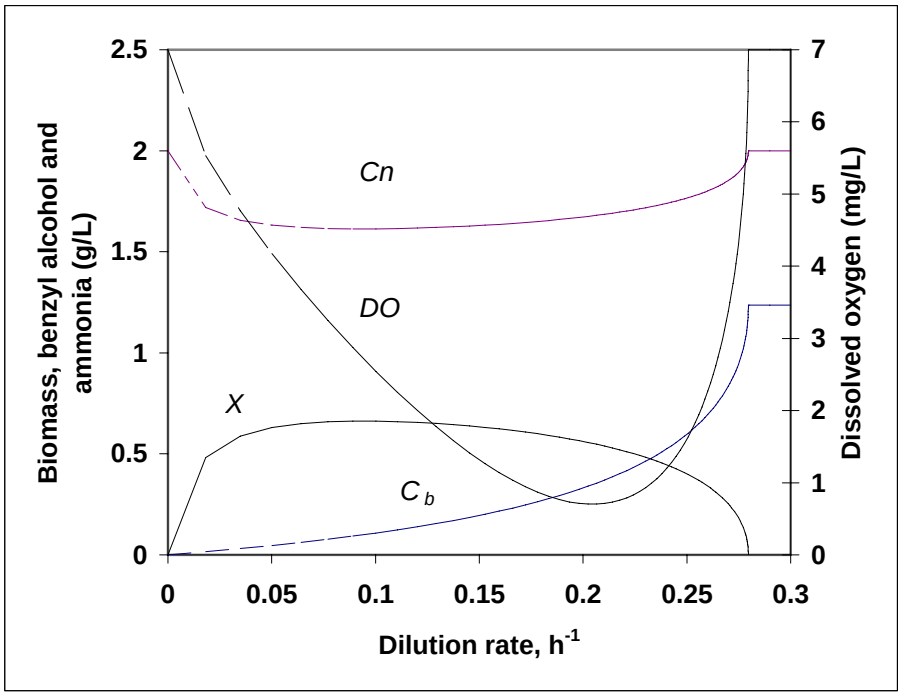

Figure 5-15b. Prediction of continuous removal of benzyl alcohol (C_{b0}=1.2 g/L)

Figure 5-15c gives the results at feed concentration of 1.54 g/L. The high level of biomass concentrations demands more oxygen for the growth, and with the increase of the dilution rates ($\mu = D$), the term Q_{O_2} in Equation 5-68 increases dramatically. Thus, the DO level drops quickly to a value that is close to the critical value. When the dilution rate reaches 0.12 h^{-1}, the DO level drops to 0.37 mg/L. With further increase of dilution rate, the DO decreases to a level that is below the critical value which results in cells being washed out. At this feed condition, the system can be operated at steady state only for dilution rates up to 0.12 h^{-1} due to oxygen limitation.

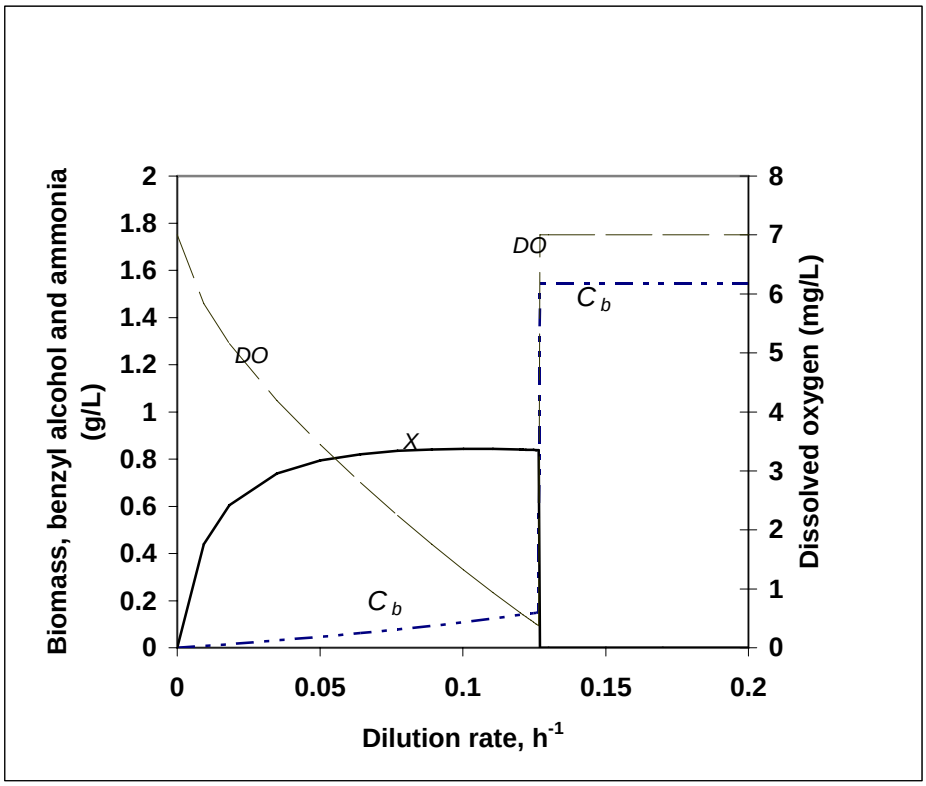

Figure 5-15c. Prediction of continuous removal of benzyl alcohol (C_{b0}=1.54 g/L)

In conclusion, for continuous removal of benzyl alcohol, when the feed concentration of benzyl alcohol is below 1.2 g/L, both oxygen and nitrogen sources are sufficient to support the growth. When the feed concentration reaches 1.54 g/L, the oxygen demand is larger than the oxygen mass transfer rate at dilution rates higher than 0.12 h^{-1}. Clearly, this case could only be operated at dilution rates below 0.12 h^{-1} . In the cases of high feed concentrations (C_{b0} > 1.54 g/L), oxygen enriched air or a pure oxygen supply would be required.

5.6.3 Theoretical Predictions of Steady State Simultaneous Removal of Ethanol and Toluene Mixtures

For the growth on the mixture of ethanol/toluene or benzyl alcohol/toluene, toluene acts as a growth inhibitor only (Bailey and Ollis, 1986; Chang *et al*, 1993; Bielefeldt and Stensel, 1999). There is no growth on toluene, but toluene gets consumed proportional to the growth rate on the actual growth substrate. The following assumptions are made in the prediction of the steady state removal of ethanol and toluene mixtures. The growth on the mixture of ethanol and toluene follows the two compound inhibition equation (Bailey and Ollis, 1986), which agrees with the metabolic model that applied with the data for ethanol/toluene bioremediation.

$$\mu = \frac{\mu_{\max} C_e}{C_e + K_e(1 + I / K_i)} \tag{5-70}$$

where $\mu_{max} = \mu_{e,max}$, I = liquid concentration of a competing compound (mg/L) and K_i is an inhibition constant (mg/L). In this case, $I = C_t$, and $K_i = 1.71 mg/L$ for toluene was used (Chang et al., 1993). For ethanol (see Table 5.1): $\mu_m = 0.56\,\mathrm{h}^{-1}$,and $K_e = 0.59 g/L$.

The biomass concentration can be predicted by:

$$C_x = \frac{1}{(\mu + m_{et})} \cdot (\phi_e \cdot Y_{ex}^{\max} + \phi_T \cdot Y_{tx}^{\max}) \tag{5-49}$$

where ϕ_e and ϕ_T are the net amounts of ethanol and toluene flowing into the system (In-Out), respectively. Considering the fact that ethanol in the outlet gas steam is

negligible $(y_{out,e} = 0)$, and ethanol was introduced into the reactor from a gas stream, not by a liquid stream $(C_{e,0} = 0)$, and $\frac{F}{V} = D$, then:

$$\phi_e = \frac{Q(y_{in} - y_{out})}{V} + \frac{F(C_{e0} - C_e)}{V} = \frac{Q}{V} y_{in,e} - DC_e, \qquad (5\text{-}49a)$$

Considering that toluene was also introduced into the reactor by a gas stream and not a liquid stream ($C_{T0} = 0$), then:

$$\phi_T = \frac{Q(y_{in,T} - y_{out,T})}{V} + \frac{F(C_{T0} - C_T)}{V} = \frac{Q}{V}(y_{in,t} - y_{out,t}) - DC_T \qquad (5\text{-}49b)$$

Combing Equations (5-49), (5-49a) and (5-49b):

$$C_x = \frac{1}{(\mu + m_{et})} \cdot \{(\frac{Q}{V} y_{in,e} - DC_e) \cdot Y_{ex}^{\max} + [\frac{Q}{V}(y_{in,t} - y_{out,e}) - DC_t] \cdot Y_{tx}^{\max}\} \qquad (5\text{-}71)$$

Equations (5-70*)* and (5-71) are applied to predict ethanol, and biomass concentrations during the steady state continuous removal of ethanol and toluene mixtures in a CSTR. The prediction results are shown in Figures 5-16 to 5-18.

Figure 5-16 shows biomass (X) and ethanol (C_e) concentrations and DO levels (calculated from Equation 5-68) for removal of ethanol/toluene mixture at toluene gas inlet concentration of 5 mg/L. The results show that with a constant toluene inlet concentration of 5 mg/L, the biomass concentration decreases with increase of dilution rates. When the dilution rate approaches 0.12 h^{-1}, the dissolved oxygen concentration drops below the critical oxygen concentration for the growth of bacteria (0.35 mg/L). Thus the bacteria will no longer grow, i.e. $\mu<D$, the cells are washed out and the biomass concentration rapidly drops to zero. At this dilution rate, the ethanol

concentration reaches the value such that all of the ethanol from the gas steam is dissolved in the liquid. Toluene in the liquid phase is at equilibrium with the inlet toluene gas. Toluene in the exit gas stream equals the inlet gas concentration because no consumption happens after cells are washed out. Thus, when the system is operating with a dilution rate above 0.12 h^{-1}, oxygen mass transfer becomes a rate-limiting factor at these conditions.

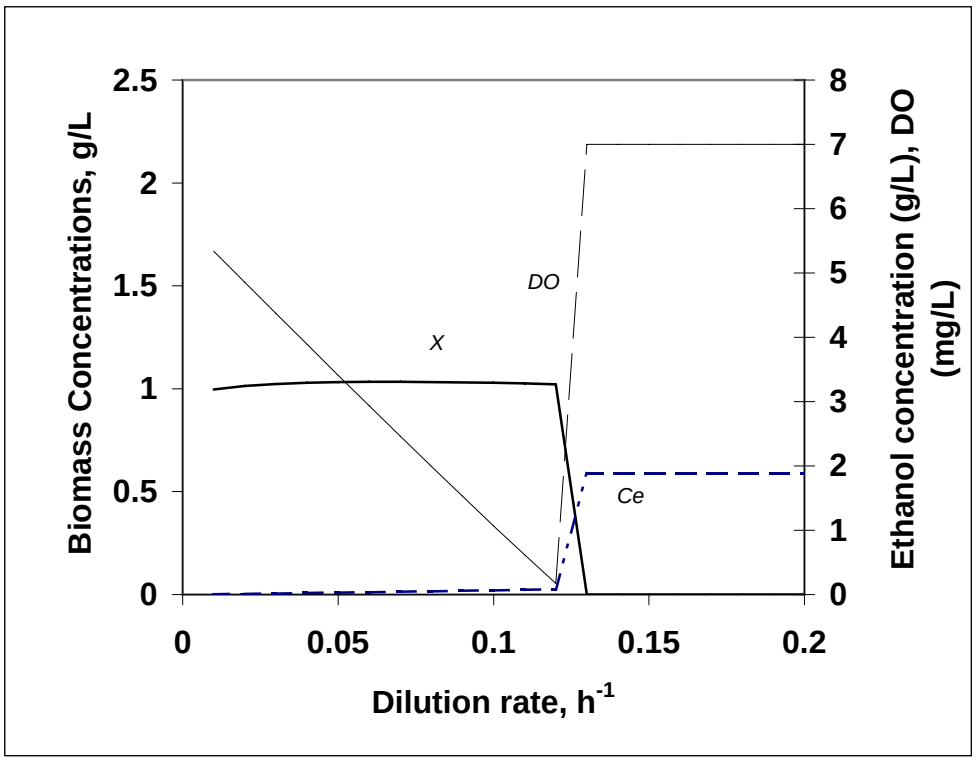

Figure 5-16. Continuous removal of ethanol and toluene

($C_{g,e}$ = 0.082 $D(V/Q)$; $y_{t,in}$ = 5 mg/L)

Figure 5-17 shows the results at a toluene inlet gas concentration of 6 mg/L. The system is at steady state for dilution rates up to 0.11 h^{-1}. When the dilution rate is lower than 0.11 h^{-1}, the ethanol (C_e) mass concentrations in the liquid phase follow Equation (5-70). After the dilution rate reaches levels higher than 0.11 h^{-1}, dissolved oxygen concentrations are below the critical value. At these conditions, cells are washed out. Figure 5-18 shows the results at toluene inlet concentration of 7 mg/L. As the dilution rate increases due to the high level of biomass in the liquid, the DO level drops quickly. When the dilution rate is higher than 0.09 h^{-1}, the DO level falls to a level that is lower than the critical oxygen value (C_{cr}) and cells are washed out. We can conclude that at these inlet conditions, the system could only be at steady state for dilution rates up to 0.09 h^{-1} due to the limitation of oxygen mass transfer. For cases at higher toluene inlet concentrations (>7 mg/L) or at higher ethanol inlet concentrations, oxygen-enriched air would be recommended as the oxygen supply for the system to operate at steady state conditions.

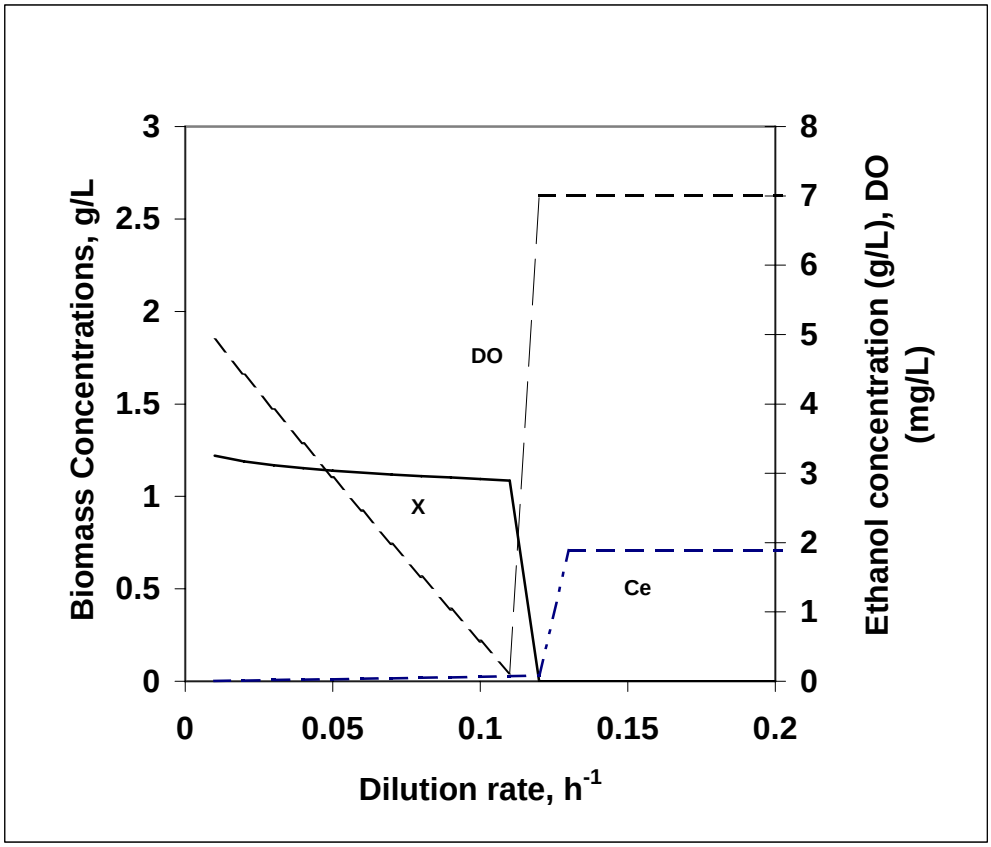

Figure 5-17. Continuous removal of ethanol and toluene

($C_{g,e}$ = 0.082 $D(V/Q)$; $y_{t,in}$ = 6.0 mg/L)

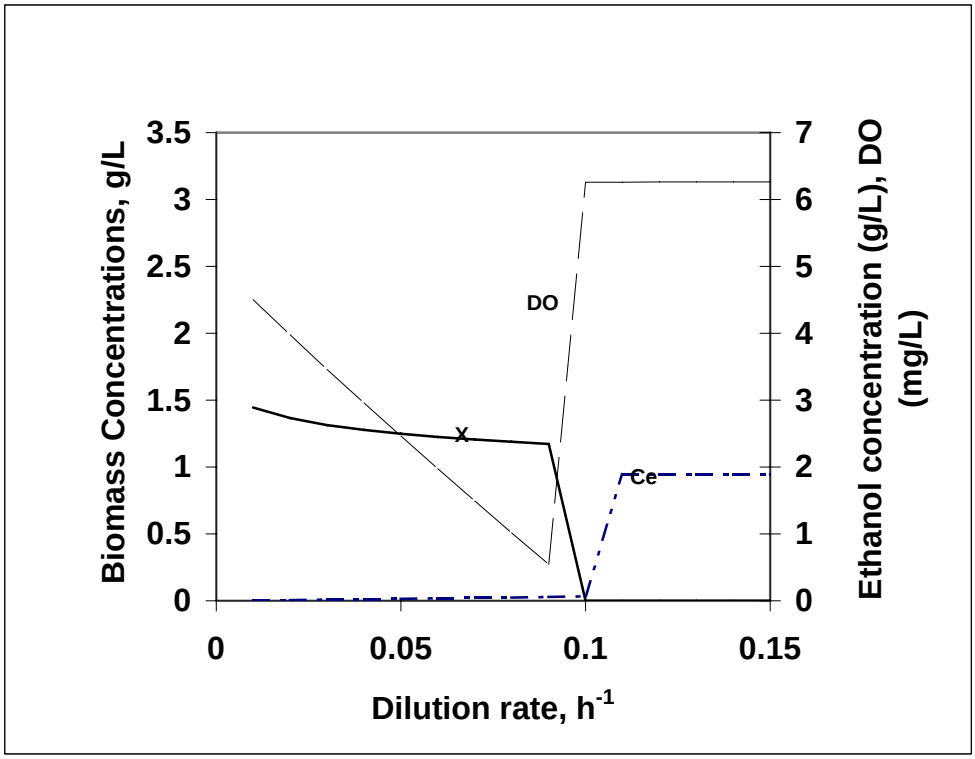

Figure 5-18. Predicted results of continuous removal of ethanol and toluene

($C_{g,e}$ = 0.082 $D(V/Q)$; $y_{t,in}$ = 7.0 mg/L)

5.6.4 Theoretical Predictions of Continuous Steady State Removal of Benzyl Alcohol and Toluene Mixtures

For growth with the benzyl alcohol/toluene mixture, toluene acts as a growth inhibitor only (Bailey and Ollis, 1986; Chang *et al*, 1993; Bielefeldt and Stensel, 1999). The growth on the mixture of benzyl alcohol and toluene follows the two-compound inhibition equation (Bailey and Ollis, 1986) which agrees with the metabolic model that applied with the data for benzyl alcohol/toluene bioremediation:

$$\mu = \frac{\mu_{\max} C_b}{C_b + K_b(1 + I/K_i)}(1 - \frac{C_b}{C_{b,\max}})^n \qquad (5\text{-}72)$$

where $\mu_{max} = \mu_{e,max}$, I = liquid concentration of a competing compound (mg/L) and K_i is an inhibition constant (mg/L). In this case, $I = C_t$, $K_i = 1.71 mg/L$ for toluene was used (Chang et al., 1993). For benzyl alcohol (see Table 5.2): $\mu_m = 0.42\,h^{-1}$, and $K_b = 0.289 g/L$.

The biomass concentration can be predicted by:

$$C_x = \frac{1}{(\mu + m_{bt})} \cdot (\phi_b \cdot Y_{bx}^{\max} + \phi_T \cdot Y_{tx}^{\max}) \qquad (5\text{-}55)$$

ϕ_b and ϕ_T represent the net amount of benzyl alcohol and toluene that flows into the system (In-Out), and they are calculated using the following equations:

$$\phi_b = \frac{F(C_{b0} - C_b)}{V} \qquad (5\text{-}55a)$$

$$\phi_T = \frac{Q(y_{in,T} - y_{out,T})}{V} + \frac{F(C_{T0} - C_T)}{V} = \frac{Q}{V}(y_{in,t} - y_{out,t}) - DC_T \qquad (5\text{-}49b)$$

Therefore, the expression of biomass concentration becomes:

$$C_x = \frac{1}{(\mu + m_{et})} \cdot \{D(C_{b0} - C_b) \cdot Y_{bx}^{\max} + [\frac{Q}{V}(y_{in,t} - y_{out,e}) - DC_t] \cdot Y_{tx}^{\max}\}$$

(5-73)

Equations (5-72), and (5-73) are applied to predict benzyl alcohol, and biomass concentrations for the steady state continuous removal of benzyl alcohol and toluene mixtures. Figures 5-19 and 5-20 show the predicted results of biomass (X), benzyl alcohol (C_b) concentrations, and the DO level (calculated from Equation 5-68) as a function of dilution rate and feed concentration.

Figure 5-19 demonstrates that at a benzyl alcohol inlet concentration of 0.6 g/L, the system can be operated at steady state conditions for toluene gas inlet concentrations up to 12.0 mg/L. The results show that with increasing dilution rates, the biomass concentration (X) decreases and that the system can be operated at dilution rates up to 0.21 h^{-1} with the DO levels above 0.87 mg/L. Therefore, oxygen mass transfer is not the rate-limiting factor at these conditions. When the dilution rate is higher than 0.21 h^{-1}, cells are washed out, and no consumption occurs. At these dilution rates, the benzyl alcohol concentration equals the feed concentration ($C_b = C_{b0}$), toluene in the liquid phase reaches equilibrium with the gas phase, and the gas outlet toluene concentration reaches the same level as the gas inlet concentration ($y_t = y_{t,in}$). The predicted results also indicate that at benzyl alcohol feed concentration of 0.6 g/L, the system could not be operated at steady state when the toluene gas inlet is higher than 12.0 mg/L unless an oxygen-enriched air is used as the oxygen supply.

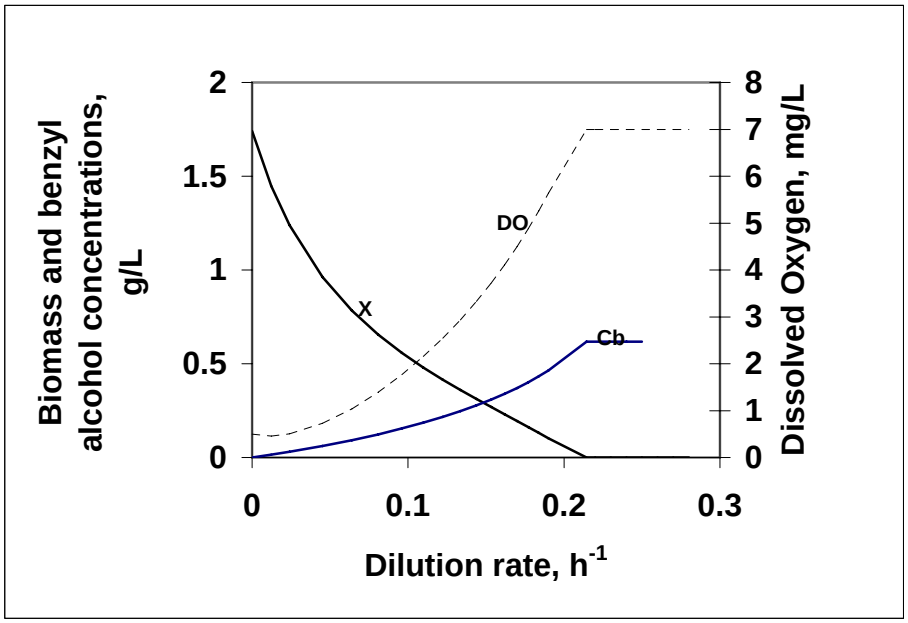

Figure 5-19. Continuous removal of toluene and benzyl alcohol

(C_{b0} = 0.6 g/L; $y_{t,in}$ = 12.0 mg/L)

Figure 5-20 reveals that at a benzyl alcohol concentration of 1.2 g/L, the system could be operated at steady state for dilution rates up to 0.11 h^{-1} with a toluene gas inlet concentration of 5 mg/L. When dilution rates are higher than 0.11 h^{-1}, the DO level drops to a value that is below the critical value for bacteria growth. Thus oxygen mass transfer becomes a rate–limiting factor at these conditions while cells are washed out, and no consumption occurs. The sharp corner observed in the predicted DO curve shown in Figure 5-20 occurs due to the program setting the biomass concentration to zero. The prediction results also indicate that at a benzyl alcohol feed concentration of

1.2 g/L, the system could not be operated at steady state when the toluene gas inlet is higher than 5 mg/L due to the limitation of the DO level. The system would require oxygen-enriched air as an oxygen supply.

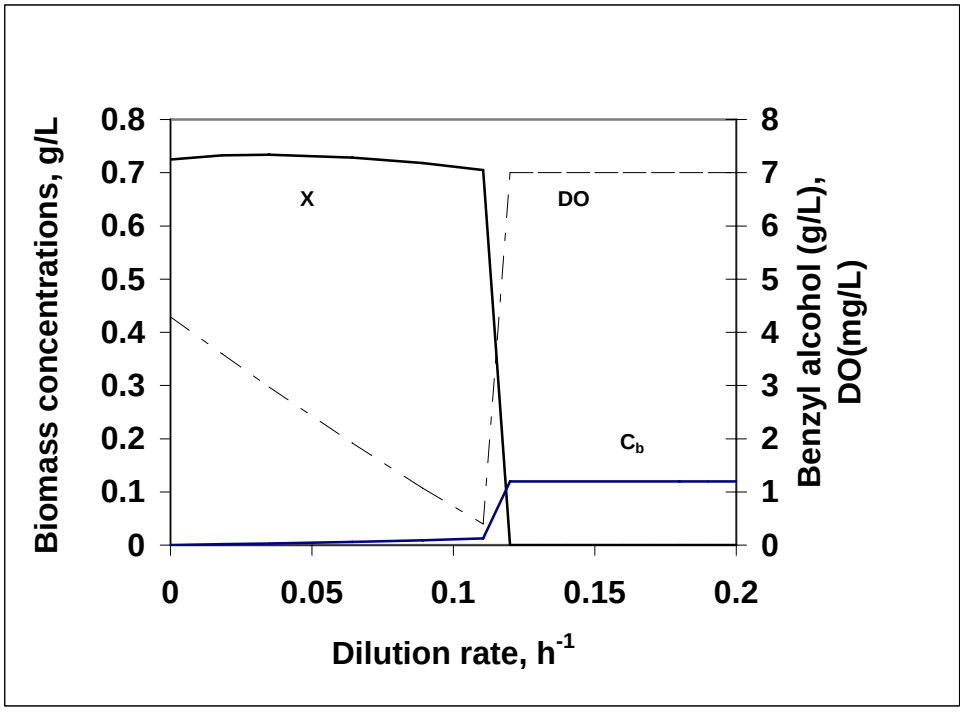

Figure 5-20 Continuous removal of toluene and benzyl Alcohol

(C_{b0} = 1.2 g/L; $y_{t,in}$ = 5 mg/L)

5.6.5 Conclusion of Modeling

In conclusion, when biomass concentrations reach high levels, the oxygen demand will also be high. If the oxygen supply is from the air stream only, then the dissolved oxygen level will be below the critical value for bacteria to grow. This has been proven by experimental observations in this work. Figure 5-21 shows the experimental results (same as Figure 4-12 plus dissolved oxygen results) for continuous

removal of ethanol at 25 mg/L of gas inlet concentration. At the instant of the gas inlet concentration being changed to 25 mg/L, the biomass reaches a higher level, which requires more oxygen for growth. The dissolved oxygen level decreased rapidly to zero, which is obviously below the critical value. At this condition an unwanted product, acetic acid, was formed which caused the pH level to decrease, which in turn inhibited the growth of the bacteria. The derivation of the unsteady state operation of the reactor is given in Appendix F. The transient, continuous flow model can appropriately capture the transient experimental data such as variation of gas inlet concentrations (See Figure 5-7 and Appendix F).

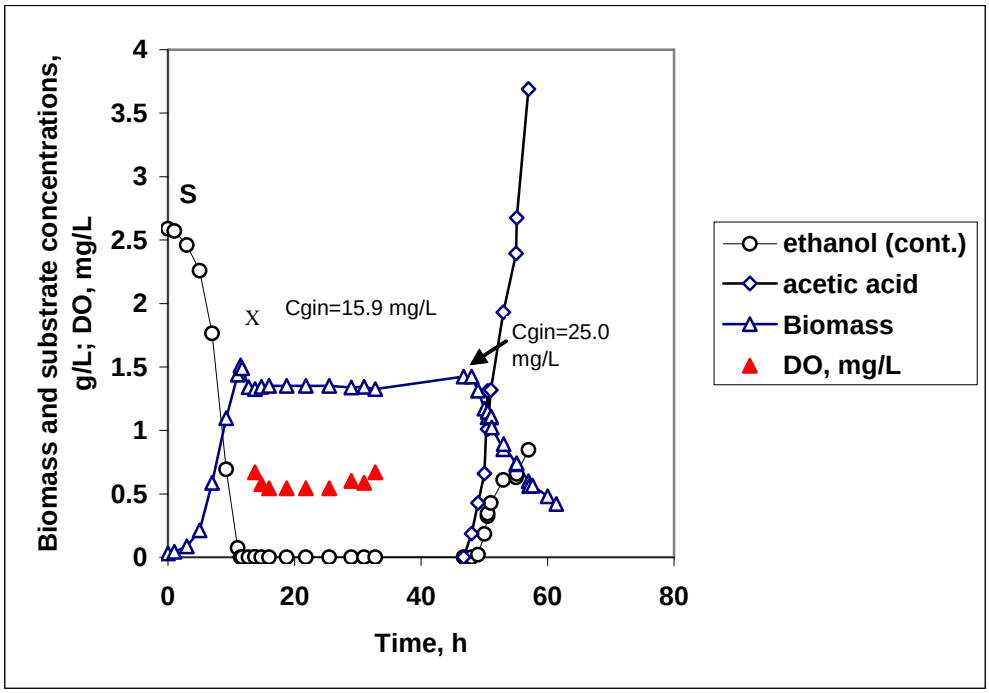

Figure 5-21. Removal of ethanol from gas stream in a continuous mode at dilution rate of 0.1 h^{-1}

The continuous models can capture all significant physical phenomena since they were derived based on fundamental biochemical principles and mass balances. Equations (5-65), (5-69), (5-71), and (5-73) illustrate that biomass concentrations are a function of the operating conditions such as inlet and outlet concentrations in liquid and gas phases, dilution rates, yield coefficients on each substrate, and the maintenance terms under different conditions. If the operating conditions change, the model reflects the physical reality of this change. For instance, for continuous removal of ethanol at steady state conditions, biomass concentration increases as the amount of ethanol introduced from gas phase increases when other conditions remain the same (see Figures 5-14a and 5-14b). For example, results in Figure 5-7 show that the steady state continuous model predicts the changes in biomass concentrations due to the increase of ethanol gas inlet concentration. However, there was not sufficient time to generate more data to determine the predictive ability of the model.

The limitation of the simulation is the parameters obtained from the limited (but time consuming) number of experiments such as m, Y_m. As discussed in Section 5.4.2, this maintenance term of growth depends on the growth environment such as the type of substrate and its concentration, operating mode (batch or continuous), and conditions of other nutrients such as pH, oxygen and ammonia. Moreover, in reality the P/O ratio (δ) may also vary with the operating conditions. Therefore, it is recommended that more detailed on-line measurements, including ATP, oxygen and carbon dioxide, be carried out in order to verify and improve the model in the future.

CHAPTER SIX – CONCLUSIONS AND RECOMMENDATIONS

6.1 CONCLUSIONS

The original contributions of this research are that both high and low solubility VOCs (ethanol and toluene) can readily be captured and bioremediated using a traditional CSTR. The major conclusions are presented in the order of discoveries from mass transfer studies, from bioremediation studies, and from metabolic modeling. Specific discoveries from mass transfer studies include:

- Mass transfer studies indicated that ethanol was transferred from a contaminated air stream into the liquid phase of a well-mixed bioreactor completely for gas inlet concentrations up to 95.0 mg/L and air flow rates up to 2 L/min.
- Toluene mass transfer studies from contaminated air into the well-mixed bioreactor indicated that the overall mass transfer coefficient increases with agitation speeds from 300 to 600 rpm, reaching a high value of 1.0×10^{-3} s^{-1}.
- Oxygen mass transfer studies showed that the presence of ethanol in the liquid phase enhances oxygen overall mass transfer coefficients, with maximum measured values of 0.049 and 0.076 s^{-1} at an ethanol concentration of 8g/L and agitation speeds of 450 and 600 rpm, respectively.

- Air stripping coefficients obtained in this study for toluene were 1000 times higher than for ethanol. The highest measured value for toluene was 12.6 h^{-1} at air flowrate of 2.1 L/min and agitation speed of 450 rpm.

The results from bioremediation studies showed that water soluble VOCs such as ethanol that are readily consumed by bacteria can be continuously captured from contaminated air and biologically treated using a CSTR. This study also demonstrated that using *Pseudomonas putida* as the biological agent, toluene cannot be biodegraded as sole substrate due to toxicity and inhibition. This study revealed that a traditional CSTR is capable of appreciable removal rates of toluene from a contaminated air stream. A practical strategy to improve the removal efficiency is to use ethanol or benzyl alcohol as co-substrate and to keep the biomass at an appropriate level, resulting in high toluene removal rates. Specific discoveries from batch and continuous bioremediation studies include:

- No inhibition effect of ethanol on the growth of *P. putida* was observed for ethanol initial concentrations up to 5.8 g/L. Growth on ethanol follows the Monod model with a maximum specific growth rate of 0.56 h^{-1}.
- Inhibition effect of benzyl alcohol on the growth of *P. putida* was observed in the batch growth experiments and was modeled by the inhibition model with a maximum benzyl alcohol concentration of 2.9 g/L above which growth is completely inhibited.

- At an inlet air concentration of 19.5 mg/L, ethanol was consumed 100% at maximum removal rates of 304 mg/L-h, which is better than existing biofilter systems currently in use by industry.
- Steady state removal of ethanol-toluene mixture from a contaminated air stream was conducted using a CSTR. The removal efficiency reached 100% for ethanol and 89% for toluene at ethanol inlet concentration of 15.9 mg/L and toluene inlet concentration of 4.5 mg/L. The fastest toluene removal rate was 93 mg/L-h.
- Using benzyl alcohol as the co-substrate, toluene was again successively removed from a contaminated air stream using a CSTR. The removal efficiency of toluene reached 97% with the fastest toluene removal rate of 93 mg/L-h.

The metabolic models were developed for bioremediation of ethanol/benzyl alcohol based on the published metabolic pathways. Specific discoveries from metabolic modeling are:

- Simple Monod and substrate inhibition kinetics generated curves that were able to represent the experimental batch biodegradation of ethanol and benzyl alcohol, respectively, within 95% confidence level. The metabolic model then allowed the incorporation of these kinetic coefficients to predict the in-situ concentrations of other key metabolites (ATP, CO_2, etc.) during batch growth cultures.
- The metabolic models have also been developed to simulate simultaneous bioremediation of ethanol / toluene and benzyl alcohol/toluene mixtures.

Toluene acts as an inhibitor on the growth of *P. putida* on these mixtures, and does not contribute to increased growth rates or biomass production.

- For continuous steady state operations, the more readily degradable substrate, ethanol, requires less maintenance for biomass growth on its own (0.10 C-mol/C-mol-h) than bioremediation in the presence of toluene, such as bioremediation of ethanol/toluene mixture (0.27 C-mol/C-mol-h), and benzyl alcohol/toluene mixture (0.069 C-mol/C-mol-h).
- When biomass concentrations reach high levels, the oxygen demand will also be high, which can limit growth, and may require an oxygen enriched air supply.

6.2 RECOMMENDATIONS

- More thorough chemical analyses of the cultures, including ATP, CO_2, acetic acid, etc., is recommended to provide more data for fitting the metabolic models.
- More CSTR experiments at wider operating conditions are recommended. In particular, the lowering of the concentrations of the co-substrates should be studied in the hopes that higher amounts of toluene can be captured and bioremediated.
- A wider range of VOCs should be investigated in order to determine the minimum water solubility chemicals that can actively be consumed by *Psuedomonas putida*.
- A wider range of bacteria should be investigated to determine if bioremediation of toluene as a sole substrate could be achieved in a CSTR.

REFERENCES

Abu-Salah, K.; G. Shelef, D. Levanon; R. Armon, and C. G. Dosoretz, 1996. "Microbial degradation of aromatic and polyaromatic toxic compounds adsorbed on powdered activated carbon", *J. Biotechnol*., 51:265-272.

Alvarez, P. J. J., and T. M. Vogel, 1991. "Substrate interactions of benzene, toluene, and para-xylene during microbial degradation by pure cultures and mixed culture aquifer slurries", *Appl. Environ. Microbiol*., October: 2981-2985.

Arulneyam, D.; and T. Swaminathan, 2000. "Biodegradation of ethanol vapour in a biofilter", *Bioprocess Eng*., 22:63-67.

Bailey, J. E., and Ollis, D. F., 1986, Biochemical Engineering Fundamentals, 2nd ed., McGraw-Hill, Inc., Toronto.

Bevington, P. R., 1969. Data reduction and error analysis for the physical sciences. New York : McGraw-Hill.

Benedek, A. and Heideger, W. J., 1971. "Effect of additives on mass transfer in turbine aeration", *Biotechnol. Bioeng*., XIII, 663-684.

Bibeau, L.; K. Kiared,; A. Leroux; R. Brzezinski; G. Viel, and M. Heitz, 1997. "Biological purification of exhaust air containing toluene vapor in a filter-bed reactor", *Can. J. Chem. Eng*., 75: 921-929.

Bielefeldt, A. R., and Stensel, H. D., 1999, "Modeling Competitive Inhibition Effects During Biodegradation of BTEX Mixtures", *Wat. Res*., 33(3):707-714.

Blanch, H. W., and Clark, D. S., 1997, Biochemical Engineering, Marcel Dekker, Inc., Hong Kong.

Bohn, H., 1992. "Consider biofiltration for decontaminating gases", *Chem. Eng. Prog*., 88(4): 34-40.

Bohn, H. L., 1993. "Bioprocessing of organic gases in waste air", Symposium on Bioremediation and Bioprocessing, 205th National Meeting, Am. Chem. Soc., p287-289.

Box, E. P. G., Hunter, W. G., and Hunter, J. S., 1978, Statistics for Experimenters, An introduction to Design, Data Analysis, and Model Building, John Wiley & Sons.

Brown, W. A., D. G. Cooper, and S. N. Liss, 2000. "Toluene Removal in an Automated Cyclical Bioreactor", *Biotechnol. Bioeng*., 16: 378-384.

Bruining, W. J., G. E. H. Joosten, A. A. C. M. Beenackers, and H. Hofman, 1986. "Enhancement of gas-liquid mass transfer by a dispersed second liquid phase", *Chem. Eng. Sci*., 41:1873-1877.

Brusseau, M. L., 1993. Complex Mixtures and Water Quality, EPA/600/S-93/004. U. S. Environmental Protection Agency, Washington, DC.

Calderbank, P. H., and M. B.Moo-Young, 1961. "The continuous phase heat and mass-transfer properties of dispersions", *Chem. Eng. Sci*., 16: 39-54.

Carno, J.; M. Berg and S. Jaras, 1996. "Catalytic abatement of emissions from small-scale combustion of wood", *Fuel*, 75: 959-965.

Cesario, M. T., W. A. Beverloo, J. Tramper, and H. H. Beeftink, 1997. "Enhancement of gas-liquid mass transfer rate of apolar pollutants in the biological waste gas treatment by a dispersed organic solvent", *Enzyme Micro. Tech*., 21: 578-588.

Chandak, M. V.; and Y. S. Lin, 1998. "Hydrophobic zeolites as adsorbents for removal of volatile organic compounds from air", *Environ. Technol*., 19:941-948.

Chang, M. K., Voice, T., and Criddle, C. S., 1993. "Kinetics of Competitive Inhibition and Cometabolism in the Biodegradation of Benzene, Toluene, and *p*-Xylene by Two Pseudomonas Isolates", *Biotechnol. Bioeng.*, 41: 1057-1065.

Chapelle, F. H., 1993. Ground-Water Microbiology and Geochemistry, John Wiley & Sons, Inc., New York, NY.

Chozick, R., and R. L. Irvine, 1991. "Preliminary studies on the granular activated carbon-sequencing batch biofilm reactor", *Environ. Progress*, 10 (4): 282-289.

Chuang, K. T.; S. Cheng, and S. Tong, 1992. "Removal and destruction of benezene, toluene, and xylene from wastewater by air stripping and catalytic oxidation", *Ind. Eng. Chem. Res.*, 31: 2466-2472.

Cioci, F.; R. Lavecchia, and M. M. Ferranti, 1997. "High-performance microbial removal of ethanol from contaminated air", *Biotechnol. Tech*., 11(12): 893-898.

Collins, L. D., and A. J. Daugulis, 1999a. "Benzene/toluene/p-xylene degradation. Part I. Solvent selection and toluene degradation in a two-phase partitioning bioreactor", *Appl. Microbiol. Biotechnol*., 52: 354-359.

Collins, L. D., and A. J. Daugulis, 1999b. "Benzene/toluene/p-xylene degradation. Part II. Effect of substrate interactions and feeding strategies in toluene/benzene and toluene/p-xylene fermentations in a partitioning bioreactor", *Appl. Microbiol. Biotechnol.*, 52: 360-365.

Collins, L. D., and A. J. Daugulis, 1999c. "Simultaneous biodegradation of benzene, toluene, and p-xylene in a two-phase partitioning bioreactor: concept demonstration and practical application", *Biotechnol. Prog*., 15: 74-80.

Corseuil, H., and P. J. J. Alvarez, 1996. "Natural bioremediation perspective for BTX-contaminated groundwater in Brazil: Effect of ethanol", *Wat. Sci. Tech*., 34 (7-8): 311-318.

Corseuil, H.; C. Hunt; R. dos Santos Ferreira, and P. Alvarez, 1998. "The influence of the gasoline oxygenate ethanol on aerobic and anaerobic BTX biodegradation", *Wat. Res.,* 32(7): 2065-2072.

Criddle, C. S., 1993. "The kinetics of cometabolism", *Biotechnol. Bioeng*., 41:1048-1056.

Cross Jr., F. L., and J. Howell, 1992. "New technology to meet air toxics regs", *Pollution Eng*., March 15, 41-47.

Darlington, A. B.; J. F. Dat, and M. A. Dixon, 2001. "The biofiltration of indoor air: Air flux and temperature influences the removal of toluene, ethylbenzene, and xylene", *Environ. Sci. Technol*., 35(1): 240-246.

Doerr, W. W., 1993. "Plan for the future with pollution prevention", *Chem. Eng. Prog*., January , 24-29.

Dueso, N., 1994. "Volatile organic compounds treatment techniques", *Stud. Environ. Sci*., 61:263–276.

Edwards, F. G. and N. Nirmalakhandan, 1996. "Biological treatment of airstreams contaminated with VOCs : an Overview", *Wat. Sci. Tech*., 34(3-4): 565-571.

Environment Canada, 2005a. http://www.msc.ec.gc.ca/cd/factsheets/smog/index_e.cfm; created: 2000-08-23, Reviewed: 2002-12-18, Visited: 2005-03-07.

Environment Canada, 2005b. http://www.ec.gc.ca/pdb/cac/ape_tables/canada2000_e.cfm; last updated: 2004-12-30, last reviewed: 2004-12-30, Visited: 2005-03-07.

EPA, 2005, http://www.epa.gov/ttn/chief/trends/trends02/trendsreportallpollutants010505.xls, 1/5/2005. Visited: 2005 – 03-07

Falatko, D. M., and J. T. Novak, 1992. "Effects of biologically produced surfactants on the mobility and biodegradation of petroleum hydrocarbons", *Water Environ. Res.*, 64: 163-169.

Fang, C. S., and S.-L. Khor, 1989. "Reduction of volatile organic compounds in aqueous solutions through air stripping and gas-phase carbon adsorption", *Environ. Prog.*, 8 (4): 270-278.

Gaudy, Jr., F. A. and Gaudy, E. T, 1980. Microbiology for Environmental Scientists and Engineers. McGraw-Hill Book Company.

Gibson, D. T.; M. Hensley; H. Yoshioka, and T. J. Mabry, 1970. "Formation of (+)-cis-2,3-dihydroxy-1-methylcyclohexa-4,6-diene from toluene by Pseudomonas putida", *Biochem*., 9 (7): 1626-1630.

Goldsmith, C. D., and R. K. Balderson, 1988. "Biodegradation and growth kinetics of enrichment isolates on benzene, toluene and xylene", *Wat. Sci. Tech*., 20 (11/12):505-507.

Gossett, J. M., 1987. "Measurement of Henry's Law Constants for C1 and C2 Chlorinated Hydrocarbons", *Environ. Sci. Technol*., 21:202-208.

Goudar, C.; K. Strevett, and J. Grego, 1999. "Competitive substrate biodegradation during surfactant-enhanced remediation", *J. Environ. Eng*., December, 1142-1148.

Guha, S., Peters, C. A., and Jaffe, P. R., 1999. "Multisubstrate biodegradation kinetics of naphthalene, phenanthrene, and pyrene mixtures", *Biotechnol. Bioeng.,* 65:491-499.

Hamer, G.; N. Al-Awadhi and Th. Egli, 1989. "Biodegradation of petrochemical industry pollutants at elevated temperatures", DECHEMA Meeting of Biotechnologists (7^{th} 1989: Frankfurt Am Main, Germany), 3:823-827.

Hartmans, S., 1997. "Biological waste gas treatment: kinetics and reactors", *Med. Fac. Landbouww. Univ. Gent*., 62/4b: 1501 – 1504.

Hassan, I. T. M. and C. W. Robinson, 1977. "Oxygen transfer in mechanically agitated aqueous systems containing dispersed hydrocarbons", *Biotechnol. Bioeng*., 19: 661-682.

Hassan, I. T. M. and C. W. Robinson, 1980. "Mass transfer coefficients in mechanically agitated gas-aqueous electrolyte dispersions", *Can. J. Chem. Eng*., 58: 198-205.

Heinen, A. W.; J. A. Peters, and H. van Bekkum, 2000. "Competitive adsorption of water and toluene on modified activated carbon supports", *Appl. Catalysis A: General*, 194-195:193-202.

Hekmat, D., and D. Vortmeyer, 1994. "Modelling of biodegradation processes in trickled-bed bioreactors", *Chem. Eng. Sci*., 49(24A):4327-4345.

Hill, G. A., 1974, Kinetics of Phenol Degradation by Pseudomonas putida. M.Sc Thesis, University of Waterloo.

Hill, G.A. and C.W. Robinson, 1975. "Substrate Inhibition Kinetics: Phenol Degradation by *Pseudomonas putida*", *Biotechnol. Bioeng*. 17:1599-1615.

Hill, G.A., B. J. Ritchie, H. Baheri, and S. Textor, 1996, Mixed-Flow Hydrodynamics: Advances in Engineering Fluid Mechanics Series, Nicholas P. Cheremisinoff, Editor, Gulf Publishing Company, pp 499-519.

Hill, G. A., and A. J. Daugulis, 1999. "Phenol inhibition kinetics for growth of Acetobacter aceti on ethanol", *Appl. Microbiol. Biotechnol*, 51: 841-846.

Hodge, D. S.; J. S. Devinny, 1994. "Biofilter treatment of ethanol vapors", *Environ. Prog*., 13:167-173.

Hounsell, G., 1995. "Case studies: selection of high efficiency VOC removal technologies for process air streams", *Proceedings, Annual Meeting - Air and Waste Management Association,* Vol. 1A, page 95-MP3.01, 24 pp.

Hussey, F., and A. Gupta, 1998. "Meet VOC regs with the right adsorbent", *Ind. Paint & Powder*, 3: 6-50.

Hunt, C.; P. Alvarez; R. dos Santos Ferreira, and H. Corseuil, 1997. "Effect of ethanol on aerobic BTEX degradation", In: *In situ and Onsite Bioremediation*, B. C. Alleman and A. L. Leeson (Eds.). Batelle Press, Columbus, OH, Vol. 1, pp. 49-54.

Jorio, H., K. Kiared, R. Brzezinski, A. Leroux, G. Viel , and M. Heitz, 1998. "Treatment of air polluted with high concentrations of toluene and xylene in a pilot-scale biofilter", *J. Chem. Technol. Biotechnol*., 73:184 – 196.

Kastner, J. R.; D. N. Thompson, and R. S. Cherry, 1999. "Water-soluble polymer for increasing the biodegradation of sparingly soluble vapors", *Enzyme Microbial. Technol*., 24: 104-110.

Kennedy, J. B. and Neville, A. M., 1974, Basic Statistical Methods for Engineers and Scientists, 2nd Edition, Harper and Row Publishers.

Keuning, S., and D. Jager, 1994. "Simultaneous degradation of chlorobenzene, toluene, xylene, and ethanol by pure and mixed *Pseudomonas* cultures", in Appl. Biotechnol. for Site Remediation, Hinchee, R.E., D.B. Anderson, F.B. Metting and G.D. Sayles (Eds.), Lewis Publishers, Boca Raton, USA, pp. 332-336.

Kiared, K.; L. Bibeau; and R. Brzezinski, 1996. "Biological elimination of VOCs in biofilter", Environ. Prog., 15 (3):148 – 152.

Kim, H.-S. and P.R. Jaffe, "Simulating the biodegradation of toluene at the macroscopic and pore-level scale for aerobic and nitrate reducing conditions", ACS National Meeting, Division of Environ. Chem. Preprints of Extended Abstract, 42(2): 363-365, August, 2000.

Kirchner, K.; G. Hauk, and H. J. Rehm, 1987. "Exhaust gas purification using immobilized monocultures (biocatalysts)", *Appl. Microbiol. Biotechnol*., 26:579-587.

Kirchner, K.; U. Schlachter, and H. J. Rehm, 1989. "Biological purification of exhaust air using fixed bacterial monocultures", *Appl. Microbiol. Biotechnol*., 31: 629-632.

Kirchner, K.; C. A. Gossen, and H. J. Rehm, 1991. "Purification of exhaust air containing organic pollutants in a trickled-bed bioreactor", *Appl. Microbiol. Biotechnol*., 35: 396-400.

Kirchner, K.; S. Wagner, and H. J. Rehm, 1992. "Exhaust gas purification using biocatalysts (Fixed bacteria monocultures) – the influence of biofilm diffusion rate (O2) on the overall reaction rate", *Appl. Microbiol. Biotechnol*., 37: 277-279.

Kirchner, K.; S. Wagner, and H. J. Rehm, 1996. "Removal of pollutants from exhaust gases in the trickle-bed bioreactor. Effect of oxygen", *Appl. Microbiol. Biotechnol*., 45: 415-419.

Klainer, A. S. and C. J. Betsch, 1970. "Scanning –Beam Eletron Microscopy of Selected Microorganisms", *J. Infectious Disease*, 121(3):339-343.

Kozliak, E. I.; T. L. Ostlie-Dunn, 1997. "Efficient air purification from VOC using a fiber-based trickle-bed bioreactor", Preprints *Am. Chem. Soc., Division of Petroleum Chem.,* 42(3): 694-698.

Kozliak, E. I.; T. L. Ostlie-Dunn, M. L. Jacobson, S. R. Mattson; and R. T. Domack, 2000. "Efficient steady-state volatile organic compound removal from air by live bacteria immobilized on fiber supports", *Bioremediation J*., 4(1):81-96.

Lee, J. C., and D. L. Meyrick, 1970. "Gas-liquid interfacial areas in salt solutions in an agitated tank", *Trans. Instn. Chem. Engrs.* (London), 48: T37.

Leson, G. and A. M. Winer, 1991. "Biofiltration: An innovative air pollution control technology for VOC emissions", *J. Air and Waste Manage. Assoc.*, 41(8):1045-1054.

Levenspiel, O., 1972. Chemical Reaction Engineering. John Wiley & Sons, Inc., New York, N. Y., 476.

Lodaya, M.; F. Lakhwala; E. Rus; M. Singh; G. Lewandowski, and S. Sofer, 1991. "Biodegradation of benzene and a BTX mixture using immobilized activated sludge", *J. Environ. Sci. Health*, A26(1):121-137.

Luong, J. H. T., 1987. "Generalization of Monod Kinetics for Analysis of Growth Data With Substrate Inhibition", *Biotechnol. Bioeng*., 29: 242-248.

Lyman, W.J., W.F. Reehl, and D. H. Rosenblatt, 1982. Handbook of Chemical Property Estimation Methods, McGraw-Hill Book Company.

Machado, R. J., and Leslie Grady, Jr., C. P., 1989. "Dual Substrate Removal by an Axenic Bacterial Culture", *Biotechnol. Bioeng*., 33:327-337.

Marek, J.; J. Paca, and A. M. Gerrard, 2000. "Dynamic responses of biofilters to changes in the operating conditions in the process of removing toluene and xylene from air", *Acta Biotechbol*., 20(1): 17-29.

Mason, C. A.; G. Ward; K. Abu-Salah; O. Keren, and C. G. Dosoretz, 2000. "Biodegradation of BTEX by bacteria on powdered activated carbon", *Bioprocess Eng*., 23: 331-336.

Merchuk, J. C., S. Yona, M. H. Siegel, and A. B. Zvi, 1990. "The first-order approximation to the response of dissolved oxygen electrodes for dynamic k_La estimation", *Biotechnol. Bioeng*., 35: 1161-1163.

Morales, M.; F. Perez; R. Auria, and S. Revah, 1994. "Toluene removal from air stream by biofiltration", in "Advances in Bioprocess Engineering", E. Galindo and O.T. Ramlrez (eds.), Kluwer Academic Publishers. pp. 405-411.

Nakao, K.; M. A. Ibrahim; Y. Yasuda, and K. Fukunaga, 2000. "Removal of volatile organic compounds from waste gas in packed column with immobilized activated sludge gel beads", *Bioseparation Eng*., 16: 187-192.

Nielsen, J., J. Villadsen, and G. Liden, 2003. Bioreaction Engineering Principles, 2nd Edition, Kluwer Academic /Plenum Publishers, New York.

Orshansky, F., and N. Narkis, 1997. "Characteristics of organics removal by PACT simultaneous adsorption and biodegradation", *Wat Res*., 31 (3): 391-398.

Ottengraf, S. P. P., 1986. "Exhaust gas purification", *Biotechnol.,* H. J. Rehm and G. Reed (eds.), VHC, Weinhem, 8: 425-451.

Parvatiyar, M. G.; R. Govind, and D. F. Bishop, 1996. "Biodegradation of toluene in a membrane biofilter", *J. Membrane Sci*., 119: 17-24.

Passant, N. R.; S. J. Richardson; R. P. J. Swannell; M. Woodfield; J. P. van der Lugt; J. H. Wolsink; P.G.M. Hesselink; V. Hecht; D. Brebbermann and H. Bischoff, 1992. "Biodegradability of the volatile organic compound (VOC) emissions from the food, drink and metal degreasing industries", *Studies in Environ. Sci*., 51:315 – 320.

Pederson, A. R., and E. Arvin, 1999. "The function of a toluene-degrading bacterial community in a waste gas trickling filter", *Wat. Sci. Tech*., 39(7): 131-137.

Purwaningsih, I.S, 2002, Mass transfer and Bioremediation of solid polycyclic aromatic hydrocarbon (PAH) particles in bioreactors, Ph.D Thesis, University of Saskatchewan.

Ramirez-Lopez, E. M.; A. Montillet; J. Comiti and P. Le Clolrec, 2000. "Biofiltration of volatile organic compounds – application to air treatment", *Wat. Sci. Technol*., 41 (12):183-190.

Reardon, K. F.; J. R. Conuel, and D. C. Mosteller, 1994. "Biodegradation kinetics and bioreactor strategy for aromatic hydrocarbon and trichloroethylene mixtures", Proceedings of the 9th Annual Conferences on Hazardous Waste Remediation, June 8-10, pp. 51-65.

Reardon, K. F.; D. C. Mosteller; and J. D. B. Rogers, 2000. "Biodegradation kinetics of benzene, toluene, and phenol as single and mixed substrates for Pseudomonas putida F1", *Biotechnol. Bioeng*., 69(4): 385-400.

Reece, C. S.; M. Lordgooei, and M. J. Rood, "Activated carbon fiber cloth adsorber with cryogenic condensation to capture and recover MEK and toluene from gas streams", Air & Waste Management Association's 91st Meetings & Exhibition, June 14-18, 1998, San Diego, California.

Robinson, C. W. and C. R. Wilke, 1973. "Oxygen absorption in stirred tanks: a correlation for ionic strength effects", *Biotechnol. Bioeng*., XV: 755-782.

Robinson, C. W. and C. R. Wilke, 1974. "Simultaneous measurement of interfacial area and mass transfer coefficients for a well-mixed gas dispersion in aqueous electrolyte solutions", *AIChE J.*, 20(2): 285-294.

Roels, J. A., 1980. "Simple Model for the Energetics of Growth on Substrates with Different Degrees of Reduction", *Biotech. Bioeng*., 22: 33-53.

Roels, J. A., 1983, Energetics and Kinetics in Biotechnology, Elsevier Biomedical Press, NY.

Rols, J. L., J. S. Condoret, C. Fonade, and G. Goma, 1991. "Modeling of oxygen transfer in water through emulsified organic liquids", *Chem. Eng. Sci.,* 46:1869-1873.

Romine, M. F., and F. J. Brockman, 1996. "Recruitment and Expression of toluene /trichloroethylene biodegradation genes in bacteria native to deep-subsurface sediments", *Appl. Envrion. Microbiol*., 62 (7):2647-2650.

Shareefdeen, Z.; B. C. Baltzis, Y-S. Oh; and R. Bartha, 1993. "Biofiltration of methanol vapor", *Biotechnol. Bioeng*., 41: 512-514.

Shareefdeen, Z., and B. C. Baltzis, 1994 "Biological removal of hydrophobic solvent vapors from airstreams", Int. Symposium on Bioprocess Engineering, 1st, pp. 397-404.

Shim, J. S.; J. T. Jung; and S. Sofer, 1995. "Oxidation of ethanol vapors in a spiral bioreactor", *J. Chem. Tech. Biotechnol*., 64: 49-54.

Shuler, M. L., F. Kargi, 2002. Bioprocess engineering: basic concepts, Prentice, Englewood Cliffs, NJ.

Singh, N., and G. A. Hill, 1987. "Air stripping effects on cell growth with volatile substances", *Biotechnol. Bioeng*., 30: 521-527.

Smolders, G. J. F., J. van der Meij, M. C. M. van Loosdrecht, and J. J. Heijnen, 1994. "Stoichiometric Model of the Aerobic Metabolism of the Biological Phosphorus Removal Process", *Biotech. Bioeng*., 44: 837-848.

Song, J.-H., and K. A. Kinney, 1999. "Biomass distribution in a vapor phase bioreactor for toluene removal", International In Situ and On-Site Bioremediation Symposium, 5th , pp. 117-122.

Stanier, R. Y.; N. J. Palleroni and M. Doudoroff, 1966. "The aerobic Pseudomonads: a taxonomic study", *J. Gen. Microbiol*., 43: 159-271.

Strous, M.; J. J. Heijnen; J. G. Kuene, and M. S. M. Jetten, 1998. "The sequencing batch reactor as a powerful tool for the study of slowly growing anaerobic ammonium-oxidizing microorganisms", *Appl. Microbio. Biotechnol*., 50: 589-596.

Togna, A. P, M. Singh, 1994. "Biological vapor-phase treatment using biofilter and biotrickling filter reactors: Practical operating regimes", *Envrion. Prog*., 13(2): 94-97.

Tsao, G. T., and Hanson, T. P., 1975, "Extended Monod equation for batch culture with multiple exponential phases", *Biotechnol. Bioeng*., 17:1591-1598.

Uhl, W.; R. Gimbel; G. Bundermann, and D. Wittich, 1996. "A two-step process for biodegradation and activated carbon – a means to improve removal of AOC and natural organics and to achieve longer operation times of GAC-adsorbers", *Wat. Supply*, 14(2):243-251.

Van der Meer, A. B., A. A. C. M Beenackers, R. Burghard, N. H. Mulder, and J. J. Fok., 1992. "Gas/liquid mass transfer in a four-phase stirred fermentor: Effects of organic phase hold-up and surfactant concentration", *Chem. Eng. Sci*., 47:2369-2374.

Van Groenestijn, J. W.; and P. G. M. Hesselink, 1993. "Biotechniques for air pollution control", *Biodegradation*, 4: 283-301.

Vecht, S. E.; M. W. Platt; Z. Er-El, and I. Goldberg, 1988. "The growth of Pseudomonas putida on m-toluic acid and on toluene in batch and in chemostat cultures", *Appl. Microbiol. Biotechnol*., 27: 587-592.

Vega, J. L.; E. C. Clausen; and J. L. Gadday, 1989. "Study of Gaseous substrate fermentation: carbon monoxide conversion to acetate. I. Batch culture", *Biotechnol. Bioeng*., 34: 774-784.

Vipulanandan, C.; R. Willson and G. Ghurye, 2000. "Effect of clay and biosurfactant on the biodegradation of toluene", *Geoenvironment,* 1479-1492.

Voigt, J. and K. Schugerl, 1979. "Absorption of oxygen in countercurrent multistage bubble columns – I Aqueous solutions with low viscosity", *Chem. Eng. Sci*., 34: 1221-1229.

Wackett, L, 2005. "Toluene Pathway Map", from website: http://umbbd.ahc.umn.edu/tol/tol_map.html, University of Minnesota.

Wang, N., 2001. Experimental Study and Mathematical Modeling of Enhanced Biological Phosphorus Removal Using Glucose as the Dominant Substrate, Ph.D Thesis, University of Saskatchewan.

Wang, N., G. Hill and J. Peng, 2002. “Mathematical model for the microbial metabolism of glucose induced enhanced biological phosphorus removal in an anaerobic/aerobic sequential batch reactor", *Environ. Eng. Policy*, 3:87-99.

Weber, F. J., and S. Hartmans, 1995. “Use of activated carbon as a buffer in biofiltration of waste gases with fluctuating concentrations of toluene”, *Appl. Microbiol. Biotechnol*., 43: 365-369.

Weber, F. J., and S. Hartmans, 1996. “Prevention of clogging in a biological trickle-bed reactor removing toluene from contaminated air”, *Biotechnol. Bioeng*., 50: 91-97.

Wei, V.Q.; G. A. Hill, and D. G. Macdonald, 1999. “Bioremediation of contaminated air using an external-loop airlift bioreactor”, *Can. J. Chem. Eng*., 77: 955-962.

Wilcox, J. B. and F. J. Agardy, 1990. “Thermal destruction of air toxic VOC’s using packed bed technology”, proceedings: 83rd A&WMA Meeting, United States Air and Waste Management Association, pages: 90/106.6, 12 pp.

You, J. H.; H. L. Chiang, and P. C. Chiang, 1994. “Comparison of adsorption characteristics for VOCs on activated carbon and oxidized activated carbon”, *Environ. Prog*., 13 (1): 31-36.

APPENDIX A. Important Metabolic Pathways

I. **Ethanol Pathway** (Adapted from Gaudy and Gaudy, 1980)

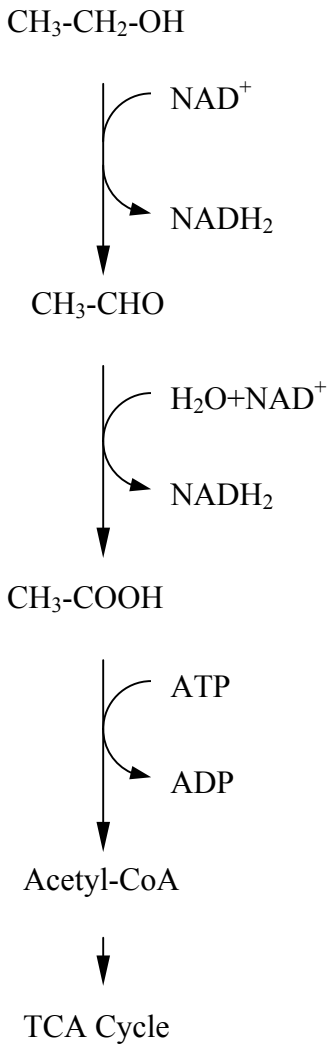

II. The Tricarboxylic Acid (TCA) Cycle*

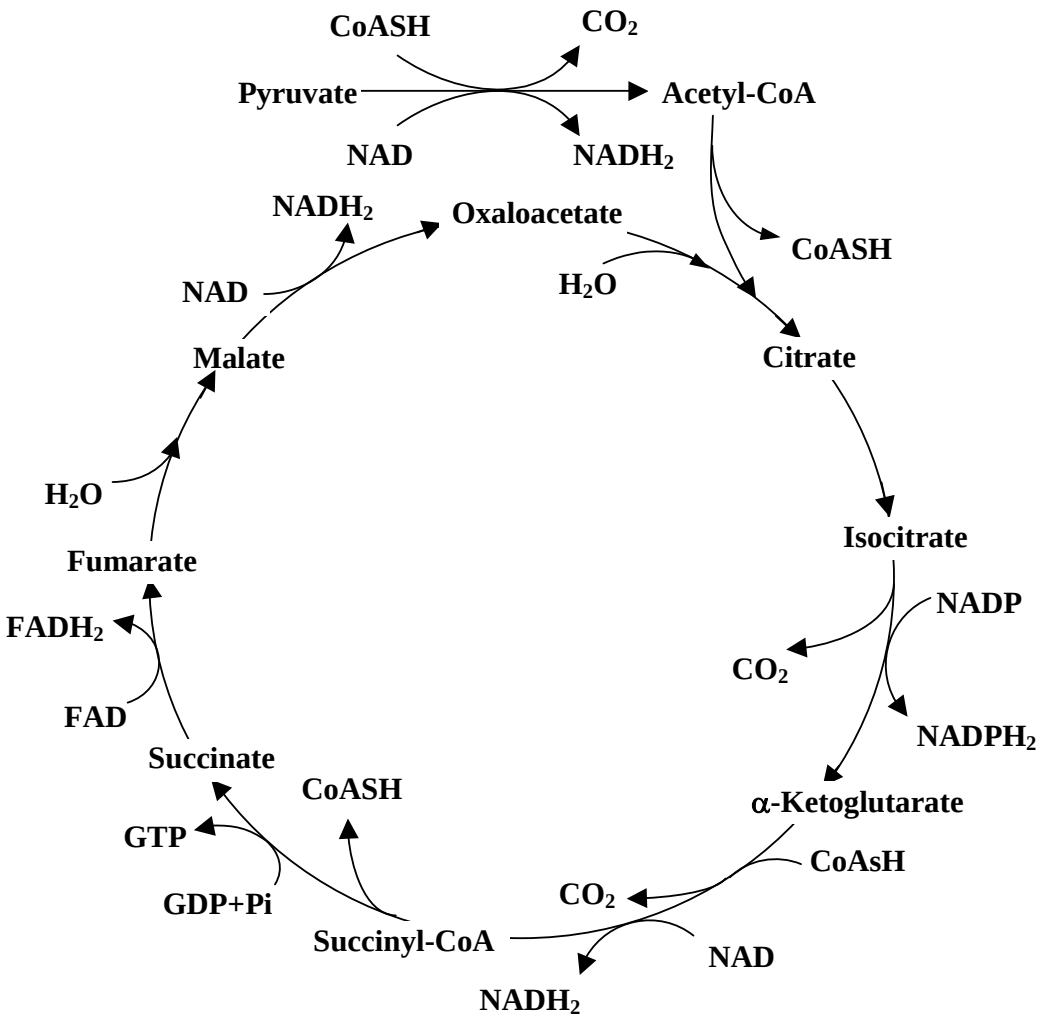

*Adapted from Gaudy and Gaudy, 1980.

III. Toluene Pathway (Adapted from Wackett, 2005)

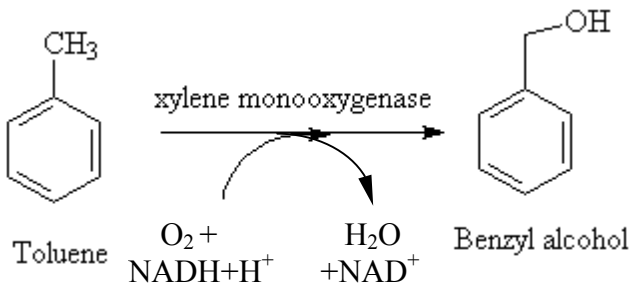

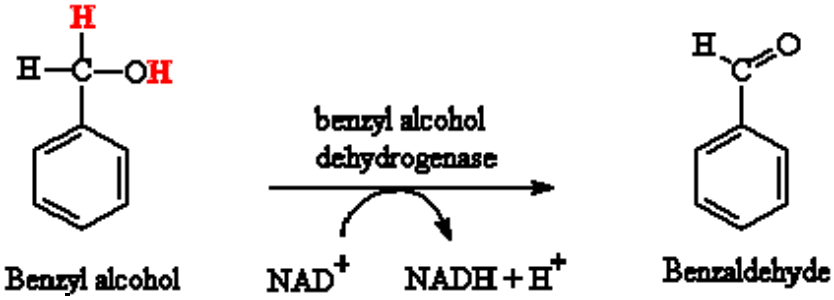

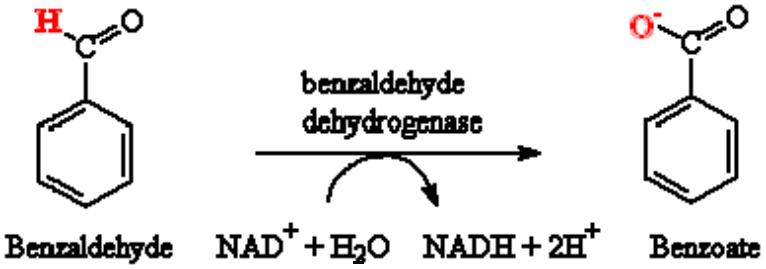

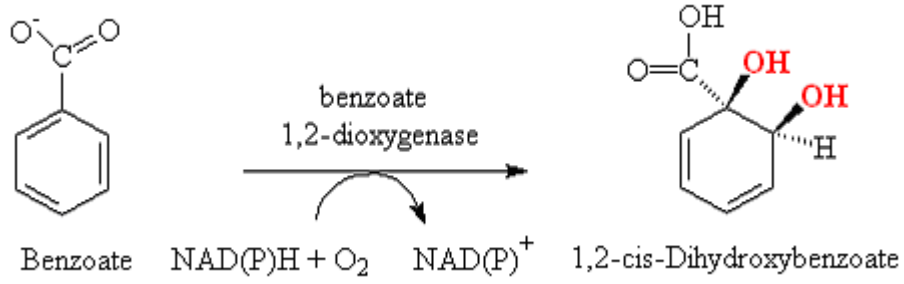

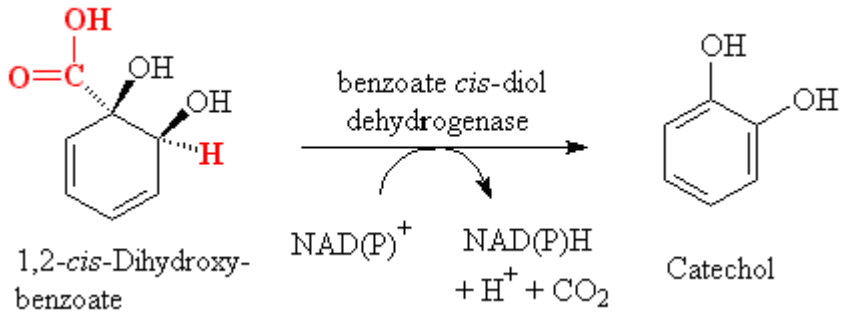
OH
O=C
OH
OH
H
benzoate *cis*-diol
dehydrogenase
NAD(P)+
NAD(P)H
+ H+ + CO2
OH
OH
1,2-*cis*-Dihydroxy-
benzoate
Catechol

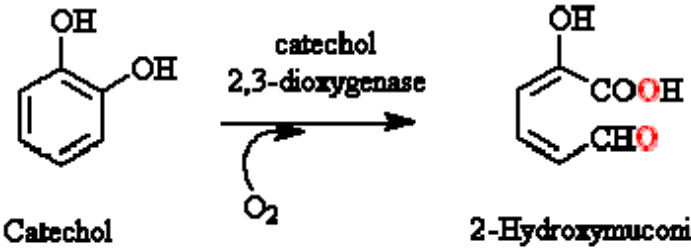
OH
OH
catechol
2,3-dioxygenase
O2
OH
COOH
CHO
Catechol
2-Hydroxymuconic
semialdehyde

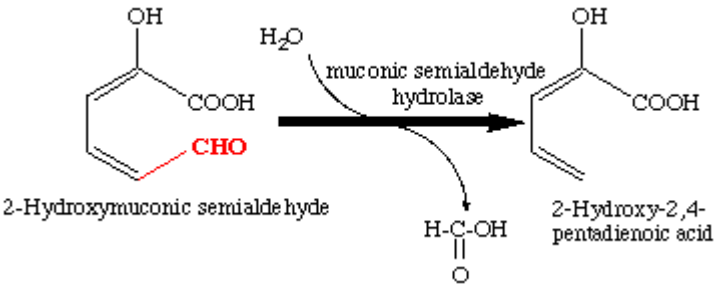
OH
COOH
CHO
2-Hydroxymuconic semialdehyde
H2O
muconic semialdehyde
hydrolase
OH
COOH
2-Hydroxy-2,4-
pentadienoic acid
H-C-OH
O

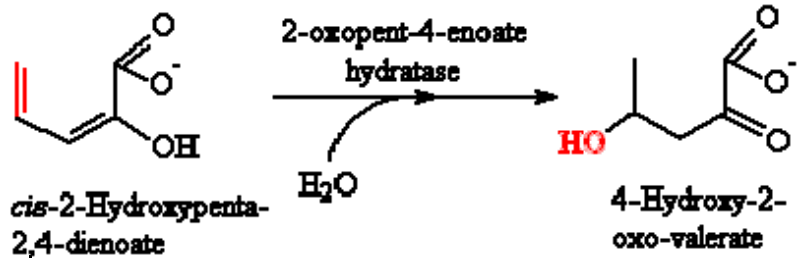
O
O-
OH
2-oxopent-4-enoate
hydratase
H2O
HO
O
O-
O
cis-2-Hydroxypenta-
2,4-dienoate
4-Hydroxy-2-
oxo-valerate

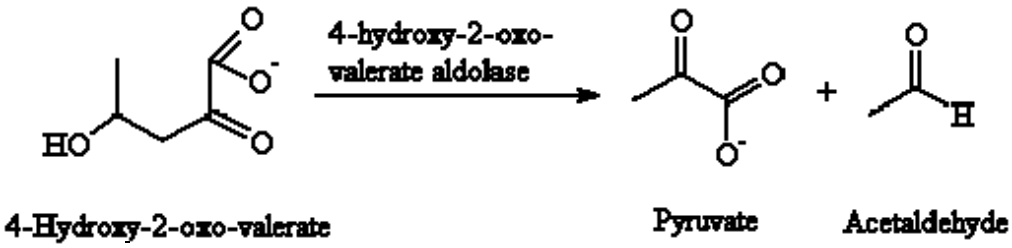
O
O-
HO
O
4-hydroxy-2-oxo-
valerate aldolase
O
O
O-
+
O
H
4-Hydroxy-2-oxo-valerate
Pyruvate
Acetaldehyde

Appendix B. Calibration Procedure and Calibration Curves

Appendix B-1. The Bacteria

Preparation Scanning-Beam Electron Microscopy (SEM)

Bacteria were cultured in benzyl alcohol medium solution (See Section 3.2.3). Normal morphology was defined as that cell form exhibited during free exponential growth. The organisms were harvested by centrifugation at 2,000 rpm for 5 minutes and were washed 3 times in 5-10 ml distilled water; mixed and re-centrifuged for 5 minutes. The organisms were then fixed in buffered 2% (vol%) glutaraldehyde (pH 7.2) for 2 hours at room temperature. The organisms were again centrifuged at 2,000 rpm for 5 minutes, and were then washed 3 times and re-suspended in 5 ml of sterile, distilled, demineralized water. A drop of the suspension was placed on 5-mm disks of heavy-duty aluminum foil and allowed to dry at room temperature (29.0 ^{o}C). The disks were then attached to specimen stubs. Specimens were coated with pure gold on a rotary turntable high-vacuum coating unit to obtain a uniform coating.

SEM

A SEM 505 Philips (Holland) in the Department of Biology, University of Saskatchewan, was employed. Specimens were examined and photographed at accelerating voltage of 30 kv. Figure B-1 (9,600 X) and B-2 (4,780 X) show the SEM graph of *Pseudomonas putida* (ATCC23973) used in this study.

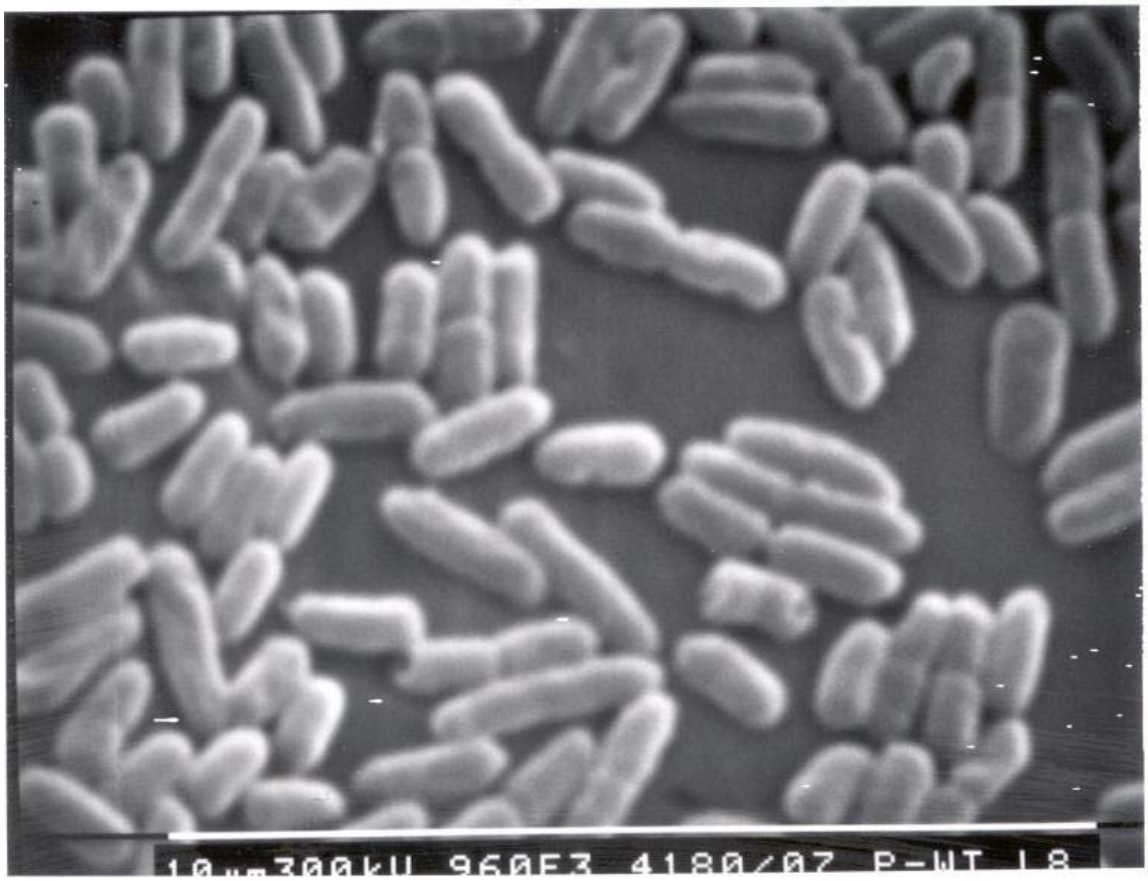

Figure B-1 *Pseudomonas Putida* (ATCC 23973) (9,600 X) by SEM

Figure B-2. *Pseudomonas putida* (ATCC 23973) (4,780 X) using SEM

Appendix B-2 Calibration of Biomass Measurement

The calibration was verified by three independent samples, and the calibration curve for biomass measurement is shown in Figure B-3 by plotting the results from all three samples.

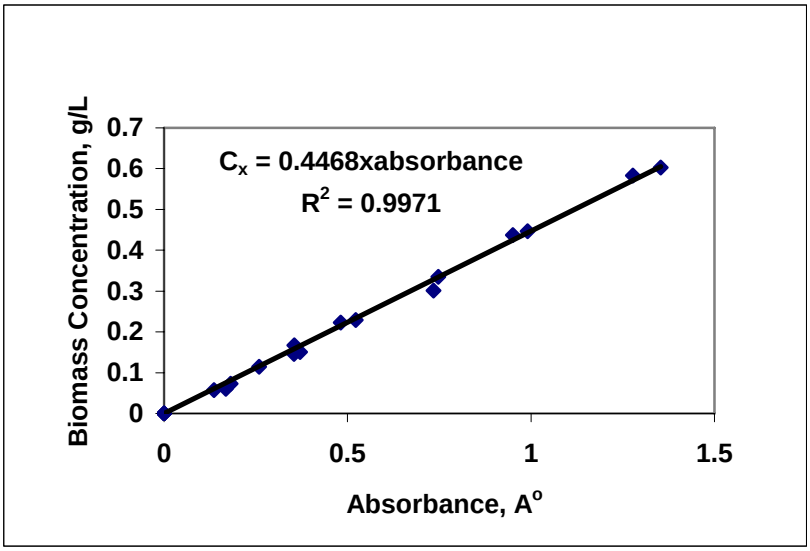

Figure B-3. Biomass calibration curve

Appendix B-3. Calibration of Chemicals (ethanol, benzyl alcohol and toluene)

Ethanol, toluene and benzyl alcohol standards were prepared as aqueous solutions for the calibration of GC analyses. The calibration curves are shown in Figures B-4 to B-6.

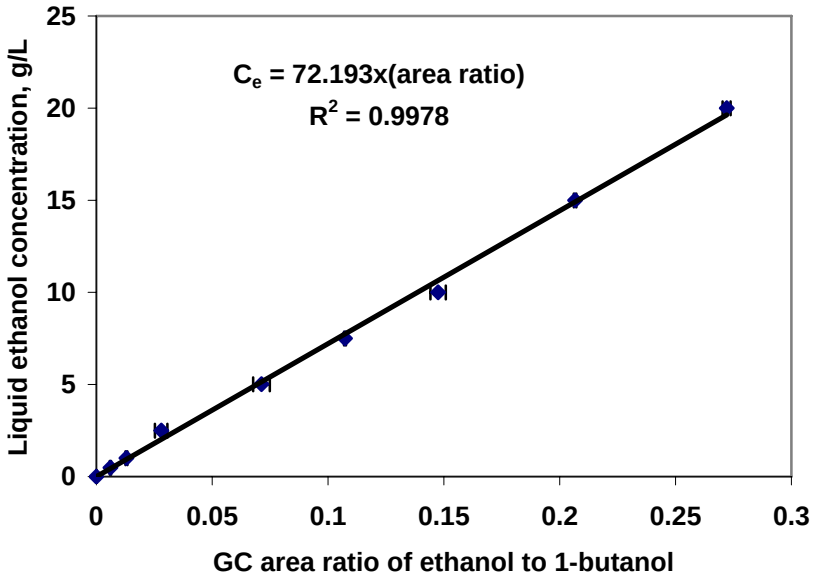

Figure B-4. Calibration curve for ethanol liquid standard

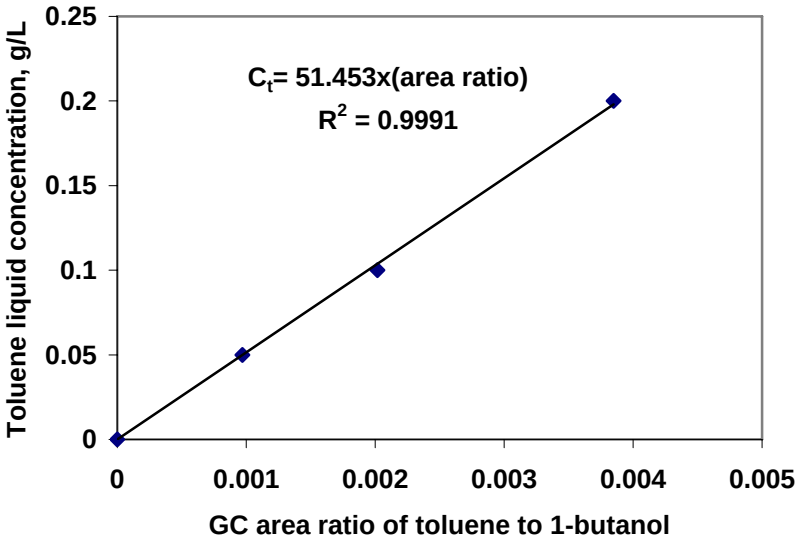

Figure B-5. Calibration curve of toluene liquid standard

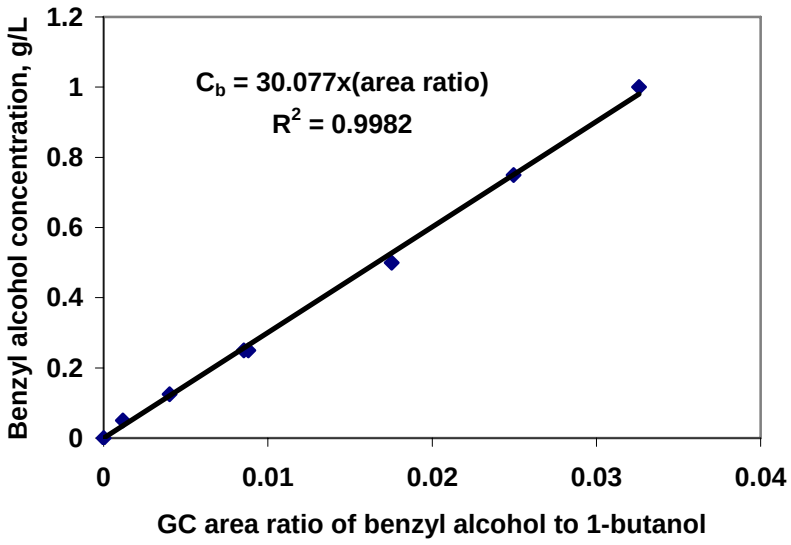

Figure B-6 Calibration curve for benzyl alcohol standard

Appendix B-4. Calibration of Toluene Gas Samples

Air phase calibration standards for toluene concentrations were prepared by adding an amount of liquid toluene in the range of 10 to 60 μL into 160 mL, sealed serum bottles containing of 55 mL of water at 25 ºC. Using the known Henry's constant and volumes of the gas and water phases in the bottles, the toluene concentrations in the gas phase could be calculated (Gossett, 1987; Cesario *et al*., 1997). Reproducibility studies using calibration standards demonstrated that GC measurements for both liquid and gas toluene concentrations were repeatable to ± 8 %. The calibration curve for toluene gas samples is shown in Figure B-7.

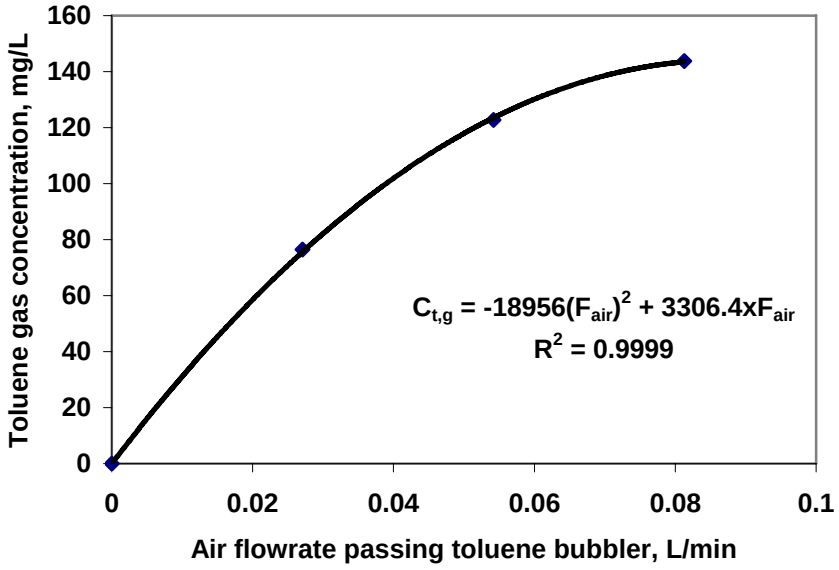

Figure B-7. Calibration of toluene gas concentration

Appendix B-5. Calibration of Air Flowmeter

The calibration curve of the air flowmeter used in this project is given in Figure B-8.

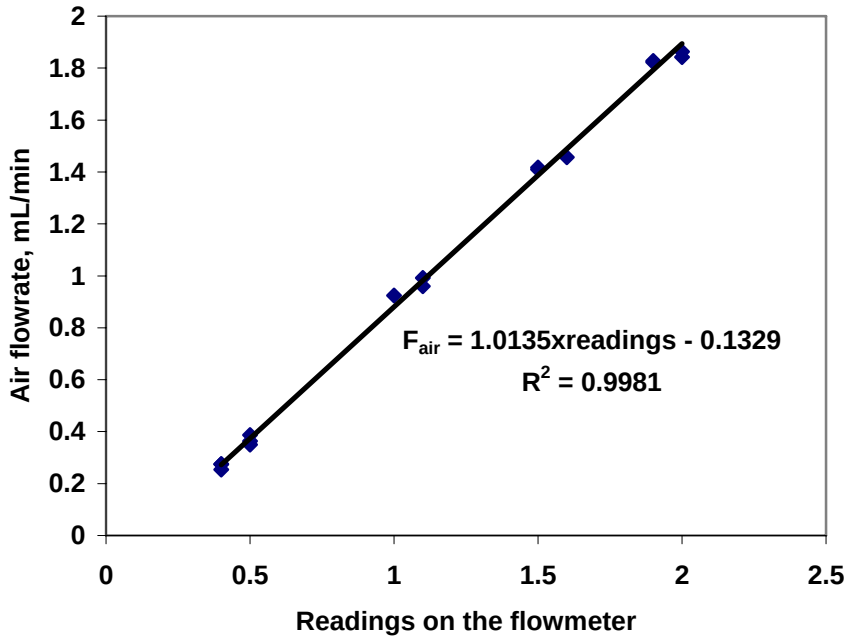

Figure B-8. Calibration curve of air flowmeter on the reactor setup

Appendix C. Experimental Results:

Appendix C-1. Oxygen Mass Transfer

Oxygen transfer from air to an aqueous phase is frequently the rate-limiting step in aerobic fermentations due to the low solubility of oxygen in water. One of the approaches to improve the oxygen transfer rate is by the dispersion into the aqueous medium of a water-immiscible organic solvent (Hassan and Robinson, 1977; Bruining et al., 1986; Rols et al., 1991; Van der Meer et al., 1992; Cesario et al., 1997). Another approach involves using electrolyte solutions (Calderbank and Moo-Young, 1961; Lee and Meyrick, 1970; Benedek and Heideger, 1971; Robinson and Wilke, 1973 and 1974; Hassan and Robinson, 1980). Lee and Meyrick (1970) reported that with pure water in their stirred tank, the average bubble size varied between 2 to 9 mm but in a 35.5 g/L aqueous solution of sodium sulfate the bubble size varied between 0.7 to 1.6 mm. Benedek and Heideger (1971) reported the same phenomenon for 11.7 g/L aqueous solution of sodium chloride but also observed that the mass transfer coefficient increased by a factor of two when sodium chloride was added. Robinson and Wilke (1974) reported that solutions of potassium hydroxide (1.2 to 4.6 g/L) and dipotassium carbonate (0.8 to 3.5 g/L) produced small air bubbles with average diameters between 0.34 to 2.3 mm, while the mass transfer coefficients ranged between 0.0717 to 0.248 s^{-1}.

The response time of the oxygen probe was measured for each of the ethanol-water solutions using two 200-ml beakers with the same ethanol concentration. One beaker was purged of oxygen using a nitrogen gas stream and the other was saturated by oxygen using an air gas stream. The probe was first immersed in the oxygen free liquid until the oxygen sensor stabilized at 0 mg/L. The probe was then instantly immersed

into the oxygen-saturated liquid and the sensor reading was recorded every 10 seconds until the reading reached a constant value. The response time of the probe was then determined by best fitting the oxygen concentration - time profile using non-linear, least square regression.

The first step in conducting the measurements of oxygen transfer to the aqueous phase in the bioreactor involved deaerating the liquid using nitrogen gas. Once the oxygen meter indicated a stable concentration near zero, the flow of nitrogen gas was stopped and air was introduced at a constant flow rate of 3.5 L/min (0.3 vvm). The concentration of oxygen in the aqueous phase was recorded every 10 seconds until the oxygen concentration was constant. The experiments were carried out at different impeller speeds (135, 300, 450 and 600 rpm) and at different ethanol concentrations (0, 1, 3, and 8 g/L ethanol in distilled water).

C-1.1 Determination of Probe Response Time

The probe response tests were carried out at different concentrations of ethanol. The equation used for best fitting the response time (using non-linear, least square regression) was:

$$C_t = C^*_{o_2}(1 - e^{t/t_e}) \qquad \text{(C-1)}$$

The results of the probe response time are shown in Figure C-1. Probe response time is related to O_2 permeability through the probe membrane. The results in Figure C-1 show that increasing ethanol concentration increases the probe response time, and therefore must hinder the O_2 diffusion through the membrane pores. This phenomenon was modeled by the following empirical equation:

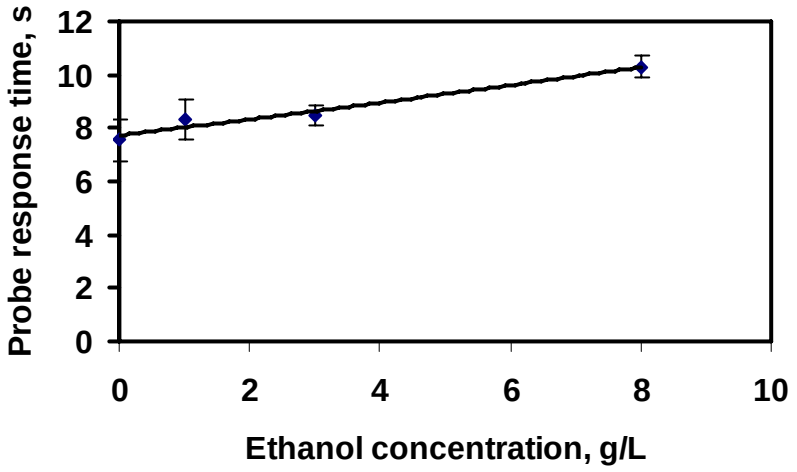

Figure C-1. Effect of ethanol on the response time of the probe (dots represent the experimental data; error bars represent experimental standard deviations; line represents Equation C-2).

$$t_e = 7.73 + 0.292\,[E] + 0.00351\,[E]^2 \qquad \text{(C-2)}$$

Both the mass transfer coefficient and gas holdup at an ethanol concentration of 20 g/L were also measured, but there were no further significant increases (3.2% increase compared to the values measured at an ethanol concentration of 8 g/L). For this reason, studies were not undertaken at higher ethanol concentrations. Undoubtedly, one of the factors contributing to increased mass transfer is the reduction in bubble coalescence due to the presence of alcohol molecules in the aqueous phase (Ziemaski et al., 1967; van de Donk et al., 1979). Another factor observed in this study is due to the formation of much smaller bubbles in alcohol solutions.

Table C-1. Dimensions of the stirred tank bioreactor

Property	Value
Reactor diameter	0.247 m
Reactor height	0.320 m
Number of impellers	2
Position of impellers (from bottom)	0.05, 0.18 m
Impeller diameter	0.06 m
Blade width	0.01 m
Volume	0.014 m^3

Appendix C-2. Fed-batch Operation

Batch growth experiments performed at very high substrate concentrations often result in very poor bacterial biomass yield because of substrate inhibition, oxygen insufficiency, and the generation of toxic metabolic byproducts. Fed-batch processes are often employed in fermentation to minimize substrate inhibition, or to avoid oxygen insufficiency and possible overheating (resulting from high biomass growth).

In this study, a working medium volume of 1.5 L was added to the bioreactor for fed-batch operation. The inoculum was prepared in shake flasks using the same chemical as the growth substrate (See Section 3.2.3 for preparation procedure) and then transferred into the bioreactor at time zero. The substrate, ethanol, was continuously introduced from a contaminated air stream. The ethanol gas concentrations both in the inlet and outlet gas streams were measured and in the liquid phase as well.

An ethanol inlet concentration of 25.0 mg/L was introduced into the bioreactor at an air flowrate of 0.4 L/min with a working volume of 1.5 L. Figure C-2 shows a fed-batch operation conducted at 450 RPM and 25.0°C. Initially, ethanol metabolism was low and the ethanol concentration in the liquid increased similar to an ethanol mass transfer alone (shown by the straight line in Figure C-2). After about three hours, biomass growth for the next five hours prevented further build-up of ethanol in the liquid phase.

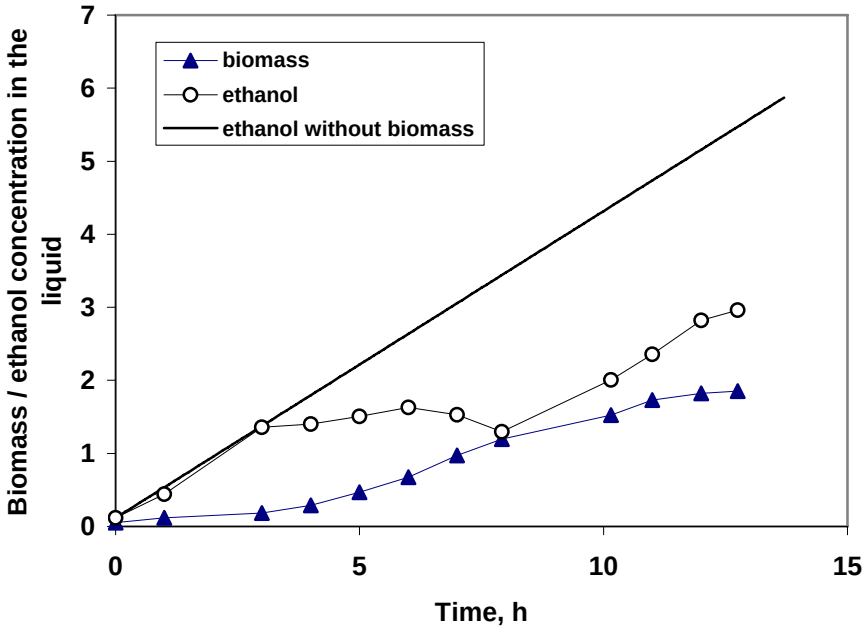

Figure C-2. Removal of ethanol from air stream by *Pseudomonas putida* in a fed-batch operation at 450 rpm and 25.0°C, ethanol inlet concentration of 25.0 mg/L (___ Predicted ethanol liquid concentration with absence of biomass in the bioreactor).

However, ethanol eventually started once again to accumulate at the same rate as mass transfer alone due to the depletion of mineral nutrients. Although this could probably be overcome with a time-dependant addition of mineral nutrients, this would require a sophisticated control strategy, so it was decided to operate the bioreactor on a continuous basis with continuous medium solution flow in and out, and with simultaneous continuous addition of the organic substrate from the contaminated air stream.

Appendix D: Mathematical Solutions and Derivations

Appendix D-1. Model for Ethanol Bioremediation

For ethanol bioremediation, the overall conversion rates of the key compounds are given in Section 5.1.2 as:

$$r_e = -1.27\nu_1 - \nu_2 \tag{5-14a}$$

$$r_x = \nu_1 \tag{5-14b}$$

$$r_{o_2} = -0.5\nu_3 \tag{5-14c}$$

$$r_{co_2} = 0.27\nu_1 + \nu_2 \tag{5-14d}$$

$$-\alpha_{1E} \cdot \nu_1 - 0.5 \cdot \nu_2 + \delta \cdot \nu_3 = 0 \tag{5-14e}$$

$$1.81 \cdot \nu_1 + 3\nu_2 - \nu_3 = 0 \tag{5-14f}$$

From the above equations it is possible to express the overall conversion rates of ethanol, oxygen, and carbon dioxide, in terms of r_x (overall conversion rate of biomass). Solving Equations (5-14f) and (5-14g) simultaneously, the reaction rates for the second and third reactions, ν_2 and ν_3, can be expressed as a function of the biomass synthesis rate ($r_x=\nu_1$) as shown in Equation (D-1):

$$\nu_2 = \frac{(\alpha_{1E} - 1.81\delta)}{(3\delta - 0.5)} \cdot \nu_1 \tag{D-1}$$

Considering Equation (5-4): $\alpha_{1E} = K + \frac{m_{ATP}}{\mu}$

$$\begin{aligned} \nu_3 &= 1.81\nu_1 + 3\nu_2 = \frac{(3\alpha_{1E} - 0.905)}{(3\delta - 0.5)} \cdot \nu_1 \\ &= \left\{\frac{3(K + \frac{m_{ATP}}{\mu}) - 0.905}{3\delta - 0.5}\right\} \cdot r_x \end{aligned} \tag{D-2}$$

Considering $r_x = \mu \cdot C_x$

$$\nu_3 = \frac{3K - 0.905}{3\delta - 0.5} \cdot r_x + \frac{3m_{ATP}}{3\delta - 0.5} \cdot C_x \tag{D-3}$$

Therefore, the oxygen consumption rate becomes:

$$-r_{o_2} = 0.5\nu_3 = (\frac{3K - 0.905}{6\delta - 1})r_x + (\frac{3m_{ATP}}{6\delta - 1})C_x \tag{D-4}$$

Carbon dioxide production rate is:

$$r_{co_2} = 0.27\nu_1 + \nu_2 = (\frac{\alpha_{1E} - \delta - 0.135}{3\delta - 0.5})r_x = (\frac{K - \delta - 0.135}{3\delta - 0.5}) \cdot r_x + (\frac{m_{ATP}}{3\delta - 0.5}) \cdot C_x \tag{D-5}$$

Ammonium consumption rate is:

$$r_N = -0.2r_x \tag{D-6}$$

The overall conversion rate of ethanol becomes:

$$-r_e = (\frac{-0.635 + 2\delta + K}{3\delta - 0.5})r_x + (\frac{m_{ATP}}{3\delta - 0.5}) \cdot C_x = \frac{1}{Y_{ex}^{\max}} r_x + m_e C_x \tag{5-15}$$

Equation (5-15) describes the amount of ethanol required for the production of biomass and maintenance.

The macroscopic yield and maintenance factors can be defined by the introduction of the following equations:

$$r_e = \frac{1}{Y_{ex}} r_x + m_s C_x \tag{D-7}$$

$$r_{o_2} = \frac{1}{Y_{ox}} r_x + m_o C_x \tag{D-8}$$

$$r_{co_2} = \frac{1}{Y_{cx}} r_x + m_c C_x \tag{D-9}$$

The microscopic model allows the formation of expressions for the macroscopic parameters $Y_{ex}, Y_{ox}, Y_{cx}, m_e, m_o$ and m_c as follows:

$$Y_{ex} = \frac{(3\delta - 0.5)}{(K + 2\delta - 0.635)} \tag{D-10}$$

$$m_e = \frac{m_{ATP}}{(3\delta - 0.5)} \tag{D-11}$$

$$Y_{ox} = \frac{(6\delta - 1)}{(3K - 0.905)} \quad = 0.644 \tag{D-12}$$

$$m_o = \frac{3m_{ATP}}{(6\delta - 1)} \tag{D-13}$$

$$Y_{cx} = \frac{(3\delta - 0.5)}{(K - \delta - 0.135)} \tag{D-14}$$

$$m_c = \frac{m_{ATP}}{(3\delta - 0.5)} \tag{D-15}$$

Appendix D-2. Model for Benzyl Alcohol Bioremediation

For benzyl alcohol bioremediation, the overall conversion rates of the key compounds are given in Section 5.2.2 as:

$$-r_b = 1.27\nu_1 + \nu_2 \tag{5-28a}$$

$$r_x = \nu_1 \tag{5-28b}$$

$$-\alpha_{1b} \cdot \nu_1 + \delta \cdot \nu_3 = 0 \tag{5-28c}$$

$$1.084 \cdot \nu_1 + \frac{13}{7}\nu_2 - \nu_3 = 0 \tag{5-28d}$$

$$r_N = -0.2\nu_1 \tag{D-16}$$

$$r_{o_2} = -\frac{2}{7}\nu_2 - 0.5\nu_3 \tag{D-17}$$

$$r_{co_2} = 0.27\nu_1 + \nu_2 \tag{D-18}$$

Solving Equations (5-28f) and (5-28d) simultaneously, the reaction rates for the second and third reactions (see reaction Equations (5-25) (5-11) in Section 5.2.2), ν_2 and ν_3, can be expressed as a function of the biomass synthesis rate ($r_x=\nu_1$) as:

$$\nu_2 = \frac{1}{(\frac{13}{7}\delta)}(\alpha_{1b} - 1.084\delta)\cdot\nu_1 \tag{D-19}$$

$$\nu_3 = \frac{\alpha_{1b}}{\delta}\cdot\nu_1 \tag{D-20}$$

Combination of Equations (D-19), (D-20) with Equations (5-28a) to (5-28d) by considering Equation (5-4): $\alpha_{1E} = K + \frac{m_{ATP}}{\mu}$, the following relations can be obtained:

$$-r_b = \frac{(K+1.274\delta)}{(13/7)\delta}r_x + [\frac{m_{ATP}}{(13/7)\delta}]\cdot C_x \tag{5-29}$$

$$-r_N = 0.2r_x \tag{D-21}$$

$$-r_{o_2} = \frac{(8.5K - 2.168\delta)}{13\delta}\cdot r_x + \frac{8.5}{13\delta}\cdot m_{ATP}\cdot C_x \tag{D-22}$$

$$r_{co_2} = \frac{(K - 0.584\delta)}{(\frac{13}{7}\delta)}\cdot r_x + \frac{m_{ATP}}{(\frac{13}{7}\delta)}\cdot C_x \tag{D-23}$$

Considering the same equation forms as Equations (D-7) to (D-9), the following relations can be drawn:

$$\frac{1}{Y_{bx}^{\max}} = \frac{(K+1.274\delta)}{(13/7)\delta} \tag{5-30a}$$

$$Y_{o_2,x} = \frac{13\delta}{(8K - 2.168\delta)} = 0.585 \tag{D-24}$$

$$\frac{1}{Y_{c,x}} = \frac{(K - 0.584\delta)}{(\frac{13}{7}\delta)} \tag{D-25}$$

Appendix E. Determination of Parameter Uncertainty

Combining Equations (5-15a) and (5-30a), the expressions of the parameters δ and K, can be described by Equations (E-1) and (E-2):

$$\delta = \frac{(0.635 - 0.5 / Y_{xe}^{\max})}{(\frac{13}{7}\frac{1}{Y_{xb}^{\max}} + 0.726 - \frac{3}{Y_{xe}^{\max}})} \tag{E-1}$$

$$K = (\frac{13}{7}\frac{1}{Y_{xb}^{\max}} - 1.274) \cdot \delta \tag{E-2}$$

We assume that the most probable values for δ is given by Equation (E-3):

$$\delta = f(\overline{Y_{xe}}, \overline{Y_{xb}}) \tag{E-3}$$

The uncertainty in the resulting value for δ can be found by considering the spread of the values of δ resulting from combining the individual measurements $Y_{e,i}$, $Y_{b,i}$, … into individual results of δ_i. The approximation for the standard deviation σ_δ for δ can be expressed as (Bevington, 1969):

$$\sigma_\delta^2 \cong \sigma_{Y_{xe}}^2 (\frac{\partial \delta}{\partial Y_{xe}})^2 + \sigma_{Y_{xb}}^2 (\frac{\partial \delta}{\partial Y_{xb}})^2 + 2\sigma_{Y_{xe}Y_{xb}} (\frac{\partial \delta}{\partial Y_{xe}})(\frac{\partial \delta}{\partial Y_{xb}}) \tag{E-4}$$

$$\sigma_K^2 \cong \sigma_{Y_{xe}}^2 (\frac{\partial K}{\partial Y_{xe}})^2 + \sigma_{Y_{xb}}^2 (\frac{\partial K}{\partial Y_{xb}})^2 + 2\sigma_{Y_{xe}Y_{xb}} (\frac{\partial K}{\partial Y_{xe}})(\frac{\partial K}{\partial Y_{xb}}) \tag{E-5}$$

The variance and covariance were obtained as:

$$\frac{\partial \delta}{\partial Y_{xe}} = 29.98 \tag{E-6}$$

$$\frac{\partial \delta}{\partial Y_{xb}} = -0.204 \tag{E-7}$$

$$\sigma_{Y_{xe}} = 0.001 \tag{E-9}$$

$$\sigma_{Y_{xb}} = 0.01 \tag{E-10}$$

$$\sigma^2_{Y_{xe}Y_{be}} = -1.3E-06 \tag{E-11}$$

$$\sigma^2_{\delta} = 9.19E-04 \tag{E-12}$$

$$\sigma_{\delta} = 0.03 \tag{E-13}$$

$$\delta = 0.91 \pm 0.03 \tag{E-14}$$

The uncertainty for K is estimated as follows:

From Equation (E-2),

$$\frac{\partial K}{\partial Y_{xe}} = (\frac{13}{7}\frac{1}{Y_{xb}} - 1.274) \cdot (\frac{\partial \delta}{\partial Y_{xe}}) \tag{E-15}$$

$$\frac{\partial K}{\partial Y_{xb}} = (-\frac{13}{7}\frac{1}{Y^2_{xb}}) \cdot \delta + (\frac{13}{7}\frac{1}{Y_{xb}} - 1.274) \cdot (\frac{\partial \delta}{\partial Y_{xb}}) \tag{E-16}$$

$$\sigma^2_K \cong \sigma^2_{Y_{xe}} (\frac{\partial K}{\partial Y_{xe}})^2 + \sigma^2_{Y_{xb}} (\frac{\partial K}{\partial Y_{xb}})^2 + 2\sigma_{Y_{xe}Y_{xb}} (\frac{\partial K}{\partial Y_{xe}})(\frac{\partial K}{\partial Y_{xb}}) \tag{E-17}$$

$$\frac{\partial K}{\partial Y_{xe}} = 85.53 \tag{E-18}$$

$$\frac{\partial K}{\partial Y_{xb}} = -9.25 \tag{E-19}$$

$$\sigma^2_K = 1.79E-02 \tag{E-20}$$

$$\sigma_K = 0.13 \tag{E-21}$$

$$K = 2.61 \pm 0.13 \tag{E-22}$$

Appendix F. Prediction Results at Unsteady State

If the dissolved oxygen (DO) is less than the critical value (C_{cr}), the system would no longer be operated at steady state, and Equations (5-65) or (5-66) will no longer be valid. Instead, the unsteady state equation has to be considered, thus Equation (5-61) becomes:

$$\frac{dC_x}{dt} = (\mu - D) \cdot C_x \tag{F-1}$$

At this condition, bacteria are no longer growing, i.e., $\mu = 0$

$$\frac{dC_x}{C_x} = -D \cdot dt \tag{F-2}$$

Integrated solution of Equation (F-1) is:

$$C_x = C_{x0} \cdot \exp(-D \cdot t) \tag{F-3}$$

The results of prediction from Equation (F-3) is given in Figure F-1. This proves that the model developed in this study can predict the transient process.

For ethanol balance:

$$\frac{dC_e}{dt} = -r_e + \phi_e \tag{F-4}$$

where $-r_e = \frac{1}{Y_{ex}} \cdot r_x + \frac{1}{Y_{ep}} \cdot r_p + m_e \cdot C_x$

$r_x = \mu \cdot C_x$ =0, formation rate of biomass.

$r_p = k_p \cdot C_e \cdot C_x$, formation rate of by-product (acetic acid).

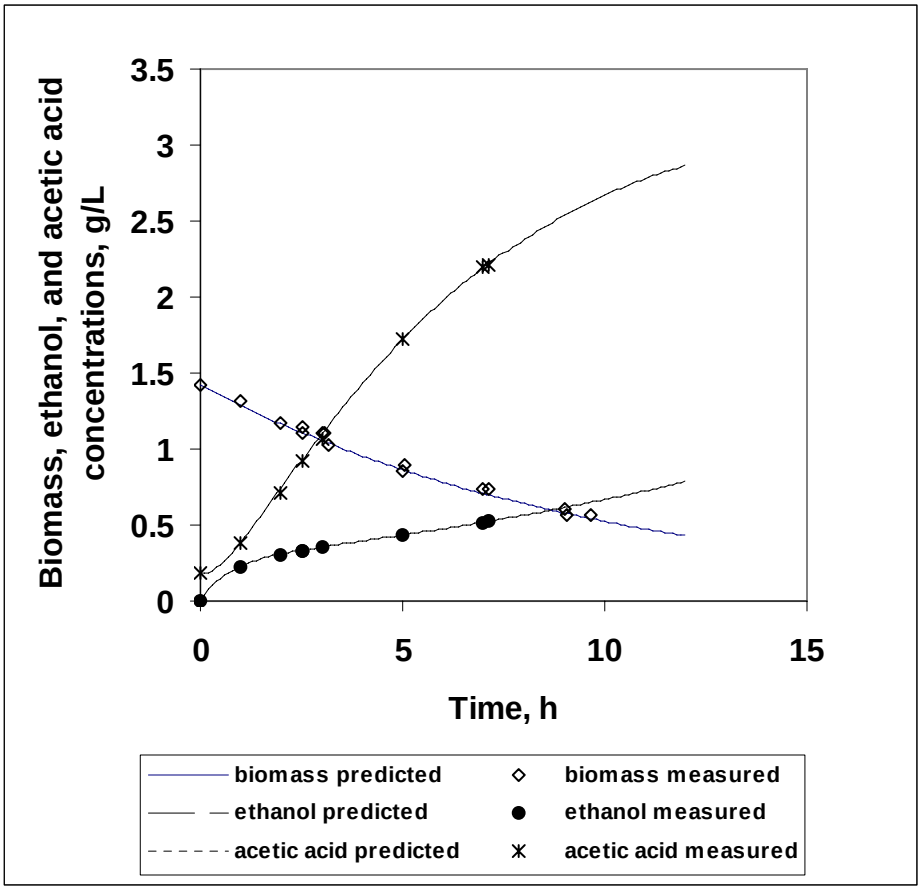

Figure F-1. Simulation results for continuous removal of ethanol at inlet gas concentration of 25.0 mg/L and dilution rate of 0.1 h^{-1}.